

DATA-EFFICIENT KERNEL METHODS FOR LEARNING DIFFERENTIAL EQUATIONS AND THEIR SOLUTION OPERATORS: ALGORITHMS AND ERROR ANALYSIS

YASAMIN JALALIAN ^{1,*}, JUAN FELIPE OSORIO RAMIREZ ^{2,*}, ALEXANDER HSU ^{2,*}, BAMDAD HOSSEINI ²,
AND HOUMAN OWHADI ¹

ABSTRACT. We introduce a novel kernel-based framework for learning differential equations and their solution maps that is efficient in data requirements, in terms of solution examples and amount of measurements from each example, and computational cost, in terms of training procedures. Our approach is mathematically interpretable and backed by rigorous theoretical guarantees in the form of quantitative worst-case error bounds for the learned equation. Numerical benchmarks demonstrate significant improvements in computational complexity and robustness while achieving one to two orders of magnitude improvements in terms of accuracy compared to state-of-the-art algorithms.

SIGNIFICANCE STATEMENT

We present a novel algorithm inspired by kernel methods and Gaussian processes for learning differential equations and their solution operators in scarce data regimes. Our approach: (a) is significantly more efficient than state-of-the-art methods, including neural networks, in terms of required data and computational time. In fact, we obtain one to two orders of magnitude improvement in accuracy on a number of benchmarks; (b) is supported by rigorous theory featuring the first quantitative worst-case error bounds for equation learning; and (c) can solve previously intractable scientific computing problems such as one-shot operator learning and learning of variable-coefficient PDEs in extremely scarce data regimes.

1. INTRODUCTION

In recent years, machine learning (ML) has revolutionized the way data is combined with mathematical models to infer and predict the behavior of physical systems. This wide adoption of ML in science has given rise to a new area of computational science and engineering often referred to as physics-informed ML [50]. Broadly speaking, the goal here is to simulate physical processes driven by differential equations (DEs) by combining data and expert knowledge in an automated manner. In this article we focus on the problem of learning DEs and their solution operators from scarce data, two tasks that constitute the vast majority of problems in physics-informed ML. We introduce a general computational framework for solving these problems based on the theory of kernels and Gaussian processes (GPs) which we call Kernel Equation Learning (KEqL). Our approach offers significant advantages over existing methods, including state-of-the-art neural network techniques, in terms of: (a) Accuracy, data efficiency, and computational efficiency, achieving superior performance across multiple benchmarks; (b) Rigorous theoretical guarantees, providing the first known quantitative worst-case error bounds for equation learning; (c) Robust and efficient training, leveraging second-order optimization algorithms for improved convergence and stability; and (d) New capabilities in physics-informed machine learning, enabling one-shot operator learning and the discovery of variable-coefficient partial differential equations (PDEs) even in severely data-scarce settings.

Due to space constraints, limitations on figures, and citation restrictions, we defer several details to the Supplementary Information (SI). These include a comprehensive literature review, in-depth theoretical arguments and algorithmic details, as well as additional numerical results. We will introduce KEqL for the case of PDEs but note that it naturally includes ordinary differential equations (ODEs) as demonstrated in our numerical experiments. Let $u : \mathcal{Y} \rightarrow \mathbb{R}$ be a function that describes the state of a physical system and consider a PDE of the form

$$(1) \quad \mathcal{P}(u)(y) = f(y) \quad y \in \mathcal{Y}, \quad \mathcal{B}(u)(y) = g(y) \quad y \in \partial\mathcal{Y},$$

with \mathcal{P} denoting a differential operator that describes a PDE in the interior of $\mathcal{Y} \subset \mathbb{R}^d$, \mathcal{B} denotes the boundary operator, and f and g denote the source term and boundary data/initial conditions. We emphasize that in the above formulation y is considered as an abstract input variable that may be spatial only (in the case of steady state PDEs) or a space-time variable (in the case of dynamics). Following [15], the three main types of problems in Physics-informed ML are: *equation learning/discovery* where \mathcal{P} or \mathcal{B} are unknown and must be inferred from a data set of (u, f, g)

* EQUAL CONTRIBUTION BY FIRST THREE AUTHORS

¹ CALIFORNIA INSTITUTE OF TECHNOLOGY, PASADENA, CA, 91125, EMAILS: YJALALIA@CALTECH.EDU, OWHADI@CALTECH.EDU

² UNIVERSITY OF WASHINGTON, SEATTLE, WA, 98195, EMAILS: JOSORIOR@UW.EDU, OWLX@UW.EDU, BAMDADH@UW.EDU

tuples [17, 91]; *operator learning* where the solution map $\mathcal{P}^{-1} : (f, g) \mapsto u$ is learned from a similar data [56, 6]; and finally *PDE solvers* where the solution u is computed given complete or partial information on (f, g) [88, 18].

An important consequence of our work is the unification of the aforementioned tasks within the abstract framework of computational graph completion (CGC) [82, 16]. The intuition behind this unification is as follows: Learning the inverse map \mathcal{P}^{-1} (operator learning) is equivalent to the problem of learning the forward map \mathcal{P} (equation learning) and then computing the inverse (PDE solvers). In scarce data regimes, where very limited measurements of u are available, it is hopeless to try to learn \mathcal{P}^{-1} directly, but it is possible to learn \mathcal{P} and u simultaneously due to the prior knowledge that the pair must satisfy (1), i.e., the learned solution should solve the learned PDE. This simultaneous learning of \mathcal{P} and u is the key idea behind our methodology, but it leads to challenging optimization problems which motivate our algorithmic contributions.

2. THE PROPOSED METHOD

In this section we outline our proposed KEqL methodology for equation learning based on the theory of reproducing kernel Hilbert spaces (RKHSs) and GPs. We consider the problem of learning the differential operator \mathcal{P} only since this is often the problem of interest in practice and note that our methodology can be generalized to learning the boundary operator \mathcal{B} in a similar way. Finally, we consider only the case where u and f are scalar fields on \mathcal{Y} and postpone the learning of systems to future work. Throughout the paper we assume \mathcal{P} has the form

$$(2) \quad \mathcal{P}(u)(y) = P \circ \Phi(u, y), \quad \Phi : (u, y) \mapsto (y, \delta_y \circ L_1 u, \dots, \delta_y \circ L_Q u) \in \mathbb{R}^{Q+d}.$$

For brevity we henceforth write $\mathcal{S} = \mathbb{R}^{Q+d}$. In the above $P : \mathcal{S} \rightarrow \mathbb{R}$ is a (possibly nonlinear) function, δ_y denotes the pointwise evaluation functional at y , and the $(L_q)_{q=1}^Q$ are bounded and linear differential operators that are assumed to be known. For ease of presentation we always assume $L_1 = \text{Id}$ so that P takes y and the point values $u(y)$ as input even though it may not depend on these quantities. Note that the map Φ is linear in u but it is nonlinear in y whenever u is nonlinear. The function P and the solution u are the main objects of interest that we wish to learn from data. Figure 1(A) depicts an instance of the computation graph (in the parlance of [82]) associated with equation (2). The red elements in that figure denote the unknown edges/elements of the computational graph in the setting of equation learning. Blue elements are input data, and the black element Φ is assumed to be known.

The above assumption on the form of \mathcal{P} encompasses most PDEs of interest in physics and engineering. As an example, consider the one dimensional variable coefficient nonlinear heat equation:

$$(3) \quad \begin{cases} \mathcal{P}(u)(t, x) = \partial_t u(t, x) - \partial_x (a(x) \partial_x u(t, x)) - u^3(t, x) = f(t, x), \text{ for } (t, x) \in (0, T] \times (0, 1), \\ u(0, x) = u(t, 0) = u(t, 1) = 0, \end{cases}$$

with a smooth coefficient $a : [0, 1] \mapsto (0, +\infty]$. Writing $y = (t, x)$ and letting $\mathcal{Y} = (0, T] \times (0, 1)$ and introducing the differential operators $L_1 : u \mapsto u$, $L_2 : u \mapsto \partial_t u$, $L_3 : u \mapsto \partial_x u$, and $L_4 : u \mapsto \partial_{xx} u$ we can cast (3) in the form (2) by writing $\mathcal{P}(u)(t, x) = P(t, x, u(t, x), L_2 u(t, x), L_3 u(t, x), L_4 u(t, x))$ with the nonlinear map

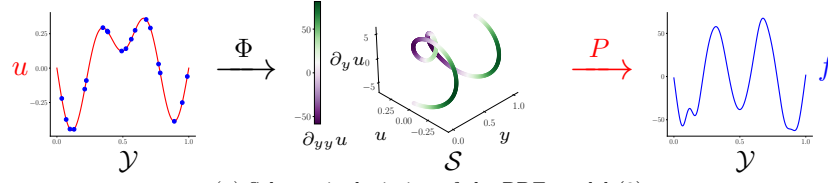
$$P : \mathbb{R}^6 \rightarrow \mathbb{R}, \quad P(s_1, s_2, s_3, s_4, s_5, s_6) = s_4 - \partial_x a(s_2) s_5 - a(s_2) s_6 - s_3^3.$$

We emphasize that the example PDE mentioned above is precisely the type of equations that we are motivated by, i.e., nonlinear equations with variable coefficients that may not have sparse representations in a known basis. In this light, we merge equation learning, the problem of learning P [11, 17], with inverse problems, the problem of inferring unknown coefficients such as a [45]; see SI A for more discussion.

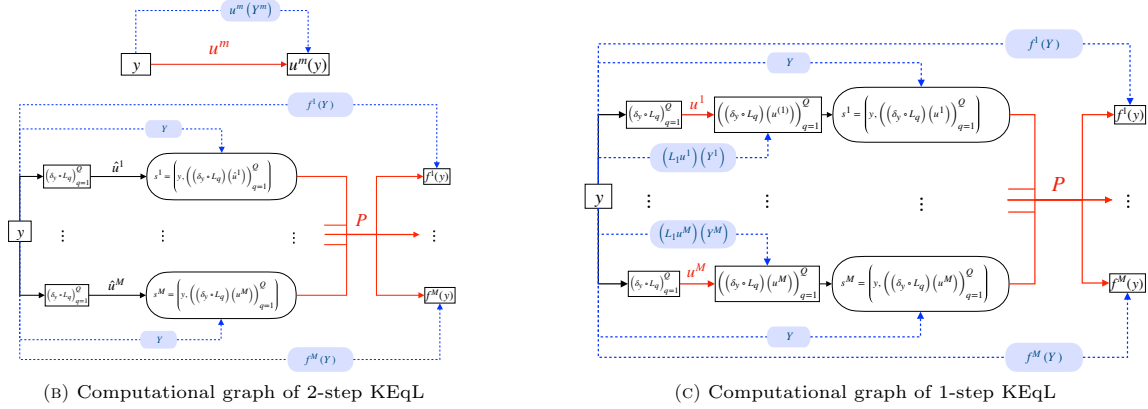
Now consider an index $m = 1, \dots, M$ and pairs (u^m, f^m) that solve (1) along with a finite set of points $Y^m = \{y_1^m, \dots, y_N^m\} \subset \Gamma$ which we refer to as the *observation points*¹. Further introduce the compact notation $u^m(Y^m) := (u^m(y_1^m), \dots, u^m(y_N^m)) \in \mathbb{R}^N$. Then our goal throughout the article is to learn P from training data $(u^m(Y^m), f^m)_{m=1}^M$, i.e., u^m is only observed on the Y^m while f^m is assumed to be known everywhere; this is a simplifying assumption for us and can be relaxed to having finite information on the f^m under some circumstances. Since the training data only contains limited information on the functions u^m the process for learning P should inevitably involve the learning of u^m as well which essentially constitutes the filtering problem in data assimilation [59].

With the above setup, we propose three approaches for learning P and the u^m : (i) a 2-step method where we first learn the u^m 's from data and then approximate P . This method was introduced in [67] as a kernel analog to the PDE-FIND algorithm of [91]; and (ii) a 1-step method where u^m and P are learned jointly akin to [82, 16] and can be viewed as a kernel analogue to [21]; (iii) we further present an intermediate method called the reduced 1-step method that interpolates between our 1-step and 2-step methods, inheriting the desirable performance of the 1-step method while improving computational efficiency. We show that the underlying computational graphs for our 1 and 2 step methods in Figure 1(B,C). As before, the red edges in these graphs are unknown nonlinearities that should be inferred and data is depicted using dashed blue lines and is injected into the nodes which represent variables.

¹One may also let N change with the index m but we keep the size of the mesh fixed to keep our notation light



(A) Schematic depiction of the PDE model (2)



(B) Computational graph of 2-step KEqL

(C) Computational graph of 1-step KEqL

FIGURE 1. (A) Schematic depiction of the computational graph of (2) in the context of equation learning for a single pair (u, f) . Red objects are unknown nonlinearities that need to be learned. Blue objects are data for the problem, while black objects (the map Φ) are assumed to be known. The left and right panels show the solution and right-hand side of an example second order PDE depending on $y, u, \partial_y u$, and $\partial_{yy} u$ while the middle panel shows $\Phi(y, u)$; (B) The computational graph of 2-step KEqL. Red edges are unknown nonlinear maps to be learned. Blue boxes denote data that is known for various nodes with dashed lines denoting where the data is injected. Note that the graphs for u^m and P are disconnected, hence the learning of u^m and P is performed sequentially in two steps; (C) The computational graph for 1-step KEqL. Coloring conventions follow panel (B) with the main difference being that the u^m and P are now connected and have to be learned simultaneously.

We note that, while our exposition and theoretical analysis are focused on the implementation of our methods using kernels, many of our results can be extended to an abstract optimal recovery framework by replacing RKHSs with Banach spaces. Such a generalization would encompass sparse regression techniques like SINDy and PDE-FIND [17, 91] as well as neural net methods such as [68, 21]. However, while these different approaches can be unified under the umbrella of optimal recovery, our kernel implementation leads to crucial gains in terms of data and computational efficiency as it enables us to use various techniques from smooth optimization and RKHS theory to solve the resulting difficult optimization problems; these same issues are known to be the main hurdle in applications of physics-informed neural nets (PINNs) as well [57].

2.1. 2-step KEqL: first learn the u^m , then learn P . Let $\mathcal{U} : \mathcal{Y} \times \mathcal{Y} \rightarrow \mathbb{R}$ denote a positive definite and symmetric (PDS) kernel with its associated RKHS \mathcal{U} with inner product $\langle \cdot, \cdot \rangle_{\mathcal{U}}$ and norm $\| \cdot \|_{\mathcal{U}}$; see SI B for a review of RKHS theory. Then the first step in 2-step KEqL approximates u^m via the optimal recovery problems ²

$$(4) \quad \hat{u}^m := \arg \min_{v^m \in \mathcal{U}} \|v^m\|_{\mathcal{U}} \quad \text{subject to (s.t.)} \quad v^m(Y^m) = u^m(Y^m).$$

We can also relax the equality constraints using a penalty method leading to a quadratic optimization problem with nugget parameter (or observation noise standard deviation) $\sigma_u^2 > 0$,

$$(5) \quad \hat{u}^m := \arg \min_{v^m \in \mathcal{U}} \|v^m\|_{\mathcal{U}}^2 + \frac{1}{2\sigma_u^2} \|v^m(Y^m) - u^m(Y^m)\|_2^2.$$

²Note that one could also employ a different kernel \mathcal{U}^m for each instance of the problem but we will not pursue this for brevity.

With \hat{u}^m at hand we proceed to step two where we approximate P through a second optimal recovery problem. To do this, let us consider an independent set of points $Y = \{y_1, \dots, y_K\} \subset \mathcal{Y}$ which we call the *collocation points*. This set of points may be chosen independent of the individual Y^m but to make our formulation simpler we will assume it is chosen such that $\cup_{m=1}^M Y^m \subset Y$, i.e., the collocation points Y contain all of the observation points Y^m .

Now observe that the differential operators L_q can be directly applied to the \hat{u}^m , in fact, as we show in Section 4 the functions $L_q \hat{u}^m$ can be computed analytically or using automatic differentiation. Then given a PDS kernel $\mathbf{P} : \mathcal{S} \times \mathcal{S} \rightarrow \mathbb{R}$ with RKHS \mathcal{P} we can approximate P via the optimal recovery problem

$$(6) \quad \hat{P} := \arg \min_{G \in \mathcal{P}} \|G\|_{\mathcal{P}} \quad \text{s.t.} \quad G \circ \Phi(\hat{u}^m, Y) = f^m(Y), \quad m = 1, \dots, M,$$

where $f^m(Y) := (f^m(y_1), \dots, f^m(y_K)) \in \mathbb{R}^K$ and we used the shorthand notation $\Phi(\hat{u}^m, Y) = (\Phi(\hat{u}^m, y_1), \dots, \Phi(\hat{u}^m, y_K)) \subset \mathcal{S}$. Similar to (5) this problem can also be relaxed using a nugget parameter $\sigma_P^2 > 0$,

$$(7) \quad \hat{P} := \arg \min_{G \in \mathcal{P}} \|G\|_{\mathcal{P}}^2 + \frac{1}{2\sigma_P^2} \sum_{m=1}^M \|G \circ \Phi(\hat{u}^m, Y) - f^m(Y)\|_2^2.$$

In either case \hat{P} also admits an analytic formula akin to the \hat{u}^m which we present in Section 4. Note that in (6, 7) we are using the collocation points Y to impose the infinite PDE constraint $G \circ \Phi(\hat{u}^m, y) = f(y)$ for all $y \in \mathcal{Y}$, on a finite discrete set, which justifies our choice of terminology as this is precisely the role of collocation points in PDE solvers [18]. This also motivates our preference to choose Y to be dense within computational budget constraints.

In many practical settings we have some prior knowledge about the differential operator \mathcal{P} , for example in many dynamic problems we know that a time derivative of the form $\partial_t^h u$ for some integer h is present. In such cases we can simply work with the model $\mathcal{P}(u) = (P + \bar{P}) \circ \Phi(u, \cdot)$ with \bar{P} representing the known part of the differential operator. This modification amounts to a simple reformulation of (7) (and similarly (6)) as

$$(8) \quad \hat{P} := \arg \min_{G \in \mathcal{P}} \|G\|_{\mathcal{P}}^2 + \frac{1}{2\sigma_P^2} \sum_{m=1}^M \|(G + \bar{P}) \circ \Phi(\hat{u}^m, Y) - f^m(Y)\|_2^2.$$

Henceforth we will include \bar{P} in our discussion to account for prior information about \mathcal{P} .

The 2-step approach described above can also be viewed within the framework of CGC [82]: CGC considers a computational graph where nodes represent variables and directed edges represent nonlinear functions. Then given data on various nodes and prior knowledge of certain edges, one aims to recover unknown nonlinear functions within the computational graph. Since our 2-step method approximates the u^m and P separately, it naturally leads to two disjoint computational graphs as shown in Figure 1(B); recall that the red arrows in that figure denote unknown nonlinear functions (edges) while dashed blue lines show data that is injected into nodes (vertices). Observe that the computational graphs for the u^m and P are disjoint and hence easy to complete. However, the 2-step method will only be successful when data is sufficient to accurately approximate the pertinent partial derivatives of the u^m . This limits the applicability of this method in scarce data regimes and motivates our 1-step formulation in Section 2.2.

2.1.1. Connection to existing methods. A slightly different version of 2-step KEqL was introduced in [67] which did not use the collocation points Y as it was assumed that the Y^m were sufficiently dense. 2-step KEqL can also be viewed as the kernel/GP analogue of SINDy/PDE-FIND [17, 91]. The kernel method is different from these works in three directions: (1) here prior knowledge about P is summarized by the choice of the kernel \mathbf{P} while in SINDy this information is given by the dictionary; (2) SINDy looks for a \hat{P} that is sparse in the dictionary while the kernel method finds a minimum RKHS norm solution that is not necessarily sparse; (3) since y is readily included as an input to P , our formulation naturally accommodates variable coefficient PDEs while dealing with such problems for SINDy is non-trivial [108] since the variable coefficients may depend on y in a complex manner that is not sparse in a particular dictionary. For detailed overview of methods related to 2-step KEqL see SI A.

2.2. 1-step KEqL: simultaneously learn the u^m and P . The primary shortcoming of 2-step KEqL is the decoupled learning of the u^m and P which limits its performance in scarce data regimes (here we have in mind the cases where the observation meshes Y^m have very few points). To remedy this we propose 1-step KEqL that estimates \hat{u}^m and \hat{P} at the same time while imposing the requisite PDE constraint on the collocation points Y . To this end, we consider the joint optimal recovery problem

$$(9) \quad (\hat{\mathbf{u}}, \hat{P}) = \arg \min_{\mathbf{v} \in \mathcal{U}^M, G \in \mathcal{P}} \|G\|_{\mathcal{P}}^2 + \lambda \sum_{m=1}^M \|v^m\|_{\mathcal{U}}^2$$

$$\text{s.t.} \quad v^m(Y^m) = u^m(Y^m), \quad \text{and} \quad (G + \bar{P}) \circ \Phi(v^m, Y) = f^m(Y), \quad \text{for} \quad m = 1, \dots, M,$$

where $\lambda > 0$ is a user defined parameter and we used the notation $\mathbf{v} := (v^1, \dots, v^M) \in \mathcal{U}^M$ to denote the vector of candidate RKHS functions with their optimal values denoted as $\hat{\mathbf{u}} \in \mathcal{U}^M$. In complete analogy with 2-step KEqL we

can also relax the equality constraint in (9) using appropriate nugget parameters $\sigma_u^2, \sigma_P^2 > 0$ to obtain the formulation,

$$(10) \quad (\widehat{\mathbf{u}}, \widehat{P}) = \arg \min_{\mathbf{v} \in \mathcal{U}^M, G \in \mathcal{P}} \|G\|_{\mathcal{P}}^2 + \sum_{m=1}^M \lambda \|v^m\|_{\mathcal{U}}^2 + \frac{1}{2\sigma_u^2} \|v^m(Y^m) - u^m(Y^m)\|_2^2 + \frac{1}{2\sigma_P^2} \|(G + \overline{P}) \circ \Phi(v^m, Y) - f^m(Y)\|_2^2.$$

Note the important distinction, compared with 2-step KEqL, that the estimation of the $\widehat{\mathbf{u}}$ and \widehat{P} is now coupled due to the composition of G and the v^m in the PDE constraint/penalty term. Indeed 1-step KEqL can also be viewed within the framework of CGC with its computational graph shown in Figure 1(C); observe that the computational graphs for the u^m and P are now connected. This coupling of the estimation of the u^m and P is the source of algorithmic challenges to solving 1-step KEqL. Nonetheless, we solve this problem after reformulation using a representer theorem and using an efficient Levenberg–Marquardt (LM) algorithm in Section 4.

2.2.1. Connection to existing methods. The concept of optimizing a loss function that jointly matches the given observations and the PDE constraint has appeared in the literature previously. Most notably, in [21], a neural network surrogate was used to approximate u^m while in [105] a spline model was used, both methods then use a sparsity prior over a dictionary to learn P and u^m . In a similar vein, there are methodologies based on SINDy that can be viewed as 1-step methods, most notably, the weak SINDy [72, 73] and the SINDy-UQ [43] although neither methods were originally developed as true 1-step methods and modifying them for scarce data settings is beyond their current implementation. What sets 1-step KEqL apart from these works is: (1) we present an explicit optimal recovery formulation based on RKHS theory; (2) the regularization due to our formulation automatically leads to a stable algorithm that is amenable to second order optimization; (3) the kernel formulation accommodates larger number of features and more flexibility in choosing and tuning the features for both u^m and P ; and (4) our formulation is readily defined with variable coefficient PDEs in mind, a topic that is often difficult for dictionary based methods. Finally, we note that 1-step RKHS methods similar to KEqL have appeared previously in [86, 58] but only for narrow classes of PDEs. For a more detailed overview of related methods to 1-step KEqL see SI A.

2.3. Operator learning. In this final subsection we turn our attention to the operator learning problem of estimating the solution map \mathcal{P}^{-1} of the PDE (1). The dominant paradigm for operator learning [56] aims to approximate the solution map \mathcal{P}^{-1} via a regression problem between function spaces from data. In our perspective, operator and equation learning problems are two sides of the same coin: where equation learning approximates \mathcal{P} , operator learning approximates the inverse \mathcal{P}^{-1} . To this end, following [67], let us write $\widehat{\mathcal{P}} := (\widehat{P} + \overline{P}) \circ \Phi$ to denote the differential operator associated with \widehat{P} . We then propose to approximate the operator \mathcal{P}^{-1} by computing the *pseudo inverse* operator $\widehat{\mathcal{P}}^\dagger$ defined variationally as

$$(11) \quad \widehat{\mathcal{P}}^\dagger(f) := \arg \min_{v \in \mathcal{U}} \|v\|_{\mathcal{U}} \quad \text{s.t.} \quad (\widehat{P} + \overline{P}) \circ \Phi(v, Y) = f(Y).$$

This optimization problem can be solved using the GP-PDE solver of [18, 7] which is a numerical PDE solver that is analogous to KEqL. We emphasize that the operator $\widehat{\mathcal{P}}$ is not invertible in general since the learned PDE is not guaranteed to be well-posed. Then (11) computes a well-defined regularized solution to this ill-posed PDE.

2.3.1. Connection to existing methods. As mentioned above most operator learning algorithms approximate mappings between Banach spaces, with neural nets being the most popular choice [56, 15], although other models such as kernel methods and GPs remain competitive [6, 74]. In most operator learning applications the training data is plentiful, i.e., the mesh size N and number of training pairs M are large. In contrast, our training data is scarce, both in terms of number of functions and the observation mesh. To our knowledge, current operator learning methods are incapable of handling such scarce data problems since \mathcal{P}^{-1} is often infinite-dimensional and non-local. On the other hand, \mathcal{P} is local and has the simple form (2) which reduces operator learning to approximating the scalar function P . This observation is the key to the success of our approach and leads to significant accuracy gain as shown in our examples in Section 5. Finally, we note that the recent family of physics-informed operator learning methods [37] take a step towards scarce data problems by augmenting their training with a PDE residual term but require complete knowledge of \mathcal{P} . For a more detailed overview of related methods for operator learning see SI A.

3. THEORETICAL ANALYSIS

Here we collect our main theoretical results concerning the convergence of KEqL in the form of quantitative error bounds for the learned functions \widehat{u}^m and the learned PDE \widehat{P} . To minimize theoretical clutter we will only present the bounds for 1-step KEqL without detailed proofs and instead focus on the key ideas and implications of the theorem. We refer the interested reader to the SI B for complete details and statements of results including analogous bounds for 2-step KEqL and an error bound for operator learning.

3.1. Setup and assumptions. For simplicity we consider 1-step KEqL without nugget terms or noise. Since we will be taking the limit of N (number of observation points) and M (size of training data) to infinity, we will supplement our notations in this section by subscripting pertinent objects with M, N indices. With this setup, we make the following assumptions:

Assumption 1. *It holds that:*

- (1) *The set $\mathcal{Y} \subset \mathbb{R}^d$ is bounded with Lipschitz boundary.*
- (2) *The kernel \mathbf{U} satisfies:*
 - (a) *Mercer's theorem holds for \mathbf{U} .*
 - (b) *\mathcal{U} is continuously embedded in the Sobolev space $H^\gamma(\mathcal{Y})$ for some $\gamma > d/2 + \text{order}(\mathcal{P})$ (where $\text{order}(\mathcal{P})$ denotes the order of the PDE).*
 - (c) *Elements of \mathcal{U} satisfy the boundary conditions in (1) (this is for ease of presentation and can be relaxed).*
- (3) *The kernel \mathbf{P} satisfies:*
 - (a) *\mathcal{P} is continuously embedded in $H^\eta(\mathcal{S})$ for some $\eta > \frac{Q+d}{2}$.*
 - (b) *Elements of \mathcal{P} are locally Lipschitz in the sense that $|P(s) - P(s')| \leq C(B)\|P\|_{\mathcal{P}}\|s - s'\|$ for all $s, s' \in B \subset \mathcal{S}$ and constant $C(B) > 0$.*

Since \mathbf{U} satisfies Mercer's theorem it has the spectral expansion $\mathbf{U}(y, y') = \sum_{j=1}^{\infty} \vartheta_j e_j(y) e_j(y')$ with eigenvalues $\vartheta_j > 0$ and eigenfunctions e_j . This expansion then allows us to define the space $\mathcal{U}^2 := \left\{ f : \mathcal{Y} \rightarrow \mathbb{R} \mid f(y) = \sum_{j=1}^{\infty} c_j(f) e_j(y) \text{ s.t. } \sum_{j=1}^{\infty} \vartheta_j^{-2} c_j(f)^2 < +\infty \right\}$. For ease of presentation let us assume that the observation points Y_N^m and the collocation points Y are the same, i.e., $Y_N^m = Y = Y_N$; we drop this assumption in our proofs in SI B. Finally, for the $Y_N \subset \mathcal{Y}$ and a set $B \subset \mathcal{S}$ we define the fill distances

$$\rho_N := \sup_{y' \in \mathcal{Y}} \inf_{y \in Y_N} \|y' - y\|_2, \quad \varrho_{M,N}(B) := \sup_{s' \in B} \inf_{s \in S \cap B} \|s' - s\|_2, \quad \text{where } S := \cup_{m=1}^M \cup_{y \in Y_N} \Phi(u^m, y).$$

3.2. Quantitative error bounds. We are now ready to state our main error bound for 1-step KEqL. The following theorem is a compressed version of Proposition 5.

Theorem 1. *Suppose Assumption 1 holds and $P, \bar{P} \in \mathcal{P}$. Let $\hat{u}_{M,N}^m$ and $\hat{P}_{M,N}$ be the solution to (9) with $Y_N^m = Y = Y_N$ for $M, N \in \mathbb{N}$ and fix a bounded set $B \subset \mathcal{S}$ with Lipschitz boundary. Then there exist constants $\rho_0, \varrho_0(B) > 0$ so that whenever $\rho_N < \rho_0$ and $\varrho_{M,N}(B) < \varrho_0(B)$, it holds that:*

- (1) *If $u^m \in \mathcal{U}$ then*

$$\sum_{m=1}^M \|u^m - \hat{u}_{M,N}^m\|_{H^{\gamma'}(\mathcal{Y})}^2 \leq C \rho_N^{2(\gamma - \gamma')} \left(\|P\|_{\mathcal{P}}^2 + \sum_{m=1}^M \|u^m\|_{\mathcal{U}}^2 \right),$$

where $0 \leq \gamma' \leq \gamma$ and $C > 0$ is a constant depending on \mathcal{Y} .

- (2) *If $u^m \in \mathcal{U}^2$ then*

$$\|P - \hat{P}_{M,N}\|_{L^\infty(B)} \leq C \left(\varrho_{M,N}(B)^{\eta - \frac{Q+d}{2}} + \rho_N^{\gamma - \gamma'} \right) \left(\|P\|_{\mathcal{P}}^2 + \|\bar{P}\|_{\mathcal{P}}^2 + \sum_{m=1}^M \|u^m\|_{\mathcal{U}^2}^2 \right)^{1/2},$$

for $d/2 + \text{order}(\mathcal{P}) < \gamma' < \gamma$ and a constant $C > 0$ that depends on \mathcal{Y} and B .

Note that our error bounds are reminiscent of Sobolev sampling inequalities (see Proposition 3 and the preceding discussion) that are the corner stone of our proof technique; indeed our rates in terms of fill-distances and the smoothness indices γ, η are familiar in this context. The key observation here is that the $\hat{u}_{M,N}^m$ interpolate the u^m on the observation points Y_N so sampling inequalities are a natural choice. However, the $\hat{u}_{M,N}^m$ are not necessarily minimum norm interpolants of the u^m due to the simultaneous optimization of functions and the equation which complicates the proof of statement (1). The bounds for $\hat{P}_{M,N}$ are more challenging since, intuitively, the input points S over which $\hat{P}_{M,N}$ approximates the value of P are themselves noisy due to the fact that the $\hat{u}_{M,N}^m$ and their requisite partial derivatives are not exact. This motivates the assumption that elements of \mathcal{P} are Lipschitz which in turn allows us to use a noisy sampling inequality to complete the proof.

We emphasize that the above error bounds are quite strong, and give pointwise control over the errors of the $\hat{u}_{M,N}^m$ and $\hat{P}_{M,N}$ over subsets of their domains provided that the training data is sufficiently space-filling. This is in line with the theory of scattered data approximation and suggests various avenues for experimental design of equation learning algorithms. Furthermore, the bound for $\hat{P}_{M,N}$ implies that the learned PDE is accurate for new input-output pairs (u, f) that are close to the training data in an appropriate sense, i.e., if $\Phi(u, \cdot) \in B$. In SI B.3 we use this observation to extend the error bound for $\hat{P}_{M,N}$ to the corresponding pseudo inverse $\hat{\mathcal{P}}_{M,N}^\dagger$.

3.2.1. *Connection to existing results.* The theoretical analysis of equation learning methods has been the subject of study in a number of previous works. Most notably [127] presents a comprehensive convergence analysis of SINDy with recovery guarantees using techniques from sparse recovery and compressed sensing. More recent articles have also considered fundamental limitations of equation learning such as identifiability [101] and PDE learning from a single trajectory [42]. More precise results have also been obtained for particular types of PDEs such as elliptic equations [95, 14]. Our analysis is different from these works in a number of directions: (1) to our knowledge previous works do not cover the case of the 1-step methods or the RKHS formulation; (2) quantitative worst-case error bounds such as ours are first of their kind; (3) some of the stronger guarantees in the literature are tailored to specific PDEs while our results apply to generic nonlinear PDEs under sufficient smoothness assumptions. For a more detailed overview of related work to our theory see SI A.

4. IMPLEMENTATION AND ALGORITHMS

We now turn our attention to the practical implementation and development of algorithms for 1-step and 2-step KEqL. We focus our discussion on the high-level and core aspects of algorithms and refer the reader to SI C as well as our GitHub repository³ for further details.

4.1. **Implementing 2-step KEqL.** Our implementation of 2-step KEqL is straightforward and utilizes standard representer theorems for kernel regression. It is well-known (see SI B) that the solution to (5) admits the formula

$$(12) \quad \hat{u}^m(y) = \mathbf{U}(Y^m, y)^T \hat{\alpha}^m, \quad \text{where} \quad \hat{\alpha}^m = (\mathbf{U}(Y^m, Y^m) + \sigma_u^2 I)^{-1} u^m(Y^m).$$

Here $\mathbf{U}(Y^m, y) := (\mathbf{U}(y_1^m, y), \dots, \mathbf{U}(y_N^m, y)) \in \mathcal{U}^N$ is a column vector field and $\mathbf{U}(Y^m, Y^m) \in \mathbb{R}^{N \times N}$ is a kernel matrix with entries $\mathbf{U}(Y^m, Y^m)_{ij} = \mathbf{U}(y_i^m, y_j^m)$. Setting $\sigma_u = 0$ further characterizes the solution (4) assuming $\mathbf{U}(Y^m, Y^m)$ is invertible. Thanks to (12) we can directly compute,

$$L_q \hat{u}(y) = L_q \mathbf{U}(Y^m, y)^T \hat{\alpha}^m, \quad \text{where} \quad L_q \mathbf{U}(Y^m, y) = (L_q \mathbf{U}(y_1^m, y), \dots, L_q \mathbf{U}(y_N^m, y)),$$

which requires us to apply the L_q operators to the kernel \mathbf{U} as a function of its second input (the y variable) for fixed values of its first input (the y_n^m values). For typical PDEs this amounts to computing partial derivatives of \mathbf{U} either analytically or using automatic differentiation software.

We can solve (8) identically to the above, using the formula

$$(13) \quad \hat{P}(s) = \mathbf{P}(S, s)^T \hat{\beta}, \quad \text{where} \quad \hat{\beta} = (\mathbf{P}(S, S) + \sigma_P^2)^{-1} (f(Y) - \bar{P}(S)), \quad \text{and} \quad S = \bigcup_{m=1}^M \Phi(\hat{u}^m, Y).$$

We used the shorthand notation $f(Y) = (f^1(Y), \dots, f^M(Y)) \in \mathbb{R}^{MK}$, the concatenation of the vectors $f^m(Y)$, and $\bar{P}(S) \in \mathbb{R}^{MK}$, the vector of point values of \bar{P} evaluated on S , both viewed as column vectors. Similar to (12), we also defined the vector field $\mathbf{P}(S, s) := (\mathbf{P}(s_1, s), \dots, \mathbf{P}(s_M, s)) \in \mathcal{P}^{MK}$, and the matrix $\mathbf{P}(S, S) = (\mathbf{P}(s_i, s_j))_{i,j=1}^M \in \mathbb{R}^{MK \times MK}$. In further analogy with the first step, setting $\sigma_P = 0$ gives the solution to (6) when $\mathbf{P}(S, S)$ is invertible.

The formulae (12) and (13) highlight the convenience and computational efficacy of 2-step KEqL since each equation requires a single linear solve involving a kernel matrix; this can be done very efficiently using sparse or randomized linear algebra techniques; see [96, 19, 20] as well as SI C.

4.2. **Implementing 1-step KEqL and its reduced version.** The implementation of 1-step KEqL is more involved and requires the solution of a compositional optimization problem. The first step is to derive an equivalent discrete formulation of (9) and (10); this amounts to the derivation of a representer theorem which we state for (9). Next we design an algorithm that can efficiently solve the aforementioned discrete optimization problem.

Towards stating our representer theorem, we need to introduce some new notation: Assuming \mathcal{U} is sufficiently regular, define the bounded and linear functionals $\phi_k^q := \delta_{y_k} \circ L_q \in \mathcal{U}^*$ for $q = 1, \dots, Q$ and $k = 1, \dots, K$, recalling our convention that L_1 denotes the identity map so that $\phi_k^1 = \delta_{y_k}$. Further observe that $\Phi(u, y_k) = (y_k, \phi_k^1(u), \dots, \phi_k^Q(u))$ by definition and so the ϕ_k^q denote the linear operators that give the subset of components of $\Phi(u, y_k)$ as a function of u , justifying our choice of notation. Write $\mathbf{U}(\phi_k^q, y) = \phi_k^q(\mathbf{U}(\cdot, y)) \in \mathcal{U}$, i.e., the RKHS function obtained by applying ϕ_k^q to $\mathbf{U}(\cdot, y)$ for every fixed value of y . Further define $\mathbf{U}(\phi_k^q, \phi_j^\ell) := \phi_j^\ell(\mathbf{U}(\phi_k^q, \cdot))$ for $\ell = 1, \dots, Q$ and $j = 1, \dots, K$. Next define the vector field $\mathbf{U}(\phi, y) := (\mathbf{U}(\phi_1^1, y), \dots, \mathbf{U}(\phi_K^1, y), \dots, \mathbf{U}(\phi_1^Q, y), \dots, \mathbf{U}(\phi_K^Q, y)) \in \mathcal{U}^{QK}$, along with the vectors $\mathbf{U}(\phi, \phi_k^q) = (\mathbf{U}(\phi_1^1, \phi_k^q), \dots, \mathbf{U}(\phi_K^1, \phi_k^q), \dots, \mathbf{U}(\phi_1^Q, \phi_k^q), \dots, \mathbf{U}(\phi_K^Q, \phi_k^q)) \in \mathbb{R}^{QK}$. Further let $\mathbf{U}(\phi^q, \phi^\ell) \in \mathbb{R}^{K \times K}$ denote the matrices with entries $\mathbf{U}(\phi^q, \phi^\ell)_{k,j} = \mathbf{U}(\phi_k^q, \phi_j^\ell)$ and the block-matrix $\mathbf{U}(\phi, \phi) \in \mathbb{R}^{QK \times QK}$ with blocks $\mathbf{U}(\phi, \phi)_{q,\ell} = \mathbf{U}(\phi^q, \phi^\ell) \in \mathbb{R}^{K \times K}$. Note that the above vectors and matrices can be computed offline using either analytical expressions (by computing appropriate partial derivatives of the kernel \mathbf{U}) or automatic differentiation akin to the 2-step KEqL. With this new notation we have the following characterization of the minimizers of (9):

³<https://github.com/TADSGroup/kernelequationlearning>

Theorem 2. Suppose that \mathcal{U} is sufficiently regular so that the operators ϕ_k^q are well-defined as elements of its dual \mathcal{U}^* . Then every minimizing tuple $(\widehat{\mathbf{u}}, \widehat{P})$ of (9) can be written in the form

$$\widehat{u}^m(y) = \mathbf{U}(\phi, y)^T \widehat{\alpha}^m, \quad \widehat{P}(s) = \mathbf{P}(\widehat{S}, s)^T \widehat{\beta},$$

for a tuple $(\widehat{\alpha}, \widehat{\beta})$ that solve the equivalent optimization problem

$$(14) \quad \begin{aligned} (\widehat{\alpha}, \widehat{\beta}) = & \arg \min_{\alpha \in (\mathbb{R}^{QK})^M, \beta \in \mathbb{R}^{MK}} \beta^T \mathbf{P}(S(\alpha), S(\alpha)) \beta + \lambda \sum_{m=1}^M (\alpha^m)^T \mathbf{U}(\phi, \phi) \alpha^m, \\ \text{s.t.} & \quad \mathbf{U}(\phi, Y^m)^T \alpha^m = u^m(Y^m), \quad \text{and} \quad \mathbf{P}(S(\alpha), S^m(\alpha))^T \beta = f^m(Y) - \overline{P}(S^m(\alpha^m)), \\ \text{where} & \quad S(\alpha) = \cup_{m=1}^M S^m(\alpha^m), \quad \text{and} \quad S^m(\alpha^m) = \Phi(\mathbf{U}(\phi, \cdot)^T \alpha^m, Y). \end{aligned}$$

Here we introduced the block vector $\alpha := (\alpha^1, \dots, \alpha^M) \in (\mathbb{R}^{QK})^M$ for coefficient vectors $\alpha^m \in \mathbb{R}^{QK}$, along with the matrices $\mathbf{U}(\phi, Y^m) \in \mathbb{R}^{QK \times N}$ with columns $\mathbf{U}(\phi, y_n^m)$, and $\mathbf{P}(S, S^m) \in \mathbb{R}^{MK \times K}$ with columns $\mathbf{P}(S, s_k^m)$.

The proof of this theorem is given in SI B. The main idea of the proof is based on the observation that conditioned on the values $L_q v^m(y_k)$, the optimization problems for the v^m and G variables in (9) will decouple. Then the result is obtained by introducing auxiliary variables representing the $L_q v^m(y_k)$ and applying representer theorems for RKHS interpolation with linear observation models. The problem (14) is the key to the design of our algorithms as it is readily implementable without the need for further discretization. This fact further implies that our theoretical analysis of (9) in Section 3 applies to the algorithms we implement in practice. We can further relax the equality constraints in (14) to obtain an equivalent problem for (10):

$$(15) \quad \begin{aligned} (\widehat{\alpha}, \widehat{\beta}) = & \arg \min_{\alpha \in (\mathbb{R}^{QK})^M, \beta \in \mathbb{R}^{MK}} \beta^T \mathbf{P}(S(\alpha), S(\alpha)) \beta + \sum_{m=1}^M \lambda (\alpha^m)^T \mathbf{U}(\phi, \phi) \alpha^m \\ & + \frac{1}{2\sigma_u^2} \|\mathbf{U}(\phi, Y^m)^T \alpha^m - u^m(Y^m)\|_2^2 + \frac{1}{2\sigma_p^2} \|\mathbf{P}(S(\alpha), S^m(\alpha^m))^T \beta + \overline{P}(S^m(\alpha^m)) - f^m(Y)\|_2^2. \end{aligned}$$

4.2.1. *An LM algorithm for 1-step KEqL.* Solving (15) is difficult in practice as a small perturbation in the α^m can lead to a large perturbation in the derivatives of the corresponding function $v^m = \mathbf{U}(\phi, \cdot)^T \alpha^m$. This large variation further translates into a large change in the $S^m(\alpha^m)$ point clouds leading to numerical instabilities. To mitigate this issue, we propose an iterative LM algorithm that will approximate the objective function of (15) with a quadratic minimization problem at each step.

Define $\mathcal{J}^m(\alpha, \beta) := \mathbf{P}(S(\alpha), S^m(\alpha^m))^T \beta + \overline{P}(S^m(\alpha^m)) - f^m(Y)$ so that the last term in (15) is simply $\frac{1}{2\sigma_p^2} \|\mathcal{J}^m(\alpha, \beta)\|_2^2$. Then we compute a minimizing sequence $(\alpha_{(j)}, \beta_{(j)})_{j=1}^\infty$ given by the scheme

$$(16) \quad \begin{aligned} (\alpha_{(j+1)}, \beta_{(j+1)}) = & \arg \min_{\alpha \in (\mathbb{R}^{QK})^M, \beta \in \mathbb{R}^{MK}} \beta^T \mathbf{P}(S(\alpha_{(j)}), S(\alpha_{(j)})) \beta + \sum_{m=1}^M \left[\lambda (\alpha^m)^T \mathbf{U}(\phi, \phi) \alpha^m \right. \\ & + \frac{1}{2\sigma_u^2} \|\mathbf{U}(\phi, Y^m)^T \alpha^m - u^m(Y^m)\|_2^2 + \frac{1}{2\sigma_p^2} \left\| \mathcal{J}^m(\alpha_{(j)}, \beta_{(j)}) + \nabla \mathcal{J}^m(\alpha_{(j)}, \beta_{(j)}) \begin{pmatrix} \alpha - \alpha_{(j)} \\ \beta - \beta_{(j)} \end{pmatrix} \right\|_2^2 \\ & \left. + \lambda_{(j)} \left[(\beta - \beta_{(j)})^T \mathbf{P}(S(\alpha_{(j)}), S(\alpha_{(j)})) (\beta - \beta_{(j)}) + \sum_{m=1}^M (\alpha^m - \alpha_{(j)}^m)^T \mathbf{U}(\phi, \phi) (\alpha^m - \alpha_{(j)}^m) \right] \right]. \end{aligned}$$

The first two terms are identical to (15) with α fixed at the previous value $\alpha_{(j)}$, the third term is unchanged, and the fourth term is a local quadratic approximation obtained by linearizing \mathcal{J}^m with $\nabla \mathcal{J}^m$ denoting the Jacobian. The last term acts as a damping term that ensures that our next estimate $(\alpha_{(j+1)}, \beta_{(j+1)})$ does not deviate too far from the current values. The $\lambda_{(j)} > 0$ is inversely proportional to a step-size parameter which is updated using a standard gain ratio heuristic that compares the decrease produced in the true objective to the decrease observed in the quadratic approximation; see SI C.

We highlight that while naive implementation of (16) leads to an effective algorithm, the computational cost due to kernel matrices $\mathbf{P}(S, S)$ and $\mathbf{U}(\phi, \phi)$ can become prohibitive when N, M are large. To address these bottlenecks we implement different computation techniques such as Nyström approximations and block matrix inversion. We will not discuss these details here but refer the reader to SI C or our Github repository ⁴. Instead, we will present an efficient relaxation of 1-step KEqL using a reduced basis that has good performance in many practical cases.

⁴<https://github.com/TADSGroup/kernelequationlearning>

4.2.2. *Reduced 1-step KEqL: an efficient approximation.* We now introduce an approximate 1-step KEqL that, at a small cost to accuracy, leads to a better conditioned and more efficient formulation. To this end, we propose to approximate (15) by restricting the v^m 's to the subspace $\text{span}\{\mathbf{U}(y_1, \cdot), \dots, \mathbf{U}(y_K, \cdot)\} \subset \mathcal{U}$, i.e., we write $v^m = \mathbf{U}(Y, \cdot)^T \alpha^m$ for $\alpha^m \in \mathbb{R}^K$ as opposed to \mathbb{R}^{QK} for 1-step KEqL. Thus this reformulation effectively constitutes a reduced basis/feature map formulation leading to the following analogous problem:

$$(17) \quad \begin{aligned} (\widehat{\alpha}, \widehat{\beta}) = & \arg \min_{\alpha \in (\mathbb{R}^K)^M, \beta \in \mathbb{R}^{MK}} \beta^T \mathbf{P}(S(\alpha), S(\alpha)) \beta + \sum_{m=1}^M \lambda(\alpha^m)^T \mathbf{U}(Y, Y) \alpha^m \\ & + \frac{1}{2\sigma_u^2} \|\mathbf{U}(Y, Y^m)^T \alpha^m - u^m(Y^m)\|_2^2 + \frac{1}{2\sigma_P^2} \|\mathbf{P}(S(\alpha), S^m(\alpha^m))^T \beta + \overline{P}(S^m(\alpha^m) - f^m(Y))\|_2^2, \end{aligned}$$

with $S(\alpha) = \cup_{m=1}^M S^m(\alpha^m)$ as before but with $S^m(\alpha^m) = \Phi(\mathbf{U}(Y, \cdot)^T \alpha^m, Y)$.

Observe that if we take $Y^m = Y$ for all m then the first constraint above completely identifies the α^m and the reduced 1-step KEqL coincides with 2-step KEqL. Therefore this method interpolates between the 1-step and 2-step methods. Furthermore, we can apply the same idea to the $\mathbf{P}(S, s)$ feature maps and choose a reduced basis for representing the learned equation \widehat{P} by, for example, subsampling the points in S in (17). Regardless, the LM algorithm of Section 4.2.1 remains applicable here.

4.3. **Choosing kernels and hyper-parameters.** While the 1- and 2-step KEqL are generic and well-defined for any choice of \mathbf{P} and \mathbf{U} (assuming sufficient regularity), the practical performance of these algorithms is closely tied to a good choice of kernels as is often the case for kernel/GP methods. Broadly speaking, the choice of these kernels imposes constraints on our model classes for the functions \widehat{u}^m and the learned PDE \widehat{P} ; in the case of the latter the choice of \mathbf{P} is analogous to choosing dictionaries in SINDy. Moreover, in many applications we may have access to expert knowledge about the u^m and the type of PDE at hand. In such scenarios it is helpful to design our kernels to reflect such prior knowledge. A standard example is periodic boundary conditions or invariance of the solution to the PDE under certain symmetries and operators. Below we discuss some instances of such kernels that are useful for prototypical PDEs that we study in Section 5.

4.3.1. *Choosing \mathbf{U} .* Since Sobolev spaces are a natural solution space for many PDEs we choose the Matérn kernel family for \mathbf{U} . In particular, we consider the anisotropic Matérn kernels:

$$\mathbf{U}_{\text{Matérn}}(y, y') := \frac{2^{1-\nu}}{\Gamma(\nu)} \left(\sqrt{2\nu} \|y - y'\|_{\Sigma} \right)^{\nu} K_{\nu} \left(\sqrt{2\nu} \|y - y'\|_{\Sigma} \right), \quad \forall y, y' \in \mathcal{Y},$$

where $\nu > 0$ is a parameter, Γ is the standard gamma function, and K_{ν} is the modified Bessel function of the second kind, and $\|y - y'\|_{\Sigma}^2 := (y - y')^T \Sigma^{-1} (y - y')$ for a PDS matrix $\Sigma \in \mathbb{R}^{d \times d}$.

It is known (see [48, Ex. 2.6, 2.8]) that under mild conditions, the RKHS of the Matérn kernel is norm equivalent to the Sobolev space $H^{\nu+d/2}$. Due to this equivalence it is crucial that the regularity parameter ν is chosen carefully in light of the order of the PDE. In the limit $\nu \rightarrow \infty$ the Matérn kernel converges to the radial basis function (RBF) kernel $\mathbf{U}_{\text{RBF}}(y, y') := \exp(-\frac{1}{2} \|y - y'\|_{\Sigma}^2)$ which has an infinitely smooth RKHS. In addition to this kernel we also use the first order rational quadratic (RQ) kernel, defined as $\mathbf{U}_{\text{RQ}}(y, y') := (1 + \|y - y'\|_{\Sigma}^2)^{-1}$. We often take Σ to be a diagonal matrix $\Sigma = \text{diag}(\gamma)$ for a vector of lengthscales $\gamma \in \mathbb{R}_{>0}^d$ to be chosen via maximum likelihood estimation (MLE), or hand tuned; standard cross validation techniques can also be utilized.

4.3.2. *Choosing \mathbf{P} .* Following the observation that many PDEs that arise in physical sciences have polynomial nonlinearities [29, Sec. 1.2], a natural choice for \mathbf{P} would be a polynomial kernel; this is also the dominant model for construction of dictionaries in SINDy-type algorithms. Here we consider $\mathbf{P}_{\text{poly}}(s, s') = ((s - c)^T B (s' - c) + 1)^{\text{deg}}$, for $s, s' \in \mathbb{R}^{Q+d}$, where $B \in \mathbb{R}^{Q+d \times Q+d}$ is a matrix akin to Σ in the previous section that allows us to scale different input coordinates or to introduce correlations, and $c \in \mathbb{R}^{Q+d}$ is a fixed vector introducing bias. We treat B, c as hyper-parameters for this kernel. In extreme scenarios, if no a priori knowledge about P exists, then one can take \mathbf{P} to be a Matérn or RBF kernel as in the case of \mathbf{U} above.

We are particularly interested in learning PDEs with variable coefficients, such as the variable coefficient diffusion model (3). In such cases we may have a priori knowledge that P has polynomial dependence on a subset of inputs (the $L_1 u(y), \dots, L_Q u(y)$ values) but general nonlinear dependence on other parameters (the y values). We encode such structures using hybrid product kernels of the form $\mathbf{P}_{\text{hybrid}}(s, s') = \mathbf{P}_{\text{RBF}}(s_{:d}, s'_{:d}) \mathbf{P}_{\text{poly}}(s_d, s'_d)$ where we used $s_{:d} \in \mathbb{R}^d$ to denote the first d coordinates of s and $s_d \in \mathbb{R}^Q$ to denote the remaining coordinates.

5. EXPERIMENTS

We now present a series of numerical experiments that demonstrate the performance of our 1-step and 2-step methodologies for the tasks of filtering the functions u^m , learning differential operators \mathcal{P} , and their solution operators \mathcal{P}^{-1} . Our examples span a wide range of problems from ODE models to PDEs with variable coefficients. For

benchmarking we compare our algorithms with SINDy [91], as a 2-step dictionary based algorithm, and the PINN-SR method of [21] as a 1-step neural net based algorithm. Here we focus on the key points regarding each experiment and postpone more results and details to SI D.

5.1. Common structure. In all of our experiments we will consider scalar valued differential equations of the form (2) under the assumption that the map Φ (equivalently the differential operators L_q) is known. In the case of dynamic models we assume $\mathcal{Y} = (0, T] \times \Omega$ for some $T > 0$ and a spacial domain Ω and take $\bar{P}(\Phi(u, y)) = \bar{P}(\Phi(u, (t, x))) = \partial_t^n u(t, x)$ to be known (the order n will be clarified for each example). Since for practical experiments we use RKHSs \mathcal{U} that do not automatically satisfy the boundary conditions of the PDEs we use additional observation points on the boundaries to impose those conditions. To this end, we write $N_{\mathcal{Y}}$ to denote the number of observation points in the interior of \mathcal{Y} while we use $N_{\partial\mathcal{Y}}$ to denote the number of observation points on the boundary, so that the total number of observation points is always $N = N_{\mathcal{Y}} + N_{\partial\mathcal{Y}}$.

For all experiments we consider training data of the form $(u^m(Y^m), f^m)_{m=1}^M$. In addition to the collocation points Y and the observation points Y^m , we also consider an independent test mesh $Y_{\text{test}} \subset \Gamma$ which will be used for reporting errors. We will consider three types of test errors:

- The *filtering error* quantifies the relative accuracy of the \hat{u}^m compared to the training data,

$$\mathcal{R}_{\text{filter}}((u^m)_{m=1}^M) := \frac{1}{M} \sum_{m=1}^M \frac{\|u^m(Y_{\text{test}}) - \hat{u}^m(Y_{\text{test}})\|_2^2}{\|u^m(Y_{\text{test}})\|_2^2}.$$

- The *equation learning error* quantifies the relative accuracy of \hat{P} over a set of functions \mathcal{W}

$$\mathcal{R}_{\text{eqL}}(\mathcal{W}) := \frac{1}{|\mathcal{W}|} \sum_{w \in \mathcal{W}} \frac{\|\mathcal{P}(w)(Y_{\text{test}}) - \hat{\mathcal{P}}(w)(Y_{\text{test}})\|_2^2}{\|\mathcal{P}(w)(Y_{\text{test}})\|_2^2},$$

where $|\mathcal{W}|$ denotes the cardinality of \mathcal{W} .

- The *operator learning error* is defined akin to the equation learning error except that it quantifies the error of the solution map corresponding to the learned equation,

$$\mathcal{R}_{\text{opl}}(\mathcal{W}) := \frac{1}{|\mathcal{W}|} \sum_{w \in \mathcal{W}} \frac{\|\mathcal{P}^{-1}(w)(Y_{\text{test}}) - \hat{\mathcal{P}}^{-1}(w)(Y_{\text{test}})\|_2^2}{\|\mathcal{P}^{-1}(w)(Y_{\text{test}})\|_2^2},$$

where $\hat{\mathcal{P}}^{-1}(w)$ is defined in (11). We highlight that \mathcal{W} constitutes initial or boundary conditions as well as source terms depending on the problem at hand.

For different experiments we report errors with \mathcal{W} taken to be: the training data (training); an in-distribution test set (ID); or out-of-distribution test sets (OOD).

5.2. The Duffing oscillator. In this example we compared the performance of 1-step and 2-step KEqL along with SINDy for learning a 1D nonlinear ODE. Our focus is on filtering and extrapolation/forecasting performance.

5.2.1. Problem setup. Consider $\mathcal{Y} = (0, 50)$ and the Duffing ODE

$$(18) \quad \mathcal{P}(u) = \partial_t^2 u - 3u + 3u^3 + 0.2\partial_t u = \cos(2t), \quad t \in \mathcal{Y}, \quad \text{s.t.} \quad u(0) = \partial_t u(0) = 0.$$

To generate the training data we solved the ODE numerically using a traditional adaptive solver. The numerical solution was then subsampled on the observation points that were also picked on a uniform grid; see Figure 2 (A). In this example we chose $M = 1$, and so we aim to learn the ODE and its solution from observations of a single trajectory. The test data sets were generated similarly but on a finer uniform mesh with different initial conditions.

5.2.2. Algorithm setup. We chose the collocation points Y to be a fine uniform grid in \mathcal{Y} . We further chose the operators $L_1 = \text{Id} : u \mapsto u$, $L_2 : u \mapsto \partial_t u$, and $\bar{P}u = \partial_t^2 u$. As for kernels we chose \mathbf{U} to be a rational quadratic kernel while we chose \mathbf{P} to be RBF. In this example we compared 1-step and 2-step KEqL with SINDy. To approximate the derivatives in SINDy we used the same kernel interpolant as 2-step KEqL. For the SINDy dictionary we chose all polynomial terms of up to third degree in the variables $\{1, u, \partial_t u\}$; we empirically found this dictionary to give the best training and test errors for both SINDy and KEqL.

5.2.3. Results. We present a summary of our numerical results for this example in Figure 2; further details and additional results can be found in SI D. In Figure 2(A) we visually compare the quality of the filtered solution \hat{u} for 1-step and 2-step KEqL. We clearly see that 1-step KEqL is superior in filtering the solution. This visual performance is further confirmed in Figure 2(B) where we observe an order of magnitude improvement between 1-step and 2-step methods in terms of relative errors.

For our next test we considered simulating the learned ODE with new initial conditions, this is essentially an extrapolation problem where we try to predict the state of the system outside of the window of observations. We

show three examples of random initial conditions in Figure 2(C), comparing the solutions computed using 1- and 2-step KEqL and SINDy. We visually observe that the 1-step method generally tracks the true solution for a longer time interval (although all solutions eventually diverge). The superior performance of 1-step KEqL is also evident in panel (B) where we use \mathcal{R}_{opl} to denote the pointwise error between the extrapolated solutions and the true states. Once again we observe an order of magnitude improvement between 1-step and 2-step methods although the performance gap is smaller for larger time windows as expected.

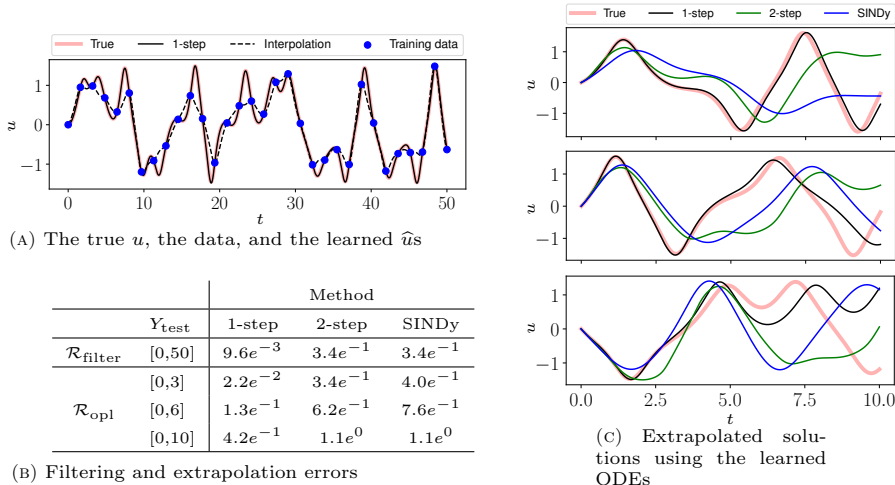


FIGURE 2. Representative numerical results for the Duffing oscillator (18): (A) Shows the training data and the ground truth state of the system u in comparison to the filtered state \hat{u} using 1-step KEqL and 2-step methods; (B) Quantitative values of relative filtering and operator learning errors. The operator learning errors are reported for different time windows and essentially constitute extrapolation errors. These values were averaged over three novel initial conditions; (C) visualization of three extrapolated dynamics used to compute \mathcal{R}_{opl} .

5.3. The Burgers' PDE. In this example we compared 1-step KEqL with SINDy and the PINN-SR algorithm of [21]; we consider the latter as a direct 1-step competitor for KEqL and compare errors for learning PDEs, filtering the solution, and operator learning in various scarce data settings.

5.3.1. Problem setup. Here we take $\mathcal{Y} = (0, 1] \times (0, 1)$ and consider the Burgers' PDE

$$(19) \quad \mathcal{P}(u) = \partial_t u + \nu u \partial_x u - \nu \partial_{xx} u = 0 \text{ for } (t, x) \in \mathcal{Y}, \quad \text{s.t. } u(0, x) = u_0(x), \text{ and } u(t, 0) = u(t, 1) = 0.$$

In all experiments we took $M = 1$ so that a single solution is observed on a scarce set of observations. These solutions were generated by prescribing the initial conditions u_0 and then solving the PDE using a traditional numerical solver on a fine mesh. The observed data was then subsampled from a set of Chebyshev collocation points that were also used in the implementation of all algorithms.

5.3.2. Algorithm setup. We took $L_1 : u \mapsto u$, $L_2 : u \mapsto \partial_x u$, $L_3 : u \mapsto \partial_x^2 u$ and also $\overline{\mathcal{P}}(u) = \partial_t u$. \mathbf{U} was taken to be RBF and \mathbf{P} was a polynomial kernel of degree 2. To approximate the derivatives for SINDy we used the same RBF kernel used in KEqL and the dictionary terms were polynomial features $\{1, u, \partial_x u, \partial_x^2 u\}$; we found that this dictionary gave the best results for SINDy. For the PINN-SR method we used the same dictionary for P along with a feed-forward neural network with 8 layers and width 20 to approximate u .

5.3.3. Results. We begin by considering the filtering and equation learning errors for one-shot learning of Burgers'. These results are shown in the top row of Figure 3(A) where we are reporting the errors for a fixed smooth initial condition with different number of observation points. Note, these errors were computed over the training data but they are different from the training error of the algorithm as they compare the filtered solution and the learned PDE on the test mesh Y_{test} . Since the observation points are random we are reporting the average errors along with the best and worst errors over different runs giving the shaded regions. We found that 1-step KEqL leads to the best filtering errors with a wider performance gap when N_y is small. Interestingly, the performance gap appears to be more pronounced in the equation learning case where we observed an order of magnitude improvement over SINDy and almost two orders improvement over PINN-SR. We observed significantly larger errors for PINN-SR here which we attribute to difficulties in tuning and optimizing PINN models. In fact, we could often bring these errors down by

hand tuning the algorithm in each instance of the experiments but automatic strategies proposed in [21] appeared to be very sensitive to the location of observation points. This issue was exacerbated further when experimenting with randomized initial conditions; see SI D.

In Figure 3(B, C) we show two enlightening examples that show the difference in performance of 1-step methods vs 2-step. In (B) we hand picked an initial condition that leads to a solution with multiple (near) shocks. We see that despite scarcity of observations, 1-step KEqL and PINN-SR are able to capture the general shape of the solution while 2-step methods are significantly worse. In (C) we show an instance where we only observed the value of the solution on the boundary of the domain while in row (D) we solved the learned equation for a new initial condition. Once again we see that 1-step methods give better performance for filtering, however, when solving the learned PDE a noticeable performance gap appears across the three methods with 1-step KEqL giving the best solution. This example further reflects the performance gaps observed in panel (A), with the equation learning performance gaps being more pronounced compared to filtering.

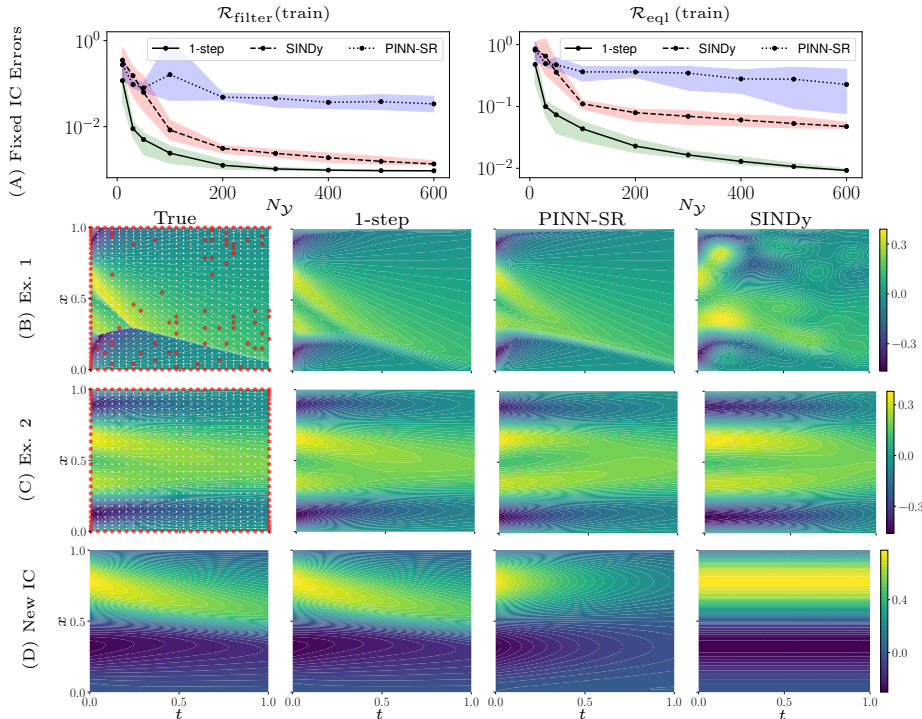


FIGURE 3. Representative numerical results for Burgers’ PDE (19): (A) The filtering and equation learning errors computed for the training functions for 1-step KEqL, SINDy, and PINN-SR using $M = 1$ training pairs with different number of interior observations N_y ; (B) An example application for an initial condition that leads to multiple shocks with scarce observations depicting the quality of filtering obtained using 1-step and 2-step methods; (C) Similar setup to row (B) with a smooth solution that is only observed on the boundary; (D) Depicting the solution to the PDEs that were learned in row (C) for a new initial condition.

5.4. Darcy’s flow PDE. In this example we performed a systematic study of the performance of 1-step (its reduced version) and 2-step KEqL for learning an elliptic PDE with a variable diffusion coefficient. In particular, we investigate the ID and OOD performance in terms of filtering, equation learning, and operator learning.

5.4.1. *Problem setup.* Here we take $\mathcal{Y} = (0, 1) \times (0, 1)$ and consider the problem

$$(20) \quad \mathcal{P}(u) = \text{div}(a\nabla u) = f(x) \text{ with } a(x) = \exp(\sin(\cos(x_1) + \cos(x_2))), \text{ for } x \in \mathcal{Y}, \text{ and } u(x) = g(x), \text{ for } x \in \partial\mathcal{Y}.$$

To generate the training data we drew functions u from a smooth GP and took $f = \mathcal{P}(u)$, also considering the value of u at $\partial\mathcal{Y}$ as the boundary condition. Each u was then subsampled on the observation points that were picked randomly in the interior of a uniform collocation grid where the PDE was enforced. The test data sets were generated similarly, with the OOD data drawn from a GP with a different length scale.

5.4.2. *Algorithm setup.* We picked the operators $L_1 : u \mapsto u$, $L_2 : u \mapsto \partial_{x_1} u$, $L_3 : u \mapsto \partial_{x_1}^2 u$, $L_4 : u \mapsto \partial_{x_2} u$, $L_5 : u \mapsto \partial_{x_2}^2 u$, $L_6 : u \mapsto \partial_{x_1 x_2} u$ and $\bar{P} \equiv 0$. We used $\mathbf{U} = \mathbf{U}_{\text{RBF}}$ for learning u and \mathbf{P} was a hybrid polynomial kernel as the product of an RBF for the spatial variables and a polynomial kernel of first degree for the rest of the variables. For all experiments we employed the reduced 1-step KEqL along with additional sparse numerical linear algebra tricks (see SI C) to scale the algorithms to large training data sizes.

5.4.3. *Results.* Figure 4 summarizes various training and test errors for this example focusing on equation learning and operator learning errors. These results were computed using randomly sampled solutions pairs and observation points. The black lines represent the average errors, while the shaded regions indicate the range of errors, spanning from the worst to the best across multiple runs.; see SI D for more details.

We observed that the reduced 1-step method consistently outperformed the 2-step method across all tasks both ID and OOD. Most notably, in very scarce observation regime (only $N_{\mathcal{Y}} = 2$ interior observations per function) we see an order of magnitude performance gap between 1-step and 2-step methods across the board. As expected, the gap reduces as we increase the observations $N_{\mathcal{Y}}$ and the size of the training data M . Finally, we note that the operator learning errors follow the same trends as the equation learning errors which suggests that ID operator learning should inherit similar rates as ID equation learning. This fact was also shown theoretically in SI B.3 under strong assumptions on the true PDE \mathcal{P} .

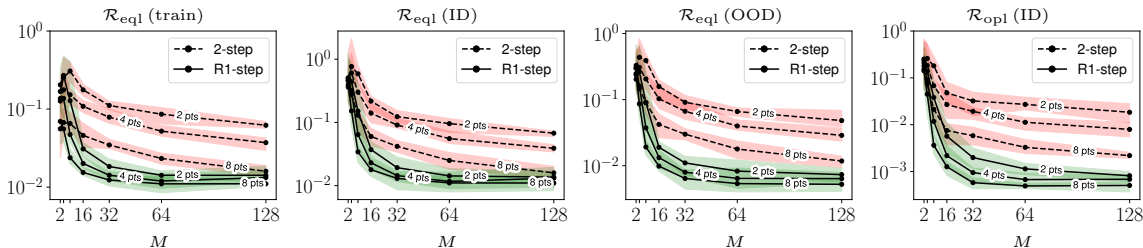


FIGURE 4. Representative numerical results for Darcy’s flow PDE (20): The first three figures from the left show the equation learning errors computed over training, ID test, and OOD test data while the last panel shows the ID operator learning errors. R1-step here denotes the reduced 1-step KEqL method and the labels on the graphs denote the number of interior observations points $N_{\mathcal{Y}}$.

6. DISCUSSION

In conclusion, we presented the 1- and 2-step formulations of KEqL as an algorithm for learning nonlinear PDEs as well as their solution operators and filtering of observed states in scarce data regimes. Our theoretical results provided quantitative error bounds and convergence rates for our algorithms while our numerical experiments demonstrated significant gains in accuracy compared to existing methods in the literature. Additionally, our exposition unifies various problems of interest to scientific machine learning under the same umbrella, i.e., equation learning, operator learning, and PDE solvers, all viewed as optimal recovery problems.

Various avenues of future research and extensions of the KEqL framework can be identified: (a) we outlined KEqL for a single PDE but its extension to systems of PDEs is an obvious next step since many physical processes of interest are governed by systems of equations; (b) our approach to operator learning, after the deployment of KEqL, relies on a PDE solver for each evaluation of $\widehat{\mathcal{P}}^\dagger$ which can be expensive. Therefore it may be interesting to investigate the emulation of this process to obtain a cheap solver that can be deployed for real time predictions; (c) In many of our experimental results we observed very competitive accuracy for 1-step KEqL, however, we still observed a relative error barrier (around 10^{-2} in Figure 4) which is not in line with our theoretical guarantees, we suspect these issues may arise due to ill-conditioning of the problems and various approximations made in the algorithms in order to scale the computations; (d) While our theoretical analysis addresses asymptotic convergence rates it does not apply to scarce data regimes where indeed we do not have small fill-distances, at least not in the physical domain \mathcal{Y} , and so a non-asymptotic analysis that justifies the scarce-data performance of KEqL would be of great interest.

ACKNOWLEDGEMENTS

JFOR, AH and BH were supported by the National Science Foundations grants DMS-2208535 ”Machine Learning for Inverse Problems” and DMS-2337678 ”Gaussian Processes for Scientific Machine Learning: Theoretical Analysis and Computational Algorithms”. YJ and HO acknowledge support from the Air Force Office of Scientific Research under MURI awards number FA9550-20-1-0358 (Machine Learning and Physics-Based Modeling and Simulation), FOA-AFRL-AFOSR-2023-0004 (Mathematics of Digital Twins), by the Department of Energy under award number DE-SC0023163 (SEA-CROGS: Scalable, Efficient, and Accelerated Causal Reasoning Operators, Graphs and Spikes

for Earth and Embedded Systems) and by the National Science Foundations under award number 2425909 (Discovering the Law of Stress Transfer and Earthquake Dynamics in a Fault Network using a Computational Graph Discovery Approach). Additionally, HO acknowledges support from the DoD Vannevar Bush Faculty Fellowship Program.

REFERENCES

- [1] R. A. Adams and J. J. Fournier. *Sobolev Spaces*. Elsevier, 2003.
- [2] A. Y. Aravkin, R. Baraldi, and D. Orban. A levenberg–marquardt method for nonsmooth regularized least squares. *SIAM Journal on Scientific Computing*, 46(4):A2557–A2581, 2024.
- [3] R. Arcangéli, M. C. López de Silanes, and J. J. Torrens. An extension of a bound for functions in Sobolev spaces, with applications to (m, s) -spline interpolation and smoothing. *Numerische Mathematik*, 107(2):181–211, 2007.
- [4] K. J. Åström and P. Eykhoff. System identification—a survey. *Automatica*, 7(2):123–162, 1971.
- [5] Y. Bar-Shalom, X. R. Li, and T. Kirubarajan. *Estimation with applications to tracking and navigation: theory algorithms and software*. John Wiley & Sons, 2004.
- [6] P. Batlle, M. Darcy, B. Hosseini, and H. Owhadi. Kernel methods are competitive for operator learning. *Journal of Computational Physics*, 496:112549, 2024.
- [7] P. Batlle, Y. Chen, B. Hosseini, H. Owhadi, and A. M. Stuart. Error analysis of kernel/gp methods for nonlinear and parametric pdes. *Journal of Computational Physics*, 520:113488, 2025.
- [8] A. Berlinet and C. Thomas-Agnan. *Reproducing kernel Hilbert spaces in probability and statistics*. Springer Science & Business Media, 2011.
- [9] T. Berry and S. Das. Limits of learning dynamical systems. *SIAM Review*, 67(1):107–137, 2025.
- [10] K. Bhattacharya, B. Hosseini, N. B. Kovachki, and A. M. Stuart. Model reduction and neural networks for parametric pdes. *The SMAI journal of computational mathematics*, 7:121–157, 2021.
- [11] J. Bongard and H. Lipson. Automated reverse engineering of nonlinear dynamical systems. *Proceedings of the National Academy of Sciences of the United States of America*, 104:9943–8, 07 2007.
- [12] G.-J. Both, S. Choudhury, P. Sens, and R. Kusters. Deepmod: Deep learning for model discovery in noisy data. *Journal of Computational Physics*, 428:109985, 2021.
- [13] N. Boullé, S. Kim, T. Shi, and A. Townsend. Learning green’s functions associated with time-dependent partial differential equations. *Journal of Machine Learning Research*, 23(218):1–34, 2022.
- [14] N. Boullé, D. Halikias, and A. Townsend. Elliptic pde learning is provably data-efficient. *Proceedings of the National Academy of Sciences*, 120(39):e2303904120, 2023.
- [15] N. Boullé and A. Townsend. Chapter 3 - a mathematical guide to operator learning. In S. Mishra and A. Townsend, editors, *Numerical Analysis Meets Machine Learning*, volume 25 of *Handbook of Numerical Analysis*, pages 83–125. Elsevier, 2024.
- [16] T. Bourdais, P. Batlle, X. Yang, R. Baptista, N. Rouquette, and H. Owhadi. Codiscovering graphical structure and functional relationships within data: A gaussian process framework for connecting the dots. *Proceedings of the National Academy of Sciences*, 121(32):e2403449121, 2024.
- [17] S. L. Brunton, J. L. Proctor, and J. N. Kutz. Discovering governing equations from data by sparse identification of nonlinear dynamical systems. *Proceedings of the National Academy of Sciences*, 113(15):3932–3937, 2016.
- [18] Y. Chen, B. Hosseini, H. Owhadi, and A. M. Stuart. Solving and learning nonlinear pdes with gaussian processes. *Journal of Computational Physics*, 447:110668, 2021. ISSN 0021-9991.
- [19] Y. Chen, E. N. Epperly, J. A. Tropp, and R. J. Webber. Randomly pivoted cholesky: Practical approximation of a kernel matrix with few entry evaluations. *Communications on Pure and Applied Mathematics*, 2023.
- [20] Y. Chen, H. Owhadi, and F. Schäfer. Sparse cholesky factorization for solving nonlinear pdes via gaussian processes. *Mathematics of Computation*, 2024.
- [21] Z. Chen, Y. Liu, and H. Sun. Physics-informed learning of governing equations from scarce data. *Nature communications*, 12(1):6136, 2021.
- [22] O. A. Chkrebtii, D. A. Campbell, B. Calderhead, and M. A. Girolami. Bayesian solution uncertainty quantification for differential equations. *Bayesian Analysis*, 11(4):1239–1267, 2016.
- [23] J. Cockayne, C. Oates, T. Sullivan, and M. Girolami. Probabilistic numerical methods for PDE-constrained Bayesian inverse problems. In *AIP Conference Proceedings*, volume 1853, page 060001, 2017.
- [24] J. Cockayne, C. J. Oates, T. J. Sullivan, and M. Girolami. Bayesian probabilistic numerical methods. *SIAM Review*, 61(4):756–789, 2019.
- [25] M. Darcy, B. Hamzi, J. Susiluoto, A. Braverman, and H. Owhadi. Learning dynamical systems from data: a simple cross-validation perspective, part ii: nonparametric kernel flows. 2021.
- [26] M. Darcy, B. Hamzi, G. Livieri, H. Owhadi, and P. Tavallali. One-shot learning of stochastic differential equations with data adapted kernels. *Physica D: Nonlinear Phenomena*, 444:133583, 2023.
- [27] T. De Ryck and S. Mishra. Generic bounds on the approximation error for physics-informed (and) operator learning. *Advances in Neural Information Processing Systems*, 35:10945–10958, 2022.

- [28] H. W. Engl, M. Hanke, and A. Neubauer. *Regularization of inverse problems*, volume 375. Springer Science & Business Media, 1996.
- [29] L. C. Evans. *Partial differential equations*. American Mathematical Society, 2022.
- [30] U. Fasel, J. N. Kutz, B. W. Brunton, and S. L. Brunton. Ensemble-sindy: Robust sparse model discovery in the low-data, high-noise limit, with active learning and control. *Proceedings of the Royal Society A*, 478(2260): 20210904, 2022.
- [31] G. F. Franklin, J. D. Powell, A. Emami-Naeini, and J. D. Powell. *Feedback control of dynamic systems*, volume 4. Prentice hall Upper Saddle River, 2002.
- [32] R. Frigola, Y. Chen, and C. E. Rasmussen. Variational gaussian process state-space models. *Advances in neural information processing systems*, 27, 2014.
- [33] H. P. Gavin. The levenberg-marquardt algorithm for nonlinear least squares curve-fitting problems. *Department of Civil and Environmental Engineering Duke University August*, 3:1–23, 2019.
- [34] Z. Ghahramani and S. Roweis. Learning nonlinear dynamical systems using an em algorithm. *Advances in neural information processing systems*, 11, 1998.
- [35] R. G. Ghanem and P. D. Spanos. *Stochastic finite elements: a spectral approach*. Dover Publications, 2003.
- [36] T. Glad and L. Ljung. *Control theory*. CRC press, 2018.
- [37] S. Goswami, A. Bora, Y. Yu, and G. E. Karniadakis. Physics-informed deep neural operator networks. In *Machine Learning in Modeling and Simulation: Methods and Applications*, pages 219–254. Springer, 2023.
- [38] E. Haber and D. Oldenburg. Joint inversion: a structural approach. *Inverse problems*, 13(1):63, 1997.
- [39] E. Haber, U. M. Ascher, and D. Oldenburg. On optimization techniques for solving nonlinear inverse problems. *Inverse problems*, 16(5):1263, 2000.
- [40] B. Hamzi and H. Owhadi. Learning dynamical systems from data: a simple cross-validation perspective, part i: parametric kernel flows. *Physica D: Nonlinear Phenomena*, 421:132817, 2021.
- [41] B. Hamzi, H. Owhadi, and Y. Kevrekidis. Learning dynamical systems from data: A simple cross-validation perspective, part iv: case with partial observations. *Physica D: Nonlinear Phenomena*, page 133853, 2023.
- [42] Y. He, H. Zhao, and Y. Zhong. How much can one learn a partial differential equation from its solution? *Foundations of Computational Mathematics*, 24(5):1595–1641, 2024.
- [43] S. M. Hirsh, D. A. Barajas-Solano, and J. N. Kutz. Sparsifying priors for bayesian uncertainty quantification in model discovery. *Royal Society Open Science*, 9(2):211823, 2022.
- [44] S. I. Kabanikhin. *Inverse and Ill-posed Problems: Theory and Applications*, volume 55. Walter de Gruyter, 2011.
- [45] J. Kaipio and E. Somersalo. *Statistical and computational inverse problems*, volume 160. Springer Science & Business Media, 2006.
- [46] B. Kaltenbacher. Regularization based on all-at-once formulations for inverse problems. *SIAM Journal on Numerical Analysis*, 54(4):2594–2618, 2016.
- [47] B. Kaltenbacher. All-at-once versus reduced iterative methods for time dependent inverse problems. *Inverse Problems*, 33(6):064002, 2017.
- [48] M. Kanagawa, P. Hennig, D. Sejdinovic, and B. K. Sriperumbudur. Gaussian processes and kernel methods: A review on connections and equivalences. arxiv:1807.02582, 2018.
- [49] S. H. Kang, W. Liao, and Y. Liu. Ident: Identifying differential equations with numerical time evolution. *Journal of Scientific Computing*, 87(1):1–27, 2021.
- [50] G. E. Karniadakis, I. G. Kevrekidis, L. Lu, P. Perdikaris, S. Wang, and L. Yang. Physics-informed machine learning. *Nature Reviews Physics*, 3(6):422–440, 2021.
- [51] K. J. Keesman. *System identification: an introduction*. Springer Science & Business Media, 2011.
- [52] M. C. Kennedy and A. O’Hagan. Bayesian calibration of computer models. *Journal of the Royal Statistical Society: Series B (Statistical Methodology)*, 63(3):425–464, 2001.
- [53] G. Kimeldorf and G. Wahba. Some results on Tchebycheffian spline functions. *Journal of mathematical analysis and applications*, 33(1):82–95, 1971.
- [54] G. S. Kimeldorf and G. Wahba. A correspondence between Bayesian estimation on stochastic processes and smoothing by splines. *Annals of Mathematical Statistics*, 41:495–502, 1970. ISSN 0003-4851.
- [55] B. C. Koenig, S. Kim, and S. Deng. Kan-odes: Kolmogorov–arnold network ordinary differential equations for learning dynamical systems and hidden physics. *Computer Methods in Applied Mechanics and Engineering*, 432:117397, 2024.
- [56] N. B. Kovachki, S. Lanthaler, and A. M. Stuart. Chapter 9 - operator learning: Algorithms and analysis. In S. Mishra and A. Townsend, editors, *Numerical Analysis Meets Machine Learning*, volume 25 of *Handbook of Numerical Analysis*, pages 419–467. Elsevier, 2024.
- [57] A. Krishnapriyan, A. Gholami, S. Zhe, R. Kirby, and M. W. Mahoney. Characterizing possible failure modes in physics-informed neural networks. *Advances in neural information processing systems*, 34:26548–26560, 2021.

- [58] K. Lahouel, M. Wells, V. Rielly, E. Lew, D. Lovitz, and B. M. Jedynek. Learning nonparametric ordinary differential equations from noisy data. *Journal of Computational Physics*, 507:112971, 2024.
- [59] K. Law, A. Stuart, and K. Zygalakis. Data assimilation. *Cham, Switzerland: Springer*, 214:52, 2015.
- [60] Q. T. Le Gia, F. J. Narcowich, J. D. Ward, and H. Wendland. Continuous and discrete least-squares approximation by radial basis functions on spheres. *Journal of Approximation Theory*, 143(1):124–133, 2006.
- [61] J. Lee, E. De Brouwer, B. Hamzi, and H. Owhadi. Learning dynamical systems from data: A simple cross-validation perspective, part iii: Irregularly-sampled time series. *Physica D: Nonlinear Phenomena*, 443:133546, 2023.
- [62] F. Leibfried, V. Dutordoir, S. John, and N. Durrande. A tutorial on sparse gaussian processes and variational inference. *arXiv preprint arXiv:2012.13962*, 2020.
- [63] Z. Li, N. Kovachki, K. Azizzadenesheli, K. Bhattacharya, A. Stuart, and A. Anandkumar. Fourier neural operator for parametric partial differential equations. In *International Conference on Learning Representations*, 2020.
- [64] Z. Li, H. Zheng, N. Kovachki, D. Jin, H. Chen, B. Liu, K. Azizzadenesheli, and A. Anandkumar. Physics-informed neural operator for learning partial differential equations. *ACM/JMS Journal of Data Science*, 1(3): 1–27, 2024.
- [65] J. Liu and M. West. Combined parameter and state estimation in simulation-based filtering. In *Sequential Monte Carlo methods in practice*, pages 197–223. Springer, 2001.
- [66] L. Ljung. Perspectives on system identification. *Annual Reviews in Control*, 34(1):1–12, 2010.
- [67] D. Long, N. Mrvaljević, S. Zhe, and B. Hosseini. A kernel framework for learning differential equations and their solution operators. *Physica D: Nonlinear Phenomena*, 460:134095, 2024. ISSN 0167-2789.
- [68] Z. Long, Y. Lu, X. Ma, and B. Dong. PDE-net: Learning PDEs from data. In *International Conference on Machine Learning*, pages 3208–3216. PMLR, 2018.
- [69] Z. Long, Y. Lu, and B. Dong. Pde-net 2.0: Learning pdes from data with a numeric-symbolic hybrid deep network. *Journal of Computational Physics*, 399:108925, 2019.
- [70] L. Lu, P. Jin, G. Pang, Z. Zhang, and G. E. Karniadakis. Learning nonlinear operators via deepnet based on the universal approximation theorem of operators. *Nature Machine Intelligence*, 3(3):218–229, 2021.
- [71] D. J. Lucia, P. S. Beran, and W. A. Silva. Reduced-order modeling: new approaches for computational physics. *Progress in aerospace sciences*, 40(1-2):51–117, 2004.
- [72] D. A. Messenger and D. M. Bortz. Weak sindy: Galerkin-based data-driven model selection. *Multiscale Modeling & Simulation*, 19(3):1474–1497, 2021.
- [73] D. A. Messenger and D. M. Bortz. Weak sindy for partial differential equations. *Journal of Computational Physics*, 443:110525, 2021.
- [74] C. Mora, A. Yousefpour, S. Hosseinmardi, H. Owhadi, and R. Bostanabad. Operator learning with gaussian processes. *Computer Methods in Applied Mechanics and Engineering*, 434:117581, 2025.
- [75] C. Moriarty-Osborne and A. L. Teckentrup. Convergence rates of non-stationary and deep gaussian process regression. *arXiv preprint arXiv:2312.07320*, 2023.
- [76] F. J. Narcowich, J. D. Ward, and H. Wendland. Sobolev error estimates and a bernstein inequality for scattered data interpolation via radial basis functions. *Constructive Approximation*, 24:175–186, 2006.
- [77] R. K. Niven, A. Mohammad-Djafari, L. Cordier, M. W. Abel, and M. Quade. Bayesian identification of dynamical systems. In *39th International Workshop on Bayesian Inference and Maximum Entropy Methods in Science and Engineering (MaxEnt 2019)*, volume 33, 2019.
- [78] J. S. North, C. K. Wikle, and E. M. Schliep. A bayesian approach for data-driven dynamic equation discovery. *Journal of Agricultural, Biological and Environmental Statistics*, 27(4):728–747, 2022.
- [79] J. S. North, C. K. Wikle, and E. M. Schliep. A bayesian approach for spatio-temporal data-driven dynamic equation discovery. *Bayesian Analysis*, 1(1):1–30, 2023.
- [80] J. S. North, C. K. Wikle, and E. M. Schliep. A review of data-driven discovery for dynamic systems. *International Statistical Review*, 91(3):464–492, 2023.
- [81] H. Owhadi. Bayesian numerical homogenization. *Multiscale Modeling & Simulation*, 13(3):812–828, 2015.
- [82] H. Owhadi. Computational graph completion. *Research in the Mathematical Sciences*, 9(2):27, 2022.
- [83] H. Owhadi and C. Scovel. *Operator-Adapted Wavelets, Fast Solvers, and Numerical Homogenization: From a Game Theoretic Approach to Numerical Approximation and Algorithm Design*. Cambridge University Press, 2019.
- [84] H. Owhadi, C. Scovel, and F. Schäfer. Statistical numerical approximation. *Notices of the AMS*, 2019.
- [85] M. Raissi. Deep hidden physics models: Deep learning of nonlinear partial differential equations. *Journal of Machine Learning Research*, 19(25):1–24, 2018.
- [86] M. Raissi, P. Perdikaris, and G. E. Karniadakis. Machine learning of linear differential equations using gaussian processes. *Journal of Computational Physics*, 348:683–693, 2017.

- [87] M. Raissi, P. Perdikaris, and G. E. Karniadakis. Numerical Gaussian processes for time-dependent and nonlinear partial differential equations. *SIAM Journal on Scientific Computing*, 40(1):A172–A198, 2018.
- [88] M. Raissi, P. Perdikaris, and G. E. Karniadakis. Physics-informed neural networks: A deep learning framework for solving forward and inverse problems involving nonlinear partial differential equations. *Journal of Computational Physics*, 378:686–707, 2019.
- [89] S. Reich and C. Cotter. *Probabilistic forecasting and Bayesian data assimilation*. Cambridge University Press, 2015.
- [90] J. A. Rosenfeld, B. P. Russo, R. Kamalapurkar, and T. T. Johnson. The occupation kernel method for nonlinear system identification. *SIAM Journal on Control and Optimization*, 62(3):1643–1668, 2024.
- [91] S. H. Rudy, S. L. Brunton, J. L. Proctor, and J. N. Kutz. Data-driven discovery of partial differential equations. *Science advances*, 3(4):e1602614, 2017.
- [92] S. Särkkä and L. Svensson. *Bayesian filtering and smoothing*, volume 17. Cambridge university press, 2023.
- [93] H. Schaeffer. Learning partial differential equations via data discovery and sparse optimization. *Proceedings of the Royal Society A: Mathematical, Physical and Engineering Sciences*, 473(2197):20160446, 2017.
- [94] H. Schaeffer, G. Tran, R. Ward, and L. Zhang. Extracting structured dynamical systems using sparse optimization with very few samples. *Multiscale Modeling & Simulation*, 18(4):1435–1461, 2020.
- [95] F. Schäfer and H. Owhadi. Sparse recovery of elliptic solvers from matrix-vector products. *SIAM Journal on Scientific Computing*, 46(2):A998–A1025, 2024.
- [96] F. Schäfer, M. Katzfuss, and H. Owhadi. Sparse cholesky factorization by Kullback–Leibler minimization. *SIAM Journal on Scientific Computing*, 43(3):A2019–A2046, 2021.
- [97] F. Schafer, T. J. Sullivan, and H. Owhadi. Compression, inversion, and approximate pca of dense kernel matrices at near-linear computational complexity. *Multiscale Modeling & Simulation*, 19(2):688–730, 2021.
- [98] W. H. Schilders, H. A. Van der Vorst, and J. Rommes. *Model order reduction: theory, research aspects and applications*, volume 13. Springer, 2008.
- [99] M. Schmidt and H. Lipson. Distilling free-form natural laws from experimental data. *Science (New York, N.Y.)*, 324:81–5, 05 2009.
- [100] B. Scholkopf and A. J. Smola. *Learning with kernels: support vector machines, regularization, optimization, and beyond*. MIT Press, 2018.
- [101] P. Scholl, A. Bacho, H. Boche, and G. Kutyniok. The uniqueness problem of physical law learning. In *ICASSP 2023-2023 IEEE International Conference on Acoustics, Speech and Signal Processing (ICASSP)*, pages 1–5. IEEE, 2023.
- [102] T. B. Schön, A. Wills, and B. Ninness. System identification of nonlinear state-space models. *Automatica*, 47(1):39–49, 2011.
- [103] J. Schoukens and L. Ljung. Nonlinear system identification: A user-oriented road map. *IEEE Control Systems Magazine*, 39(6):28–99, 2019.
- [104] I. Steinwart. *Support Vector Machines*. Springer, 2008.
- [105] F. Sun, Y. Liu, and H. Sun. Physics-informed spline learning for nonlinear dynamics discovery. In Z.-H. Zhou, editor, *Proceedings of the Thirtieth International Joint Conference on Artificial Intelligence, IJCAI-21*, pages 2054–2061. International Joint Conferences on Artificial Intelligence Organization, 8 2021. Main Track.
- [106] A. Tarantola. *Inverse problem theory and methods for model parameter estimation*. SIAM, 2005.
- [107] C. R. Vogel. *Computational methods for inverse problems*. SIAM, 2002.
- [108] D. Voina, S. Brunton, and J. N. Kutz. Deep generative modeling for identification of noisy, non-stationary dynamical systems. *arXiv preprint arXiv:2410.02079*, 2024.
- [109] H. U. Voss, J. Timmer, and J. Kurths. Nonlinear dynamical system identification from uncertain and indirect measurements. *International Journal of Bifurcation and Chaos*, 14(06):1905–1933, 2004.
- [110] G. Wahba. *Spline models for observational data*. SIAM, 1990.
- [111] E. A. Wan and A. T. Nelson. Dual extended kalman filter methods. *Kalman filtering and neural networks*, pages 123–173, 2001.
- [112] C. Wang and A. Townsend. Operator learning for hyperbolic partial differential equations. *arXiv preprint arXiv:2312.17489*, 2023.
- [113] J. Wang, A. Hertzmann, and D. J. Fleet. Gaussian process dynamical models. *Advances in neural information processing systems*, 18, 2005.
- [114] J. Wang, J. Cockayne, O. Chkrebtii, T. J. Sullivan, C. Oates, et al. Bayesian numerical methods for nonlinear partial differential equations. *Statistics and Computing*, 31(5):1–20, 2021.
- [115] M. Wells, K. Lahouel, and B. Jedynek. The stochastic occupation kernel method for system identification. *arXiv preprint arXiv:2406.15661*, 2024.
- [116] H. Wendland. *Scattered Data Approximation*. Cambridge University Press, 2004.
- [117] H. Wendland and C. Rieger. Approximate interpolation with applications to selecting smoothing parameters. *Numerische Mathematik*, 101:729–748, 2005.

- [118] G. Wynne, F.-X. Briol, and M. Girolami. Convergence guarantees for gaussian process means with misspecified likelihoods and smoothness. *Journal of Machine Learning Research*, 22(123):1–40, 2021.
- [119] J. Xiong. *An introduction to stochastic filtering theory*, volume 18. OUP Oxford, 2008.
- [120] D. Xiu and G. E. Karniadakis. The wiener–askey polynomial chaos for stochastic differential equations. *SIAM journal on scientific computing*, 24(2):619–644, 2002.
- [121] H. Xu. Dl-pde: Deep-learning based data-driven discovery of partial differential equations from discrete and noisy data. *Communications in Computational Physics*, 29(3):698–728, 2021.
- [122] H. Xu, H. Chang, and D. Zhang. Dlga-pde: Discovery of pdes with incomplete candidate library via combination of deep learning and genetic algorithm. *Journal of Computational Physics*, 418:109584, 2020.
- [123] H. Xu, D. Zhang, and J. Zeng. Deep-learning of parametric partial differential equations from sparse and noisy data. *Physics of Fluids*, 33(3), 2021.
- [124] L. Yang, B. Hamzi, Y. Kevrekidis, H. Owahdi, X. Sun, and N. Xie. Learning dynamical systems from data: A simple cross-validation perspective, part vi: Hausdorff metric based training of kernels to learn attractors with application to 133 chaotic dynamical systems. 2023.
- [125] L. Yang, X. Sun, B. Hamzi, H. Owahdi, and N. Xie. Learning dynamical systems from data: A simple cross-validation perspective, part v: Sparse kernel flows for 132 chaotic dynamical systems. *Physica D: Nonlinear Phenomena*, 460:134070, 2024. ISSN 0167-2789.
- [126] Y. Yang, M. Aziz Bhouri, and P. Perdikaris. Bayesian differential programming for robust systems identification under uncertainty. *Proceedings of the Royal Society A*, 476(2243):20200290, 2020.
- [127] L. Zhang and H. Schaeffer. On the convergence of the sindy algorithm. *Multiscale Modeling & Simulation*, 17(3):948–972, 2019.
- [128] S. Zhang and G. Lin. Robust data-driven discovery of governing physical laws with error bars. *Proceedings of the Royal Society A: Mathematical, Physical and Engineering Sciences*, 474(2217):20180305, 2018.

SUPPLEMENTARY INFORMATION A. LITERATURE REVIEW

A.1. Equation learning and system identification. The discovery or learning of differential equations from data was brought into prominence after the seminal papers [11, 99] that used symbolic regression to discover physical laws from data. However, the problem of learning the equations that govern a dynamical system from time-series data was already studied extensively in the 70s in the control literature under the name *system identification* [4, 66, 51]. Modern iterations of equation learning are often focused on learning dynamical systems and differential equation under a sparsity prior over a dictionary of terms that are likely to be present [17, 91, 93]. While the Sparse Identification of Nonlinear Dynamics (SINDy) [17] is perhaps the most widely known instance of such sparse regression algorithms, many other variants have been proposed in the literature with the main defining features being the way in which the sparsity prior is implemented [93, 49]. Since these earlier contributions, many extensions of the sparse regression approach have been proposed. Some notable examples are: weak form equation learning methods such as weak-SINDy [72, 72] that aim to reduce the order of partial derivatives to improve accuracy and robustness with noisy data; ensemble methods such as ensemble-SINDy [30] where many SINDy models are trained with different dictionaries and parameters to then be ensembled together to produce a more accurate model; and Bayesian methods [128, 77, 126, 43, 78, 79] that utilize a probabilistic formulation of the equation learning problem, often using sparsity-promoting priors over dictionary parameters, to enable uncertainty quantification. Many other extensions of the sparse regression approach to equation learning have been proposed in the literature that are outside the scope of the current article and so we refer the reader to the review article [80] and the references within. It is important to note that the overwhelming majority of the methods discussed above fall under the category of 2-step methods within our exposition where partial derivatives of the functions u^m are estimated separately from learning the equation P . Some instances, most notably weak-SINDy [72] and UQ-SINDy [43], can be formulated as 1-step methods but this goes beyond a simple modification of their current implementations. The closest method to 1-step KEqL within the sparse regression family is the PiSL algorithm of [105] that estimates the u^m as B-cubic splines and P over a dictionary, simultaneously. However, this method was primarily developed for ODE models and was not extended to the case of PDEs.

Various kernel/Gaussian process (GP) methods for equation learning, or adjacent problems, have been proposed in the literature. The connections between Bayesian/GP inference and numerical analysis were already observed in the works of Wahba and Kimeldorf [54, 53, 110] which underlay GP techniques for solution of differential equations [81, 22, 23, 87, 84, 83, 24, 114, 18]. While the aforementioned works were mainly focused on the numerical solution of differential equations, this line of thinking has lead to various kernel/GP methods for learning equations as well, most notably, [86] introduced GPs for learning linear differential equations in a 1-step manner while [58] introduced a 1-step kernel method resembling our formulation for learning ODEs. The series of papers [40, 25, 61, 41, 125, 124] also introduced a methodology that is very similar to ours for inference of ODEs from time-series data towards filtering and data assimilation. [90] introduces a kernel analogue to SINDy and weak-SINDy for dynamic problems based on

the idea of occupation kernels, kernels that correspond to integrals of RKHS functions over trajectories. The idea of occupation kernels was further used in [115] for learning the drift and diffusion of a stochastic process. [26] also used a kernel method for learning stochastic differential equations from a single trajectory. [67] introduced an early version of 2-step KEqL for learning ODEs and PDEs with unknown coefficients and observed improved performance in both equation learning and operator learning, inspiring the present paper. Finally, we note that the computational graph completion framework that contains our methodology was introduced in [82] where it was already used to learn an ODE model for an electrical circuit using scarce data, this work was further extended to hyper-graphs in [16].

More recently, various neural net models for learning and discovery of differential equations have been proposed. These methods range from symbolic regression [68, 69, 121, 122, 123] to neural net regression [85, 12, 21, 55]. The latter class of methods are based on the methodology of physics-informed neural nets (PINNs) [88] that approximates solutions of PDEs by minimizing residuals over a neural net function class. Both [85, 21] model the unknown functions u^m with neural networks. The deep hidden physics model of [85] then proceeds to also model P with a neural net while the PINN-SR algorithm of [21] models P over a sparse dictionary akin to SINDy. We should note that the deep hidden physics model was not originally presented in the setting of scarce observations but it can be easily modified for that task akin to the PINN-SR model. However, both methods are prone to difficulties with solving the resulting optimization problems as is known for other PINN models [57]. Regardless, the PINN-SR model is the closest competitor to our 1-step KEqL method and hence is used as a benchmark in our experiments.

A.2. Theory of equation learning. The problem of learning dynamical systems is a vast and old field with a mature theoretical foundation. A complete overview of this field is outside the scope of this paper, and we refer the reader to the recent survey [9]. The theoretical analysis of equation learning, on the other hand, is a more recent and less mature topic. The convergence properties of sparse regression methods for equation learning (e.g. SINDy) were studied in the series of articles [93, 127, 94, 49] where techniques from compressed sensing and random matrix theory were used to provide recovery guarantees over appropriate dictionaries. Although these results can be viewed as analogues of our error analysis for 2-step KEqL for the case of sparse regression methods, they are not applicable to 1-step methods in scarce data regimes of interest to us. The recent paper [101] studies the identifiability of equation learning for ODEs and PDEs, i.e., under what conditions is it at all possible to learn an equation even with abundant data? Conversely, [42] considers the limitations of learning a PDE from a single trajectory.

Our theoretical results give a different type of result compared to the aforementioned papers by presenting worst-case error bounds and mostly relying on smoothness assumptions on the functions u^m and P while remaining applicable to 1-step methodologies. Our techniques borrow ideas from the mature field of scattered data approximation [116] and build on Sobolev sampling inequalities from approximation theory [117, 76, 3]. Indeed, our theory is heavily inspired by the recent papers [7, 6] where error bounds of a similar flavor were derived for kernel PDE solvers and kernel operator learning algorithms.

A.3. Inverse problems. Identifying parameters (often functions) of a differential equation is the primary focus of the field of inverse problems [106, 45] with a rich history of theoretical analysis [28, 44] and computational methodologies [107]. While traditional inverse problems focus on known PDEs with unknown spatio-temporal coefficients, the methodologies developed for those problems can be extended to both 1-step and 2-step methodologies for equation learning; in fact, one can argue that equation learning, as presented in the current paper, is an inverse problem for P . Many of the ideas that we developed in the current paper including the use of RKHS regularizers and the linearizations used to define the algorithm for solving the 1-step KEqL problem are prevalent in the inverse problems literature [39]. Ideas akin to our 1-step formulation have also appeared in the inverse problems literature under the name of joint inversion [38], where parameters of related models are recovered simultaneously, as well as all-at-once inversion [46, 47] where the unknown coefficients of the PDE and the solution are estimated in a single optimization problem.

A.4. Operator learning. The field of operator learning has become very popular in recent years and since the seminal papers [10, 63, 70] where neural net techniques were developed for the approximation of solution maps of PDEs. Since then, a large body of work has been developed around operator learning focusing on methodologies as well as theory; see [56] and references within for neural operators and [6] for the kernel perspective. We should note that, while modern operator learning is largely focused on neural net models for data-driven learning of mappings between function spaces, the operator learning problem has appeared in the literature since at least the early 2000's in the fields of computer model emulation [52], polynomial chaos [120], stochastic Galerkin methods [35], reduced order modeling [71], and model order reduction [98], all of whom are supported by mature theoretical and methodological literature. We also mention the works [97, 13, 14, 112, 95] that consider the operator learning of linear PDEs with quantitative approximation rates.

It is important to note that our perspective towards operator learning, which deliberately utilizes the fact that the differential operator \mathcal{P} is local, is far from the dominant approach in the aforementioned works. However, this idea has been investigated in the context of physics-informed operators in recent years [27, 37, 64]. These models

train a neural net to learn the solution map of a PDE with an additional term in the training loss that minimizes the residual of the PDE for the predicted solutions on a collocation mesh akin to our 1-step method. The main departing feature however is that physics-informed neural operators assume knowledge of the underlying PDE.

A.5. Data assimilation. The problem of recovering the functions u^m and in turn predicting the solution of a dynamic PDE in future times falls within the field of data assimilation [59, 89] which, historically, was developed closely alongside filtering [5, 119] and control [36, 31]. The problem of filtering the state of a control system while identifying its unknown parameters (i.e., system identification) is also classical in filtering [109, 103] and can be solved using classic techniques such as extended Kalman smoothing [92, Sec. 5]. This idea has been further developed in various directions including: expectation maximization methods [34, 102]; dual extended Kalman filters [111]; GP dynamical models [113, 32] (which are reminiscent of our method as well as the work [40] and subsequent works); and sequential Monte Carlo [65]. The important distinction of these works compared to our approach is three fold, first, the works in data assimilation and control often assume particular structure for the underlying dynamic models; second, these works are almost exclusively developed for dynamical systems as opposed to PDEs; and third, data assimilation is almost exclusively concerned with time-series data. However, the close adjacency of the aforementioned work to ours suggests potential future applications of the KEQL methodology within the data assimilation literature.

SUPPLEMENTARY INFORMATION B. THEORETICAL DETAILS

In this section we collect details of the theoretical foundations behind our kernel equation learning algorithm along with detailed proofs of convergence analyses and error bounds presented in the main body of the paper.

B.1. Preliminaries. Here we collect some preliminary definitions and results from the theory of RKHSs and Sobolev spaces that are used throughout the main body of the paper as well as proofs outlined later in this section.

B.1.1. RKHS review. The following results are standard in the theory of RKHSs and can be found in many classic texts such as [100, 83, 104, 8]. Consider an open set $\Omega \subset \mathbb{R}^q$ and a kernel $\mathbf{H} : \Omega \times \Omega \rightarrow \mathbb{R}$. We say \mathbf{H} is positive definite and symmetric (PDS) if for any $N \in \mathbb{N}$ and set of points $X = \{x_1, \dots, x_N\} \subset \Omega$, the kernel matrix $\mathbf{H}(X, X) \in \mathbb{R}^{N \times N}$ with (i, j) -entries $\mathbf{H}(x_i, x_j)$ is PDS. If $\mathbf{H}(X, X)$ is strictly PDS then we say \mathbf{H} is a strictly PDS kernel.

Every PDS kernel \mathbf{H} is uniquely identified with a Hilbert space \mathcal{H} , called its corresponding RKHS, with inner product $\langle \cdot, \cdot \rangle_{\mathcal{H}}$ and norm $\| \cdot \|_{\mathcal{H}}$. The kernel \mathbf{H} and elements of \mathcal{H} satisfy the so-called reproducing property, i.e., $\langle f, \mathbf{H}(x, \cdot) \rangle_{\mathcal{H}} = f(x)$ for all $f \in \mathcal{H}$. We are particularly interested in the characterization of \mathcal{H} via Mercer's theorem.

Proposition 1. *Suppose $\Omega \subset \mathbb{R}^q$ is bounded and let \mathbf{H} be a PDS kernel that is continuous in both of its arguments on $\bar{\Omega}$. Then there exists an orthonormal set of continuous eigenfunctions $\{e_i\}_{i=1}^{\infty} \subset L^2(\Omega)$ and decreasing eigenvalues $\{\lambda_i\}_{i=1}^{\infty}$, $\lambda_1 \geq \lambda_2 \geq \dots$, such that*

$$\mathbf{H}(x, x') = \sum_{i=1}^{\infty} \lambda_i e_i(x) e_i(x').$$

The RKHS \mathcal{H} can be characterized as

$$(21) \quad \mathcal{H} = \left\{ f : \Omega \rightarrow \mathbb{R} \mid f(x) = \sum_{i \in \{i | \lambda_i \neq 0\}} c_i(f) e_i(x), \quad \sum_{i \in \{i | \lambda_i \neq 0\}} \lambda_i^{-1} c_i(f)^2 < +\infty \right\}$$

and for any pair $f, f' \in \mathcal{H}$ we have $\langle f, f' \rangle_{\mathcal{H}} = \sum_{i \in \{i | \lambda_i \neq 0\}} \lambda_i^{-1} c_i(f) c_i(f')$.

Given the spectral characterization (21), we further define the nested ladder of RKHS spaces

$$\mathcal{H}^{\gamma} := \left\{ f : \Omega \rightarrow \mathbb{R} \mid f(x) = \sum_{i=1}^{\infty} c_i(f) e_i(x), \quad \sum_{i=1}^{\infty} \lambda_i^{-\gamma} c_i(f)^2 < +\infty \right\},$$

for $\gamma \geq 1$. These are precisely the RKHSs corresponding to the kernels $\mathbf{H}^{\gamma}(x, x') := \sum_{i=1}^{\infty} \lambda_i^{\gamma} e_i(x) e_i(x')$. Naturally, larger values of γ imply more "smoothness", in particular we have the inclusion $\mathcal{H}^{\gamma_2} \subset \mathcal{H}^{\gamma_1}$ for $1 \leq \gamma_1 < \gamma_2$ following Hölder's inequality. Observe that our definition of the \mathcal{H}^{γ} resembles the spectral definition of Sobolev spaces $H^{\gamma}(\Omega)$ on compact sets in which case the $\{\lambda_i, e_i\}_{i=1}^{\infty}$ can be taken as the eigenpairs of the Green's function of the Laplacian operator. The following lemma is useful in our proofs later in this section.

Lemma 1. *Suppose $f \in \mathcal{H}^{2\gamma}$ and $f' \in \mathcal{H}^{\gamma}$. Then it holds that $\langle f', f \rangle_{\mathcal{H}^{\gamma}} \leq \|f'\|_{L^2(\Omega)} \|f\|_{\mathcal{H}^{2\gamma}}$.*

Proof. For simplicity of notation let us assume that $\lambda_i \neq 0$ so that the kernel \mathbf{H} is strictly PDS (i.e., non-degenerate). By definition of the \mathcal{H}^{γ} inner product, and using Cauchy-Schwartz, we have that

$$\langle f', f \rangle_{\mathcal{H}^{\gamma}} = \sum_{i=1}^{\infty} \lambda_i^{-\gamma} c_i(f') c_i(f) \leq \left(\sum_{i=1}^{\infty} c_i(f')^2 \right)^{1/2} \left(\sum_{i=1}^{\infty} \lambda_i^{-2\gamma} c_i(f)^2 \right)^{1/2} = \|f'\|_{L^2(\Omega)} \|f\|_{\mathcal{H}^{2\gamma}}.$$

□

Finally we recall the following representer theorem for interpolation problems in RKHSs which is fundamental to our proof of Theorem 2:

Lemma 2 (Representer theorem for interpolation [83, Cor. 17.12]). *Let \mathcal{H} be an RKHS with kernel \mathbf{H} and let $\phi_1, \dots, \phi_N \in \mathcal{H}^*$ (the set of bounded and linear functionals on \mathcal{H}). Consider*

$$\hat{f} := \arg \min_{f \in \mathcal{H}} \|f\|_{\mathcal{H}} \quad \text{s.t.} \quad \phi_i(f) = z_i, \quad i = 1, \dots, N,$$

for $z = (z_1, \dots, z_N) \in \mathbb{R}^N$. Then every minimizer \hat{f} has the form $\hat{f} = \mathbf{H}(\phi, \cdot)^T \hat{\alpha}$ where $\hat{\alpha} = \mathbf{H}(\phi, \phi)^{-1} z$. Here we followed the notation of Theorem 2 and wrote $\mathbf{H}(\phi_i, x) = \phi_i(\mathbf{H}(\cdot, x))$, $\mathbf{H}(\phi, x) = (\mathbf{H}(\phi_1, x), \dots, \mathbf{H}(\phi_N, x)) \in \mathcal{H}^N$, and $\mathbf{H}(\phi, \phi) \in \mathbb{R}^{N \times N}$ as the matrix with entries $\phi_j(\mathbf{H}(\phi_i, \cdot))$. In cases where $\mathbf{H}(\phi, \phi)$ is not invertible the vector $\hat{\alpha}$ is defined in the least squares sense.

B.1.2. Sobolev spaces. We now collect useful technical results concerning Sobolev spaces that are the corner stone of our error analysis in Section 3. For an extensive study of Sobolev spaces we refer the reader to [1]. For introduction to Sobolev sampling inequalities and related results on scattered data approximation see [116].

For an open set $\Omega \subset \mathbb{R}^q$ and $\gamma \in \mathbb{N}$ we write $H^\gamma(\Omega)$ to denote the $L^2(\Omega)$ based Sobolev space of index γ , i.e., the elements of $u \in L^2(\Omega)$ such that all partial derivatives of order γ also belong to $L^2(\Omega)$. In particular, we equip $H^\gamma(\Omega)$ with the norm

$$\|u\|_{H^\gamma(\Omega)}^2 = \sum_{|\mathbf{a}| \leq \gamma} \|D^{\mathbf{a}} u\|_{L^2(\Omega)}^2,$$

where $\mathbf{a} = (a_1, \dots, a_q)$ is a multi-index set with $a_j \in \mathbb{N}_0$ (the set of positive integers including zero) and $D^{\mathbf{a}} := \frac{\partial^{a_1}}{\partial x_1^{a_1}} \frac{\partial^{a_2}}{\partial x_2^{a_2}} \dots \frac{\partial^{a_q}}{\partial x_q^{a_q}}$, where we used x_j to denote the j -th component of x as a vector in \mathbb{R}^q . We can then define $H^\gamma(\Omega) := \{u \in L^2(\Omega) \mid \|u\|_{H^\gamma(\Omega)} < +\infty\}$ with the convention $H^0(\Omega) = L^2(\Omega)$. We recall the following classic results for Sobolev spaces:

Proposition 2 (Sobolev embedding theorem [1, Thm. 4.12]). *Suppose $\Omega \subset \mathbb{R}^q$ is a bounded set with Lipschitz boundary and that for $p \in \mathbb{N}$ it holds that $\gamma > q/2 + p$. Then $H^\gamma(\Omega)$ is continuously embedded in $C^p(\Omega)$ and it holds that $\|u\|_{C^p(\Omega)} \leq C_\Omega \|u\|_{H^\gamma(\Omega)}$ for an embedding constant $C_\Omega \geq 0$ that depends only on Ω .*

In addition to the embedding theorem we will heavily rely on the Sobolev sampling inequality which gives control over the Sobolev norm of a function that is small or zero on a discrete set. The following theorem is a distillation of [117, Prop. 2.4] in the form that we need in our proofs; see also [76, 60, 3].

Proposition 3 (Sobolev sampling inequality). *Suppose $\Omega \subset \mathbb{R}^d$ is a bounded set with Lipschitz boundary and consider a set of points $X = \{x_1, \dots, x_N\} \subset \bar{\Omega}$ with fill distance $h_X := \sup_{x \in \Omega} \inf_{x' \in X} \|x - x'\|_2$. Let $u|_X$ denote the restriction of u to the set X , viewed as a vector in \mathbb{R}^N . Further consider indices $\gamma > d/2$ and $0 \leq \eta \leq \gamma$ and let $u \in H^\gamma(\Omega)$.*

(a) (Noiseless) *Suppose $u|_X = 0$. Then there exists $h_0 > 0$ so that whenever $h_X \leq h_0$ we have the inequality*

$$\|u\|_{H^\eta(\Omega)} \leq C_\Omega h_X^{\gamma-\eta} \|u\|_{H^\gamma(\Omega)}$$

where $C_\Omega > 0$ is a constant that depends only on Ω .

(b) (Noisy) *Suppose $u|_X \neq 0$. Then there exists $h_0 > 0$ so that whenever $h_X \leq h_0$ we have the inequality*

$$\|u\|_{L^\infty(\Omega)} \leq C_\Omega h_X^{\gamma-d/2} \|u\|_{H^\gamma(\Omega)} + 2\|u|_X\|_\infty,$$

where $C_\Omega > 0$ is a constant that depends only on Ω .

B.2. Convergence proof and error analysis for KEqL (Proof of Theorem 1). Recall that we considered the training data of the form $\{u^m(Y^m), f^m\}_{m=1}^M$ with a set of N observation points $Y^m \subset \mathcal{Y}$. For our convergence analysis we need to consider the limits $M, N \rightarrow \infty$ and so we will need to index our observation points and solutions appropriately. We will write Y_N^m to highlight the number N of collocation points in the observation point set. To further simplify notation we will assume that $Y = Y_{M,N} = \cup_{m=1}^M Y_N^m$, so that the collocation points are simply the union of the observation points for any choice of N . Moreover, we write $\hat{u}_{M,N}^m$ and $\hat{P}_{M,N}$ to highlight the dependence of minimizers on the size of the observation point set N and the total number of training pairs M .

For reference let us recall our PDE problem along with the optimization problem for 1-step KEqL with our new notation. Below we also include the known function \bar{P} , representing our knowledge of existing terms in the PDE.

$$\text{(PDE)} \quad \begin{cases} \mathcal{P}(u)(y) = (\bar{P} + P) \circ \Phi(u, y) = f(y), & \forall y \in \mathcal{Y} \quad \text{where} \quad \Phi(u, y) = (y, L_1 u(y), \dots, L_Q u(y)), \\ \mathcal{B}(u)(y) = g(y), & \forall y \in \partial\mathcal{Y}. \end{cases}$$

$$\text{(1STP)} \quad \begin{cases} (\hat{u}_{M,N}, \hat{P}_{M,N}) = \arg \min_{\mathbf{v} \in \mathcal{U}^M, G \in \mathcal{P}} \|G\|_{\mathcal{P}}^2 + \sum_{m=1}^M \|v^m\|_{\mathcal{U}}^2 \\ \text{s.t.} \quad v^m(Y_N^m) = u^m(Y_N^m), \quad G(S(v^m)) = f^m(Y_{M,N}) - \bar{P}(S(v^m)). \end{cases}$$

For simplicity we took the constant $\lambda_1 = 1$ and used our usual notation $S(v) = \{s_1(v), \dots, s_K(v)\}$ where $s_k(v) = \Phi(v, y_k)$ for $y_k \in Y_{M,N}$.

Our theoretical analysis will rely on sufficient technical assumptions that we now summarize; these will be used in the rest of this section for various arguments and their accumulation is presented as Assumption 1.

First we have a standard assumption on the set \mathcal{Y} on which the PDE is defined. This assumption allows us to use Propositions 2 and 3.

Assumption 2. *The set $\mathcal{Y} \subset \mathbb{R}^d$ is bounded and has Lipschitz boundary.*

Next we will need assumptions on the kernels \mathbf{U} and \mathbf{P} to ensure sufficient regularity and compact embedding in appropriate Sobolev spaces:

Assumption 3. *The kernel $\mathbf{U} : \mathcal{Y} \times \mathcal{Y} \rightarrow \mathbb{R}$ and its corresponding RKHS satisfy:*

- (i) \mathbf{U} is PDS and continuous in its arguments.
- (ii) \mathcal{U} is compactly embedded in $H^\gamma(\mathcal{Y})$ for some $\gamma > d/2 + \text{order}(\mathcal{P})$, in particular $\exists C_{\mathcal{Y}} > 0$ such that $\|u\|_{H^\gamma(\mathcal{Y})} \leq C_{\mathcal{Y}} \|u\|_{\mathcal{U}}$ for all $u \in \mathcal{U}$.
- (iii) Elements $u \in \mathcal{U}$ satisfy the boundary conditions of (PDE), i.e., $\mathcal{B}(u) = g$ on $\partial\mathcal{Y}$.

Remark 1. *We highlight that assumption (iii) above allows us to simplify our theoretical arguments significantly since we do not need to approximate values of the functions on the boundary. However, this assumption can be removed by adding a separate approximation result for the value of estimated solutions $\widehat{u}_{M,N}^m$ near the boundary under sufficient regularity assumptions.*

Assumption 4. *The kernel $\mathbf{P} : \mathcal{S} \times \mathcal{S} \rightarrow \mathbb{R}$ and its corresponding RKHS satisfy:*

- (i) \mathbf{P} is PDS.
- (ii) \mathcal{P} is compactly embedded in $H^\eta(\mathcal{S})$ for some $\eta > \frac{Q+d}{2}$.
- (iii) Elements of \mathcal{P} are locally Lipschitz, i.e., for any compact set $B \subset \mathcal{S}$ there exists a constant $C(B) > 0$ so that $|P(s) - P(s')| \leq C(B) \|P\|_{\mathcal{P}} \|s - s'\|_2$, for all $s, s' \in B$.

Finally, recall our notation from Section 3 for the fill-distances

$$\rho_{m,N} = \sup_{y \in \mathcal{Y}} \inf_{y' \in Y_N^m} \|y - y'\|_2, \quad \varrho_{M,N}(B) = \sup_{s \in B} \inf_{s' \in \mathcal{S} \cap B} \|s - s'\|_2,$$

where $S = \cup_{m=1}^M S^m$ with $S^m = \Phi(u^m, Y_{M,N})$ and $B \subset \mathcal{S}$.

B.2.1. Proof of convergence for 1-step KEqL. We start by giving a proof of convergence for 1-step KEqL as a simpler version of our quantitative rates in the next subsection.

Proposition 4. *Consider the problem (1STP). Suppose Assumptions 2 and 3 and Assumption 4(i-ii) hold, $P \in \mathcal{P}$, and \bar{P} is continuous. Consider pairs $\{u^m, f^m\}_{m=1}^\infty$ satisfying (PDE) and a bounded set $B \subset \mathcal{S}$ with Lipschitz boundary. Finally, suppose $\rho_{m,N} \rightarrow 0$ as $N \rightarrow \infty$ for all m and $\varrho_{M,N}(B) \rightarrow 0$ as $M, N \rightarrow \infty$. Then the following holds:*

- (a) Fix M . If $u^m \in \mathcal{U}$ then $\lim_{N \rightarrow \infty} \widehat{u}_{M,N}^m = u^m$ pointwise in \mathcal{Y} and in $H^{\gamma'}(\mathcal{Y})$ for all $\gamma' < \gamma$ and $m \in \{1, \dots, M\}$.
- (b) If $u^m \in \mathcal{U}^2$ then $\lim_{M \rightarrow \infty} \lim_{N \rightarrow \infty} \widehat{P}_{M,N} = P$ pointwise in B and in $H^{\eta'}(B)$ for all $\eta' < \eta$.

Proof. Let us verify that our assumptions are sufficient for the problem to be well defined. Since \mathcal{U} is an RKHS then the problem for $\widehat{u}_{M,N}^m$ is readily well defined. Moreover, since \mathbf{U} is continuous the space \mathcal{U}^2 is well defined as in SI B.1.1. Moreover, Assumption 2 along with Assumption 3(ii) and Proposition 2 ensure that Φ is continuous and bounded, in fact, $\Phi(\cdot, y)$ is a bounded and linear operator on \mathcal{U} ; this is simply the statement that $\mathcal{P}(u)$ is defined pointwise. Finally, since \mathcal{P} is an RKHS and \bar{P} is continuous we ensure that the problem for $\widehat{P}_{M,N}$ is also well defined.

Proof of (a): Observe that the pair (\mathbf{u}, P) (notation: $\mathbf{u} = (u^1, u^2, \dots, u^M)$) are feasible for (1STP) for all values of M, N . Then the optimality of $(\widehat{\mathbf{u}}_{M,N}, \widehat{P}_{M,N})$ implies that

$$(22) \quad \|\widehat{P}_{M,N}\|_{\mathcal{P}}^2 + \sum_{m=1}^M \|\widehat{u}_{M,N}^m\|_{\mathcal{U}}^2 \leq \|P\|_{\mathcal{P}}^2 + \sum_{m=1}^M \|u^m\|_{\mathcal{U}}^2.$$

Thus, for fixed M we have that $\|\widehat{u}_{M,N}^m\|_{\mathcal{U}} \leq C(M)$ for all m , i.e., $\{\widehat{u}_{M,N}^m\}_{N=1}^\infty$ is bounded in \mathcal{U} . Then Assumption 3(ii) implies that $\widehat{u}_{M,N}^m$ has a convergent subsequence in $H^\gamma(\mathcal{Y})$. On the other hand, since $\rho_{m,N} \rightarrow 0$ and thanks to the assumption that u^m are continuous (since they belong to \mathcal{U}) we infer that all accumulation points of $\widehat{u}_{M,N}^m$ coincide with u^m . This implies that for fixed M and for any $m \in \{1, \dots, M\}$ we have $\lim_{N \rightarrow \infty} \widehat{u}_{M,N}^m = u^m$ pointwise and in $H^{\gamma'}(\mathcal{Y})$ for $\gamma' < \gamma$.

Proof of (b): Fix M and for each u^m define the optimal interpolant

$$(23) \quad \bar{u}_N^m := \arg \min_{v \in \mathcal{U}} \|v\| \quad \text{s.t.} \quad v(Y_N^m) = u^m(Y_N^m).$$

By optimality, we have the bound

$$(24) \quad \|\widehat{u}_{M,N}^m\|_{\mathcal{U}} \geq \|\bar{u}_N^m\|_{\mathcal{U}}.$$

At the same time, the representer theorem gives $\bar{u}_N^m = \mathbf{U}(Y_N^m, \cdot)^T \mathbf{U}(Y_N^m, Y_N^m)^{-1} u^m(Y_N^m)$ and a direct calculation using the reproducing property implies that $\langle u^m - \bar{u}_N^m, \bar{u}_N^m \rangle_{\mathcal{U}} = 0$ which in turn gives the identity

$$(25) \quad \|u^m - \bar{u}_N^m\|_{\mathcal{U}}^2 = \|u^m\|_{\mathcal{U}}^2 - \|\bar{u}_N^m\|_{\mathcal{U}}^2.$$

At the same time, since we assumed $u^m \in \mathcal{U}^2$ we also have, using Lemma 1,

$$\|u^m - \bar{u}_N^m\|_{\mathcal{U}}^2 = \langle u^m - \bar{u}_N^m, u^m \rangle_{\mathcal{U}} \leq \|u^m - \bar{u}_N^m\|_{L^2(\mathcal{Y})} \|u^m\|_{\mathcal{U}^2}.$$

But, an identical argument to part (a) shows that $\|u^m - \bar{u}_N^m\|_{L^2(\mathcal{Y})} \rightarrow 0$ as $N \rightarrow \infty$ and so we infer that $\lim_{N \rightarrow \infty} \|u^m - \bar{u}_N^m\|_{\mathcal{U}} = 0$. This fact, together with (24) and (25) implies that

$$\limsup_{N \rightarrow \infty} \|\widehat{u}_N^m\|_{\mathcal{U}} \geq \|u^m\|_{\mathcal{U}}.$$

Then it follows from (22) that

$$\limsup_{N \rightarrow \infty} \|\widehat{P}_{M,N}\|_{\mathcal{P}} \leq \|P\|_{\mathcal{P}}.$$

This implies that the sequence $\{\widehat{P}_{M,N}\}_{N=1}^{\infty}$ is bounded and so has a convergent subsequence due to Assumption 4(ii). From part (a) we also have that $\lim_{N \rightarrow \infty} \Phi(\widehat{u}_{M,N}^m, y) = \Phi(u^m, y)$ for all $y \in \mathcal{Y}$ and $m \in \{1, \dots, M\}$. \square

We now summarize our proof of quantitative error estimates that were summarized in Theorem 3. We will split the proof into two propositions, giving rates for the 1-step and 2-step methods separately.

B.2.2. Error analysis for 1-step KEqL. We now turn our attention to quantitative error bounds for 1-step KEqL and give a complete proof of Theorem 1. For convenience we restate that theorem below in the form of a proposition.

Proposition 5. *Consider the problem (1STP) with $M, N \in \mathbb{N}$. Suppose Assumptions 2 to 4 hold and $P, \bar{P} \in \mathcal{P}$. Consider pairs $\{u^m, f^m\}_{m=1}^M$ satisfying (PDE), and a bounded set $B \subset \mathcal{S}$ with Lipschitz boundary. Then there exist constants $\rho_0, \varrho_0(B) \in (0, 1)$ so that whenever $\rho_{m,N} < \rho_0$ and $\varrho_{M,N}(B) < \varrho_0(B)$ it holds that:*

(a) *If $u^m \in \mathcal{U}$ then*

$$\sum_{m=1}^M \|\widehat{u}_{M,N}^m - u^m\|_{H^{\gamma'}(\mathcal{Y})}^2 \leq C \left(\sup_{1 \leq m \leq M} \rho_{m,N} \right)^{2(\gamma - \gamma')} \left(\|P\|_{\mathcal{P}}^2 + \sum_{m=1}^M \|u^m\|_{\mathcal{U}}^2 \right),$$

for $0 \leq \gamma' < \gamma$ and a constant $C > 0$ that depend only on \mathcal{Y} .

(b) *If $u^m \in \mathcal{U}^2$ then*

$$\|P - \widehat{P}_{M,N}\|_{L^\infty(B)} \leq C \left[\left(\varrho_{M,N}^{\frac{\eta - \varrho + d}{2}} + \sup_m \rho_{m,N}^{\gamma - \gamma'} \right) \left(\|P\|_{\mathcal{P}}^2 + \|\bar{P}\|_{\mathcal{P}}^2 + \sum_{m=1}^M \|u^m\|_{\mathcal{U}^2}^2 \right)^{1/2} \right],$$

for $d/2 + \text{order}(\mathcal{P}) < \gamma' < \gamma$ and a constant $C > 0$ that depends on \mathcal{Y} and B .

Proof. We prove each statement of the proposition separately. We will also use some notation from the convergence proofs earlier in this section.

(a) Observe that the equality constraints $\widehat{u}_{M,N}^m(Y_N^m) = u^m(Y_N^m)$ simply state that the $\widehat{u}_{M,N}^m$ are interpolating the u^m and so our error bound is natural in light of the Sobolev sampling inequality Proposition 3(a). Indeed, directly applying that result followed by Assumption 3(ii) we obtain, for $\rho_{m,N} < \rho_0$, the bounds

$$\|\widehat{u}_{M,N}^m - u^m\|_{H^{\gamma'}(\mathcal{Y})} \leq C (\rho_{m,N})^{\gamma - \gamma'} \|\widehat{u}_{M,N}^m - u^m\|_{H^\gamma(\mathcal{Y})} \leq C (\rho_{m,N})^{\gamma - \gamma'} \|\widehat{u}_{M,N}^m - u^m\|_{\mathcal{U}},$$

with the constant $C > 0$ changing from one inequality to the next and depending only on the domain \mathcal{Y} and the choice of \mathcal{U} and γ . Using the triangle inequality, the identity $(a + b)^2 \leq 2(a^2 + b^2)$, and the optimality condition (22), we can write

$$\begin{aligned} \sum_{m=1}^M \|\widehat{u}_{M,N}^m - u^m\|_{H^{\gamma'}(\mathcal{Y})}^2 &\leq C (\sup_m \rho_{m,N})^{2(\gamma - \gamma')} \left(\sum_{m=1}^M \|\widehat{u}_{M,N}^m\|_{\mathcal{U}}^2 + \sum_{m=1}^M \|u^m\|_{\mathcal{U}}^2 \right), \\ &\leq C (\sup_m \rho_{m,N})^{2(\gamma - \gamma')} \left(\|P\|_{\mathcal{P}}^2 + \sum_{m=1}^M \|u^m\|_{\mathcal{U}}^2 \right). \end{aligned}$$

This concludes the proof of the first inequality.

(b) First, we obtain a quantitative bound on the RKHS norm of $\widehat{P}_{M,N}$. The optimality condition (22) gives

$$\|\widehat{P}_{M,N}\|_{\mathcal{P}}^2 \leq \|P\|_{\mathcal{P}}^2 + \sum_{m=1}^M [\|u^m\|_{\mathcal{U}}^2 - \|\widehat{u}_{M,N}^m\|_{\mathcal{U}}^2].$$

On the other hand, by (24) and (25) we have

$$\|\widehat{u}_{M,N}^m\|_{\mathcal{U}}^2 \geq \|u^m\|_{\mathcal{U}}^2 - \|u^m - \bar{u}_N^m\|_{\mathcal{U}}^2.$$

Combining the two inequalities above yields

$$(26) \quad \|\widehat{P}_{M,N}\|_{\mathcal{P}}^2 \leq \|P\|_{\mathcal{P}}^2 + \sum_{m=1}^M \|u^m - \bar{u}_N^m\|_{\mathcal{U}}^2.$$

Applying Lemma 1 (thanks to the assumption that $u^m \in \mathcal{U}^2$) then gives the bound $\|u^m - \bar{u}_N^m\|_{\mathcal{U}}^2 \leq \|u^m - \bar{u}_N^m\|_{L^2(\mathcal{Y})} \|u\|_{\mathcal{U}^2}$. Further applying the sampling inequality Proposition 3 (since \bar{u}_N^m interpolates u^m) to control $\|u^m - \bar{u}_N^m\|_{L^2(\mathcal{Y})}$ we further obtain the bound $\|u^m - \bar{u}_N^m\|_{\mathcal{U}}^2 \leq C\rho_{m,N}^\gamma \|u^m\|_{\mathcal{U}} \|u\|_{\mathcal{U}^2}$. Substituting into (26) gives

$$(27) \quad \|\widehat{P}_{M,N}\|_{\mathcal{P}}^2 \leq \|P\|_{\mathcal{P}}^2 + C \sum_{m=1}^M \rho_{m,N}^\gamma \|u^m\|_{\mathcal{U}} \|u\|_{\mathcal{U}^2}.$$

Now we turn our attention to controlling the error between $\widehat{P}_{M,N}$ and \mathcal{P} . Observe that the PDE constraint in (1STP) implies that, for all k and m ,

$$(\widehat{P}_{M,N} + \bar{P})(s_k(\widehat{u}_{M,N}^m)) = (P + \bar{P})(s_k(u^m)).$$

Subtracting $\widehat{P}_{M,N} + \bar{P}$ from both sides of the above equation, and recalling that $s_k(v) \equiv \Phi(v, y_k)$ is linear in v , we obtain the bound

$$\left| (P - \widehat{P})(s_k(u^m)) \right| = \left| \widehat{P}_{M,N}(s_k(u^m - \widehat{u}_{M,N}^m)) + \bar{P}(s_k(u^m - \widehat{u}_{M,N}^m)) \right| \leq \left| \widehat{P}_{M,N}(s_k(u^m - \widehat{u}_{M,N}^m)) \right| + \left| \bar{P}(s_k(u^m - \widehat{u}_{M,N}^m)) \right|.$$

Now consider indices k, m such that $s_k(u^m)$ and $s_k(\widehat{u}_{M,N}^m)$ belong to B . Then by the Lipschitz assumption on $\widehat{P}_{M,N}$ and \bar{P} (i.e., Assumption 4(iii)) we have that

$$\left| (P - \widehat{P})(s_k(u^m)) \right|^2 \leq C(B) \left(\|\widehat{P}_{M,N}\|_{\mathcal{P}}^2 + \|\bar{P}\|_{\mathcal{P}}^2 \right) \|s_k(u^m - \widehat{u}_{M,N}^m)\|_2^2.$$

Applying the bound (27) to control $\|\widehat{P}_{M,N}\|_{\mathcal{P}}^2$ under the assumption that $\rho_{m,N} < \rho_0$, we can write

$$\left| (P - \widehat{P})(s_k(u^m)) \right|^2 \leq C \left(\|P\|_{\mathcal{P}}^2 + \|\bar{P}\|_{\mathcal{P}}^2 + \sum_{m=1}^M \rho_{m,N}^\gamma \|u^m\|_{\mathcal{U}} \|u\|_{\mathcal{U}^2} \right) \|s_k(u^m - \widehat{u}_{M,N}^m)\|_2^2.$$

Let us now control the error $\|s_k(u^m - \widehat{u}_{M,N}^m)\|_2^2$. Thanks to Assumption 3(ii) and the Sobolev embedding theorem Proposition 2, we have that for any γ' satisfying $d/2 + \text{order}(\mathcal{P}) < \gamma' \leq \gamma$ that $\|s_k(v)\|_2 \leq C\|v\|_{H^{\gamma'}}$. This, together with statement (a) gives the bound

$$(28) \quad \begin{aligned} \left| (P - \widehat{P}_{M,N})(s_k(u^m)) \right|^2 &\leq C \left(\|P\|_{\mathcal{P}}^2 + \|\bar{P}\|_{\mathcal{P}}^2 + \sum_{m=1}^M \rho_{m,N}^\gamma \|u^m\|_{\mathcal{U}} \|u\|_{\mathcal{U}^2} \right) \sup_m \rho_{m,N}^{2(\gamma-\gamma')} \left(\|P\|_{\mathcal{P}}^2 + \sum_{m=1}^M \|u^m\|_{\mathcal{U}}^2 \right) \\ &\leq C \left[\sup_m \rho_{m,N}^{2(\gamma-\gamma')} \right] \left(\|P\|_{\mathcal{P}}^2 + \|\bar{P}\|_{\mathcal{P}}^2 + \sum_{m=1}^M \|u^m\|_{\mathcal{U}}^2 \right)^2, \end{aligned}$$

where we assumed $\rho_{m,N} < 1$ for the second display.

At this point, we have shown that P and $\widehat{P}_{M,N}$ are close on the discrete set S . A direct application of the noisy Sobolev sampling inequality Proposition 3(b), under the assumption that $\varrho_{M,N}(B) \leq \varrho_0$ gives

$$(29) \quad \|P - \widehat{P}_{M,N}\|_{L^\infty(B)} \leq C\varrho_{M,N}(B)^{\eta - \frac{Q+d}{2}} \|P - \widehat{P}_{M,N}\|_{H^\eta(B)} + 2\|(P - \widehat{P}_{M,N})|_S\|_\infty.$$

Thanks to Assumption 4(ii) and the bound (27) we can further bound the Sobolev norm in the first term on the right-hand side,

$$\|P - \widehat{P}_{M,N}\|_{H^\eta(B)} \leq \|P - \widehat{P}_{M,N}\|_{H^\eta(S)} \leq \|P\|_{\mathcal{P}} + \|\widehat{P}_{M,N}\|_{\mathcal{P}} \leq C \left(\|P\|_{\mathcal{P}}^2 + \sum_{m=1}^M \rho_{m,N}^\gamma \|u^m\|_{\mathcal{U}} \|u\|_{\mathcal{U}^2} \right)^{1/2}.$$

Taking the supremum over the index m under the sum and substituting this bound along with (28) into (29) we can write

$$\begin{aligned} \|P - \widehat{P}_{M,N}\|_{L^\infty(B)} &\leq C \left[\varrho_{M,N}^{\eta - \frac{Q+d}{2}} \left(\|P\|_{\mathcal{P}}^2 + \left(\sup_m \rho_{m,N} \right)^\gamma \sum_{m=1}^M \|u^m\|_{\mathcal{U}} \|u^m\|_{\mathcal{U}^2} \right)^{1/2} \right. \\ &\quad \left. + \left(\left(\sup_m \rho_{m,N} \right)^{\gamma - \gamma'} \right) \left(\|P\|_{\mathcal{P}}^2 + \|\overline{P}\|_{\mathcal{P}}^2 + \sum_{m=1}^M \|u^m\|_{\mathcal{U}^2}^2 \right)^{1/2} \right]. \end{aligned}$$

Under the assumption that $\rho_{m,N} \leq 1$ and using the embedding $\mathcal{U}^2 \subset \mathcal{U}$ we can further simplify this error bound to obtain the desired inequality

$$\|P - \widehat{P}_{M,N}\|_{L^\infty(B)} \leq C \left[\left(\varrho_{M,N}^{\eta - \frac{Q+d}{2}} + \sup_m \rho_{m,N}^{\gamma - \gamma'} \right) \left(\|P\|_{\mathcal{P}}^2 + \|\overline{P}\|_{\mathcal{P}}^2 + \sum_{m=1}^M \|u^m\|_{\mathcal{U}^2}^2 \right)^{1/2} \right].$$

□

B.2.3. Error analysis for 2-step KEqL. We now present an analogue of Proposition 5 for the 2-step KEqL. The key ideas behind the 2-step proof are the same as the case of 1-step KEqL with some modification in the way the noisy Sobolev sampling inequality is applied. Let us recall the corresponding optimization problem for 2-step KEqL in the style of (1STP). With the same notation we have

$$(2\text{STP}) \quad \begin{cases} \widehat{u}_N^m = \arg \min_{v^m \in \mathcal{U}} \|v^m\|_{\mathcal{U}} & \text{subject to (s.t.) } v^m(Y_N^m) = u^m(Y_N^m) \\ \widehat{P}_{M,N} = \arg \min_{G \in \mathcal{P}} \|G\|_{\mathcal{P}} & \text{s.t. } G(S(\widehat{u}_N^m)) = f^m(Y) - \overline{P}(S(\widehat{u}_N^m)), \quad m = 1, \dots, M, \end{cases}$$

Note that we modified our notation slightly and wrote \widehat{u}_N^m instead of $\widehat{u}_{M,N}^m$ since the optimal recovery problems the u^m are independent of each other in this case.

Proposition 6. *Consider the problem (2STP) with $M, N \in \mathbb{N}$. Suppose Assumptions 2 to 4 hold, $P, \overline{P} \in \mathcal{P}$, and $u^m \in \mathcal{U}$. Consider pairs $\{u^m, f^m\}_{m=1}^M$ satisfying (PDE), and a bounded set $B \subset \mathcal{S}$ with Lipschitz boundary. Then there exist constants $\rho_0, \varrho_0(B) \in (0, 1)$ so that whenever $\rho_{m,N} < \rho_0$ and $\varrho_{M,N}(B) < \varrho_0(B)$ it holds that:*

$$\|\widehat{u}_N^m - u^m\|_{H^{\gamma'}(\mathcal{Y})} \leq C \rho_{m,N}^{(\gamma - \gamma')} \|u^m\|_{\mathcal{U}},$$

for $0 \leq \gamma' < \gamma$ and a constant $C > 0$ that depends only on \mathcal{Y} . Furthermore,

$$\begin{aligned} \|P - \widehat{P}_{M,N}\|_{L^\infty(B)} &\leq C \max\{1, 2^{\eta - \frac{Q+d}{2}}\} \\ &\quad \cdot \left[\varrho_{M,N}^{\eta - \frac{Q+d}{2}} + \max \left\{ \left(\sup_m \rho_{m,N}^{\gamma - \gamma'} \|u^m\|_{\mathcal{U}} \right)^{\eta - \frac{Q+d}{2}}, \left(\sup_m \rho_{m,N}^{\gamma - \gamma'} \|u^m\|_{\mathcal{U}} \right) \right\} (\|P\|_{\mathcal{P}} + \|\overline{P}\|_{\mathcal{P}}) \right], \end{aligned}$$

for $d/2 + \text{order}(\mathcal{P}) < \gamma' < \gamma$ and a constant $C > 0$ that depends on \mathcal{Y} and B .

Proof. (a) The first statement is a direct application of the Sobolev sampling inequality Proposition 3(a) since the \widehat{u}_N^m are simply the kernel interpolants of the u^m .

(b) Consider the definition of P and observe that the interpolation constraint for $\widehat{P}_{M,N}$ can be written as

$$\begin{aligned} (\widehat{P}_{M,N} + \overline{P})(s_k(\widehat{u}_N^m)) &= (P + \overline{P})(s_k(u_N^m)) = (P + \overline{P})(s_k(\widehat{u}_N^m)) + (P + \overline{P})(s_k(u^m)) - (P + \overline{P})(s_k(\widehat{u}_N^m)) \\ &= (P + \overline{P})(s_k(\widehat{u}_N^m)) + (P + \overline{P})(s_k(u^m - \widehat{u}_N^m)), \end{aligned}$$

where once again we used the fact that the $s_k(v)$ is linear in v . Assuming $s_k(u^m)$ and $s_k(u_N^m)$ belong to the set B we can use the local Lipschitz property of P and \overline{P} to infer that

$$|\widehat{P}_{M,N}(s_k(\widehat{u}_N^m)) - P(s_k(\widehat{u}_N^m))| \leq C(B) (\|P\|_{\mathcal{P}} + \|\overline{P}\|) \|s_k(u^m - \widehat{u}_N^m)\|$$

By the Sobolev sampling inequality Proposition 3(a) and Assumption 3(ii) we can further bound

$$(30) \quad \|s_k(u^m - \widehat{u}_N^m)\| \leq C \rho_{m,N}^{\gamma - \gamma'} \|u^m\|_{\mathcal{U}},$$

where $\gamma > \gamma' > d/2 + \text{order}(\mathcal{P})$. This further leads to an error bound on the difference between $\widehat{P}_{M,N}$ and P on the set of points $s_k(\widehat{u}_N^m)$:

$$|\widehat{P}_{M,N}(s_k(\widehat{u}_N^m)) - P(s_k(\widehat{u}_N^m))| \leq C \rho_{m,N}^{\gamma - \gamma'} (\|P\|_{\mathcal{P}} + \|\overline{P}\|) \|u^m\|_{\mathcal{U}}$$

We can now apply the noisy Sobolev sampling inequality Proposition 3(b), viewing $\widehat{P}_{M,N}$ as the noisy interpolant on P on the set of points $s_k(\widehat{u}_N^m)$, to get the error bound

$$\|P - \widehat{P}_{M,N}\|_{L^\infty(B)} \leq C \left[\varrho_{M,N}^{\eta - \frac{Q+d}{2}} \|P\|_{\mathcal{P}} + \left(\sup_m \rho_{m,N}^{\gamma - \gamma'} \|u^m\|_{\mathcal{U}} \right) (\|P\|_{\mathcal{P}} + \|\overline{P}\|_{\mathcal{P}}) \right],$$

where we introduced the notation $\widehat{\varrho}_{M,N} := \sup_{s' \in B} \inf_{k,m} \|s' - s_k(\widehat{u}_N^m)\|$. By (30) we have that $\|s' - s_k(\widehat{u}_N^m)\| \leq \|s' - s_k(u^m)\| + C \sup_m \left(\rho_{m,N}^{\gamma-\gamma'} \|u^m\|_{\mathcal{U}} \right)$ which in turn implies $\widehat{\varrho}_{M,N} \leq \varrho_{M,N} + C \sup_m \left(\rho_{m,N}^{\gamma-\gamma'} \|u^m\|_{\mathcal{U}} \right)$. Substituting back into the bound above yields

$$\|P - \widehat{P}_{M,N}\|_{L^\infty(B)} \leq C \left[\left(\varrho_{M,N} + \sup_m \left(\rho_{m,N}^{\gamma-\gamma'} \|u^m\|_{\mathcal{U}} \right) \right)^{\eta - \frac{\varrho+d}{2}} \|P\|_{\mathcal{P}} + \left(\sup_m \rho_{m,N}^{\gamma-\gamma'} \|u^m\|_{\mathcal{U}} \right) (\|P\|_{\mathcal{P}} + \|\overline{P}\|_{\mathcal{P}}) \right].$$

Using the inequality $(a+b)^p \leq \max\{1, 2^{p-1}\}(a^p + b^p)$ for $p \in (0, +\infty]$ we can simplify this bound to take the desired form

$$\|P - \widehat{P}_{M,N}\|_{L^\infty(B)} \leq C \max\{1, 2^{\eta - \frac{\varrho+d}{2}}\} \cdot \left[\varrho_{M,N}^{\frac{\eta - \frac{\varrho+d}{2}}{2}} + \max \left\{ \left(\sup_m \rho_{m,N}^{\gamma-\gamma'} \|u^m\|_{\mathcal{U}} \right)^{\eta - \frac{\varrho+d}{2}}, \left(\sup_m \rho_{m,N}^{\gamma-\gamma'} \|u^m\|_{\mathcal{U}} \right) \right\} (\|P\|_{\mathcal{P}} + \|\overline{P}\|_{\mathcal{P}}) \right].$$

□

Remark 2. We note that our error analysis above can be extended in various directions to incorporate other types of problems that may be encountered in practice. For example, the terms concerning $\sum_{m=1}^M \|u^m\|_{\mathcal{U}^2}^2 \sup_m \rho_{m,N}$ in Proposition 5(b) (similar terms in Proposition 6(b)) can be too pessimistic in situations where a small portion of the training data are outliers with very large norm or large fill-distances. Then it is natural for us to consider a probabilistic model, i.e., the GP regression approach with a nugget term which allows us to obtain similar error bounds in expectation or high-probability. Such error bounds already exist in the literature and we refer the interested reader to [75, 118] for further reading.

B.3. Operator learning error analysis. We begin by giving an elementary lemma that allows us to control the error between the solution of a true PDE and that of an approximate equation under sufficient regularity assumptions on the forward and inverse differential operators. For this lemma we will consider $\mathcal{P} : \mathcal{U} \rightarrow \mathcal{F}$ and its inverse $\mathcal{P}^{-1} : \mathcal{F} \rightarrow \mathcal{U}$ for generic Banach spaces \mathcal{U}, \mathcal{F} .

Lemma 3. Consider sets $A \subset \mathcal{U}$ and $B \subset \mathcal{F}$ for which the following conditions holds:

(1) \mathcal{P}^{-1} is locally Lipschitz on B , i.e., for any pair $f, f' \in B \subset \mathcal{F}$, there exists a constant $L(B)$ so that

$$\|\mathcal{P}^{-1}(f) - \mathcal{P}^{-1}(f')\|_{\mathcal{U}} \leq L(B) \|f - f'\|_{\mathcal{F}}.$$

(2) $\widehat{\mathcal{P}}$ approximates \mathcal{P} on A in the sense that

$$\|\widehat{\mathcal{P}}(u) - \mathcal{P}(u)\|_{\mathcal{F}} \leq \epsilon(A) \|u\|_{\mathcal{U}},$$

for some constant $\epsilon(A) > 0$.

Fix an $f \in B$ for which $\mathcal{P}^{-1}(f) \in A$, and let $\widehat{u} \in A$ be any element that solves $\widehat{P}(\widehat{u}) = f$. Then we have the error bound

$$\|\widehat{u} - \mathcal{P}^{-1}(f)\|_{\mathcal{U}} \leq L(B) \epsilon(A) \|\widehat{u}\|_{\mathcal{U}}.$$

Proof. Let us write $u = \mathcal{P}^{-1}(f)$. Since \widehat{u} solves the approximate problem we can write

$$\widehat{\mathcal{P}}(\widehat{u}) + \mathcal{P}(\widehat{u}) - \mathcal{P}(\widehat{u}) = f = \mathcal{P}(u).$$

Combining this with the Lipschitz assumption on \mathcal{P}^{-1} and the assumed error bound for $\widehat{\mathcal{P}}$ gives the chain of inequalities

$$\|\widehat{u} - u\|_{\mathcal{U}} \leq L(B) \|\mathcal{P}(\widehat{u}) - \mathcal{P}(u)\|_{\mathcal{F}} = L(B) \|\widehat{\mathcal{P}}(\widehat{u}) - \mathcal{P}(\widehat{u})\|_{\mathcal{F}} \leq L(B) \epsilon \|\widehat{u}\|_{\mathcal{U}}.$$

□

Let us now apply this lemma to obtain an error bound for the learned equation for 1-sep KEqL; a similar result can be shown for the 2-step method by a straightforward modification of the proof.

Proposition 7. Suppose Proposition 5 is satisfied with some set B . Let $f \in C(\mathcal{Y})$ be a right-hand side function such that

(1) \mathcal{P}^{-1} is locally Lipschitz in a neighborhood of f , i.e., $\|\mathcal{P}^{-1}(f) - \mathcal{P}^{-1}(f')\|_{\mathcal{U}} \leq L \|f - f'\|_{C(\mathcal{Y})}$ for f' in some neighborhood of f .

(2) $\Phi(\mathcal{P}^{-1}(f), y) \in B$ for all $y \in \mathcal{Y}$.

Then, for sufficiently large M, N , and any \widehat{u} that satisfies $\widehat{\mathcal{P}}(\widehat{u}) = f$ we have the error bound

$$\|\widehat{u} - \mathcal{P}^{-1}(f)\|_{\mathcal{U}} \leq C \|\widehat{u}\|_{\mathcal{U}} \left[\left(\varrho_{M,N}^{\frac{\eta - \frac{\varrho+d}{2}}{2}} + \sup_m \rho_{m,N}^{\gamma-\gamma'} \right) \left(\|P\|_{\mathcal{P}}^2 + \|\overline{P}\|_{\mathcal{P}}^2 + \sum_{m=1}^M \|u^m\|_{\mathcal{U}^2}^2 \right)^{1/2} \right].$$

Proof. Let us write $u = \mathcal{P}^{-1}(f)$, and observe that thanks to hypothesis (2) of the theorem and Proposition 5, we have the bound

$$\|\widehat{\mathcal{P}}(u) - \mathcal{P}(u)\|_{C(\mathcal{Y})} \leq C \left[\left(\varrho_{M,N}^{\eta - \frac{Q+d}{2}} + \sup_m \rho_{m,N}^{\gamma - \gamma'} \right) \left(\|P\|_{\mathcal{P}}^2 + \|\bar{P}\|_{\mathcal{P}}^2 + \sum_{m=1}^M \|u^m\|_{\mathcal{U}^2}^2 \right)^{1/2} \right].$$

The result follows by a straightforward application of Lemma 3. \square

Remark 3. *The above proposition tells us that the operator learning problem associated to "solving" $\widehat{\mathcal{P}}(u) = f$ essentially inherits the same rate of convergence as the equation learning problem so long as the new right-hand side function f is not too different from those encountered in the training data. This is in line also with the local nature of the type of error bounds we have derived in this section for \widehat{P} and \widehat{u}^m from the theory of scattered data approximation.*

B.4. Representer theorems for 1-step and 2-step KEqL. Below we give the proofs of representer theorems for both versions of the KEqL algorithm as presented in the main body.

B.4.1. Representer formulas for 2-step KEqL. For completeness we will give a brief justification for the expressions (12) and (13) as direct consequences of Lemma 2: Consider (4) and apply Lemma 2 with $\mathcal{H} = \mathcal{U}$, $\phi_i = \delta_{y_i^m}$, and $z_i = u^m(y_i^m)$ for all $i = 1, \dots, N$. This gives (12). Next consider (6) and apply Lemma 2 with $\mathcal{H} = \mathcal{P}$, $\phi_i = \delta_{s_i}$ for $s_i \in S$, and $z_i = f(y_i)$ for $y_i \in Y$ to obtain (13).

B.4.2. Representer theorem for 1-step KEqL (Proof of Theorem 2). To simplify notation we first prove the theorem with $M = 1$, i.e., with training data $(u(Y^1), f)$. Let us recall the corresponding optimal recovery problem for convenience:

$$(31) \quad \begin{aligned} (\widehat{u}, \widehat{P}) &= \arg \min_{v \in \mathcal{U}, G \in \mathcal{P}} \|G\|_{\mathcal{P}}^2 + \lambda_1 \|v\|_{\mathcal{U}}^2 \\ \text{s.t.} \quad &v(Y^1) = u(Y^1), \quad \text{and} \quad G(S) = f(Y), \end{aligned}$$

where $S = \{s_1, \dots, s_K\}$, and $s_k := \Phi(v, y_k)$ for $y_k \in Y$ where we recall that Y is the dense set of collocation points that we use to impose the PDE constraint.

Then our goal is to show that under the assumptions of Theorem 2, every minimizing tuple $(\widehat{u}, \widehat{P})$ of (31) can be written in the form

$$\widehat{u}(y) = \mathbf{U}(\phi, y)^T \widehat{\alpha}, \quad \widehat{P}(s) = \mathbf{P}(\widehat{S}, s)^T \widehat{\beta},$$

for a tuple $(\widehat{\alpha}, \widehat{\beta})$ that solves the equivalent optimization problem

$$(32) \quad \begin{aligned} (\widehat{\alpha}, \widehat{\beta}) &= \arg \min_{\alpha \in \mathbb{R}^{QK}, \beta \in \mathbb{R}^{K^2}} \beta^T \mathbf{P}(S, S) \beta + \lambda_1 \alpha^T \mathbf{U}(\phi, \phi) \alpha, \\ \text{s.t.} \quad &\mathbf{U}(\phi, Y^1)^T \alpha = u(Y^1), \quad \text{and} \quad \mathbf{P}(S, S)^T \beta = f(Y). \end{aligned}$$

where $S = \{s_1, \dots, s_K\}$ but now each $s_k = (y_k, \mathbf{U}(\phi, \phi_k^1)^T \alpha, \dots, \mathbf{U}(\phi, \phi_k^Q)^T \alpha)$. Recall our notation $\mathbf{U}(\phi, Y^m) \in \mathbb{R}^{QK \times N}$ for the matrix with columns $\mathbf{U}(\phi, y_n)$, and $\mathbf{P}(S, S) \in \mathbb{R}^{K \times K}$ for the matrix with columns with columns $\mathbf{P}(S, s_k)$.

Proof. Let us write (31) in the equivalent form

$$(33) \quad \begin{cases} \arg \min_{v \in \mathcal{U}, G \in \mathcal{P}} \|G\|_{\mathcal{P}}^2 + \lambda_1 \|v\|_{\mathcal{U}}^2 \\ \arg \min_{Z \in \mathbb{R}^{K \times Q}} \begin{cases} \text{s.t.} \quad \phi_k^q(v) = Z_{k,q} \text{ and } G(s_k) = f(y_k), \text{ for all } k = 1, \dots, K, \text{ and } q = 1, \dots, Q \\ \text{where} \quad s_k := (y_k, Z_{k,1}, \dots, Z_{k,Q}) \end{cases} \\ \text{s.t.} \quad Z_{j,1} = u(y_j), \quad \text{for } j \in \{k \in \{1, \dots, K\} : y_k \in Y^1\}. \end{cases}$$

Observe that the Z variable matrix that we introduce acts as a slack variable for the inner problem and the outer constraint is enforcing the observation locations of v at $Y^1 \subset Y$.

For a fixed $Z \in \mathbb{R}^{K \times Q}$, we can solve the inner optimization problem for v and G explicitly using Lemma 2, which leads to

$$v(y) = \mathbf{U}(\phi, y)^T \mathbf{U}(\phi, \phi)^{-1} \text{vec}(Z), \quad \text{and} \quad G(s) = \mathbf{P}(S, s)^T \mathbf{P}(S, S)^{-1} f(Y).$$

The RKHS norms of these solutions can be computed explicitly as

$$\|v\|_{\mathcal{U}}^2 = \text{vec}(Z)^T \mathbf{U}(\phi, \phi)^{-1} \text{vec}(Z), \quad \text{and} \quad \|G\|_{\mathcal{P}}^2 = f(Y)^T \mathbf{P}(S, S)^{-1} f(Y).$$

Thus, we equivalently write (33) as

$$(34) \quad \begin{aligned} \arg \min_{Z \in \mathbb{R}^{K \times Q}} & f(Y)^T \mathbf{P}(S, S)^{-1} f(Y) + \lambda_1 \text{vec}(Z)^T \mathbf{U}(\phi, \phi)^{-1} \text{vec}(Z) \\ \text{s.t.} \quad & \mathbf{U}(\phi, Y^1)^T \mathbf{U}(\phi, \phi)^{-1} \text{vec}(Z) = u(Y^1), \end{aligned}$$

where we now modified the s_k to be of the form

$$s_k = (y_k, \mathbf{U}(\phi, \phi_k^1)^T \mathbf{U}(\phi, \phi)^{-1} \text{vec}(Z), \dots, \mathbf{U}(\phi, \phi_k^Q)^T \mathbf{U}(\phi, \phi)^{-1} \text{vec}(Z)).$$

Similarly, the constraint in (34) is valid since $\phi_k^q(v) = Z_{k,q}$ which particularly includes $\phi_j^1(v) = Z_{j,1}$ for $j \in \{1, \dots, K\} : y_\ell \in Y^1\}$.

Finally, if we define $\alpha = \mathbf{U}(\phi, \phi)^{-1} \text{vec}(Z)$ and $\beta = \mathbf{P}(S, S)^{-1} f(Y)$ (where in case $\mathbf{U}(\phi, \phi)$ and $\mathbf{P}(S, S)$ are not invertible, understand α and β in the least squares sense) then the problem (34) is equivalent to the desired system

$$\begin{aligned} \arg \min_{\alpha \in \mathbb{R}^{QK}, \beta \in \mathbb{R}^K} \quad & \beta^T \mathbf{P}(S, S) \beta + \lambda_1 \alpha^T \mathbf{U}(\phi, \phi) \alpha \\ \text{s.t.} \quad & \mathbf{U}(\phi, Y^1)^T \alpha = u(Y^1), \quad \text{and} \quad \mathbf{P}(S, S)^T \beta = f(Y) \end{aligned}$$

where $S = \{s_1, \dots, s_K\}$ with each $s_k = \left(y_k, \mathbf{U}(\phi, \phi_k^1)^T \alpha, \dots, \mathbf{U}(\phi, \phi_k^Q)^T \alpha \right)$. Notice that the constraint on β is trivially satisfied since $G(s_k) = f(y_k)$ for all $k \in \{1, \dots, K\}$, however, it becomes explicit due to the change of variables in terms of β in the formulation of G .

For the general proof for an arbitrary number of functions M the same idea follows since the equivalent form Equation (33) now contains the slack tensor $Z \in \mathbb{R}^{K \times Q \times M}$ instead of the matrix Z above since each v^m will be represented by a matrix Z^m in our proof. Additionally S will then contain not only K points but KM points corresponding to each of the v^m and their requisite partial derivatives evaluated at the collocation points. \square

SUPPLEMENTARY INFORMATION C. DETAILS OF ALGORITHMS

In this section, we describe additional algorithmic details relating to the 1-step KEqL method, i.e., (15). As it was mentioned in the main body of the paper, implementation of our LM formulation already leads to a convergent algorithm with good empirical performance. However, dealing with large kernel matrices often limits the scalability of that method. To address these issues we outline various strategies in this section that are implemented in our numerical experiments. These optional strategies include: a Nyström approximation to our model for P using a reduced basis; applying a change of variables in the optimization algorithms using Cholesky factors of kernel matrices to improve conditioning; and fast matrix calculations by leveraging block arrow structures.

C.1. Nyström approximations and reduced bases for P . It is often possible to replace the canonical representer basis $\mathbf{P}(S(\alpha), s)$ for P with a fixed set of $I \ll MK$ inducing points S_I [62]. These inducing points can be chosen by randomly sub-sampling the elements of $S(\alpha)$ at every iteration of the LM algorithm, but this can lead to technical difficulties since the point cloud $S(\alpha)$ changes from one iteration to the next, meaning that our reduced basis for P also needs to change. Instead, we simply choose S_I by subsampling the point clouds $\Phi(\hat{u}^m, Y)$ where the \hat{u}^m denote our estimates of the u^m from 2-step KEqL. Hence, our reduced basis for P is pre-computed before the LM algorithm is implemented. Note, that this approximation becomes exact whenever the number of inducing points $I \geq \dim(\mathcal{P})$, for example, in the case of polynomial kernels which have finite rank, choosing a sufficiently large number of inducing points ensures exact solution of the problem.

By fixing S_I , our finite dimensional optimization problem becomes

$$(35) \quad \begin{aligned} (\hat{\alpha}, \hat{\beta}) = \arg \min_{\alpha \in (\mathbb{R}^{QK})^M, \beta \in \mathbb{R}^I} \quad & \beta^T \mathbf{P}(S_I, S_I) \beta + \lambda_1 \sum_{m=1}^M (\alpha^m)^T \mathbf{U}(\phi, \phi) \alpha^m \\ & + \sum_{m=1}^M \frac{1}{2\sigma_u^2} \|\mathbf{U}(\phi, Y^m)^T \alpha^m - u^m(Y^m)\|_2^2 + \frac{1}{2\sigma_P^2} \|\mathbf{P}(S_I, S^m(\alpha^m))^T \beta - f^m(Y)\|_2^2, \end{aligned}$$

Notice that the matrix $\mathbf{P}(S_I, S_I)$ is now fixed and of much smaller size than the full matrix $\mathbf{P}(S(\alpha), S(\alpha))$.

C.2. Cholesky change of variables. Taking the Cholesky factorizations $\mathbf{P}(S_I, S_I) = C_P C_P^T$ and $\mathbf{U}(\phi, \phi) = C_U C_U^T$, we can define the transformed variables

$$w^m = C_U^T \alpha^m, \quad z = C_P^T \beta.$$

Under this transformation, we can re-write (35) as,

$$(36) \quad \begin{aligned} (\hat{\mathbf{w}}, \hat{z}) = & \arg \min_{\mathbf{w} \in (\mathbb{R}^{QK})^M, z \in \mathbb{R}^I} \|z\|^2 + \lambda_1 \sum_{m=1}^M \|w^m\|^2 \\ & + \sum_{m=1}^M \frac{1}{2\sigma_u^2} \|\mathbf{U}(\phi, Y^m)^T C_U^{-T} w^m - u^m(Y^m)\|_2^2 \\ & + \frac{1}{2\sigma_P^2} \|\mathbf{P}(S_I, S^m(w^m))^T C_P^{-T} z - f^m(Y)\|_2^2. \end{aligned}$$

While the LM algorithm is generally invariant under such changes of variables this greatly improves the conditioning of the optimization problems in practice. Indeed, we found that this change of variables enables first order methods, such as gradient descent, to also produce reasonable solutions when otherwise they would have failed.

To further clarify our implementation of the LM algorithms we abstract the objective into a general nonlinear least squares problem by rewriting (C.2) as

$$(37) \quad \begin{aligned} (\hat{\mathbf{w}}, \hat{z}) = & \arg \min_{\mathbf{w} \in (\mathbb{R}^{QK})^M, z \in \mathbb{R}^I} \|z\|^2 + \sum_{m=1}^M \|w^m\|^2 + \|F(z, \mathbf{w})\|^2 \\ F(z, \mathbf{w}) = & \begin{bmatrix} F_1(z, w^1) \\ F_2(z, w^2) \\ \vdots \\ F_M(z, w^M) \end{bmatrix} \in \mathbb{R}^{M(N+K)}, \quad F_m(z, w_m) = \begin{bmatrix} \sqrt{\frac{1}{2\sigma_u^2}} (\mathbf{U}(\phi, Y^m)^T C_U^{-T} w^m - u^m(Y^m)) \\ \sqrt{\frac{1}{2\sigma_P^2}} (\mathbf{P}(S_I, S^m(w^m))^T C_P^{-T} z - f^m(Y)) \end{bmatrix}. \end{aligned}$$

For this problem we obtain the LM updates

$$(38) \quad \begin{aligned} (\mathbf{w}_{(j+1)}, z_{(j+1)}) = & \arg \min_{\mathbf{w} \in (\mathbb{R}^{QK})^M, z \in \mathbb{R}^I} \|z\|^2 + \sum_{m=1}^M \|w^m\|^2 + \|F_{(j)}(z, \mathbf{w})\|^2 + \lambda_{(j)} \left(\|z - z_{(j)}\|^2 + \sum_{m=1}^M \|w^m - w_{(j)}^m\|^2 \right) \\ F_{(j)}(z, \mathbf{w}) = & \nabla F(z_{(j)}, \mathbf{w}_{(j)}) \begin{bmatrix} z - z_{(j)} \\ \mathbf{w} - \mathbf{w}_{(j)} \end{bmatrix} + F(z_{(j)}, \mathbf{w}_{(j)}) \end{aligned}$$

where $\lambda_{(j)}$ is a proximal regularization parameter to ensure global convergence. In many cases, applying this iteration with a reasonable update rule for λ_j and solving the least squares subproblems by computing Cholesky factorizations of the normal equations is sufficient to achieve accurate solutions. When issues with the conditioning of the normal equations arise, we use an SVD solver which is more accurate but has a higher computational cost.

C.2.1. *A heuristic for choosing $\lambda_{(j)}$.* We now discuss the adaptation of the damping parameter $\lambda_{(j)}$, which is crucial for both ensuring stability of the optimization algorithm far from a minimum, and providing fast convergence near minima. Following [2, 33], define the *gain ratio* $\rho_{(j)}$ to be the ratio of the decrease of the true objective value to the decrease predicted by the linearized objective,

$$\rho_{(j)} := \frac{\left(\|z_{(j+1)}\|^2 + \sum_{m=1}^M \|w_{(j+1)}^m\|^2 + \|F(z_{(j+1)}, \mathbf{w}_{(j+1)})\|^2 \right) - \left(\|z_{(j)}\|^2 + \sum_{m=1}^M \|w_{(j)}^m\|^2 + \|F(z_{(j)}, \mathbf{w}_{(j)})\|^2 \right)}{\left(\|z_{(j+1)}\|^2 + \sum_{m=1}^M \|w_{(j+1)}^m\|^2 + \|F_{(j)}(z_{(j+1)}, \mathbf{w}_{(j+1)})\|^2 \right) - \left(\|z_{(j)}\|^2 + \sum_{m=1}^M \|w_{(j)}^m\|^2 + \|F_{(j)}(z_{(j)}, \mathbf{w}_{(j)})\|^2 \right)}.$$

For constants $0 < c_0 < c_1 < c_2 < 1$ and an adaptation multiplier $b > 1$, we set

$$\lambda_{(j+1)} = \begin{cases} b\lambda_{(j)} & \rho_{(j)} < c_1 \\ \lambda_{(j)} & \rho_{(j)} \in (c_1, c_2) \\ \frac{1}{b}\lambda_{(j)} & \rho_{(j)} > c_2. \end{cases}$$

In the case that $\rho_{(j)} < c_0$, we reject the step, set $(\beta_{(j+1)}, \boldsymbol{\alpha}_{(j+1)}) = (\beta_{(j)}, \boldsymbol{\alpha}_{(j)})$, and attempt to compute the next step with the increased damping parameter.

C.3. **Leveraging block-arrow sparsity.** Instantiating and computing solutions to the regularized linear least squares problems within the LM iterations can be difficult in large scale problems where N, M are large. In such cases, the solution to (38) can be computed directly in $O((QK + N_1)^3 M)$ operations, by leveraging sparsity of the

gradients ∇F , rather than the naive $O((QK + N_I)^3 M^3)$. Observe that

$$\nabla F(z_{(j)}, \mathbf{w}_{(j)}) = \begin{bmatrix} \nabla_z F_1 & \nabla_{w_1} F_1 & 0 & \cdots & 0 \\ \nabla_z F_2 & 0 & \nabla_{w_2} F_1 & \cdots & 0 \\ \vdots & \vdots & \vdots & \ddots & \vdots \\ \vdots & 0 & & & 0 \\ \nabla_z F_M & 0 & 0 & \cdots & \nabla_{w_M} F_M \end{bmatrix}$$

This form of ∇F induces a block arrowhead structure for the regularized normal equations for the least squares problems within the LM update,

$$\nabla F^T \nabla F + (1 + \lambda_{(j)})I = \begin{bmatrix} * & * & \cdots & * & * \\ * & * & & & \\ \vdots & & * & & \\ * & & & \ddots & \\ * & & & & * \end{bmatrix} = \begin{bmatrix} A_P & B_{UP}^T \\ B_{UP} & D_U \end{bmatrix}$$

where $A_P \in \mathbb{R}^{N_I \times N_I}$ and $D_U \in \mathbb{R}^{QKM \times QKM}$ is a block diagonal matrix with blocks of size QK . From here, block elimination can be applied to solve the normal equations

$$\begin{bmatrix} A_P & B_{UP}^T \\ B_{UP} & D_U \end{bmatrix} \begin{bmatrix} \delta z \\ \delta \mathbf{w} \end{bmatrix} = \begin{bmatrix} F_P \\ F_U \end{bmatrix}$$

given by the formulae

$$C = \left(A_P - B_{UP}^T D_U^{-1} B_{UP} \right), \quad \delta \mathbf{w} = C^{-1} \left(F_P - B_{UP}^T D_U^{-1} F_U \right), \quad \delta \mathbf{z} = D_U^{-1} (F_U - B_{UP} \delta \beta),$$

where we note that the Schur complement C and the matrix A_P are of the moderate size $I \times I$, and the inverse of D_U is readily computable due to the block diagonal structure.

SUPPLEMENTARY INFORMATION D. NUMERICAL EXPERIMENTS AND DETAILS

We now present details of the numerical experiments summarized in the main body of the paper, covering various details such as data generation processes, selection of observation and collocation points, hyperparameter, and additional results and observations. Further implementation details can be found in our GitHub repository⁵ where we collect code for regenerating our numerical results and figures.

D.1. The Duffing oscillator. In this example we compared the performance of 1-step and 2-step KEqL along with SINDy for learning a 1D nonlinear ODE. Our focus is on the performance of the methods in filtering and extrapolation/forecasting of the dynamics.

Let us recall our problem setup where we took $\mathcal{Y} = (0, 50)$ and considered the Duffing oscillator

$$(39) \quad \begin{cases} \mathcal{P}(u) = \partial_t^2 u - 3u + 3u^3 + 0.2\partial_t u = \cos(2t), & t \in \mathcal{Y}, \\ u(0) = \partial_t u(0) = 0. \end{cases}$$

To generate the training data for this example we solved the ODE numerically using a Dopri5 solver in Python with adaptive step size and initial value $1e - 3$. The numerical solution was then subsampled on $N = 32$ observation points that were also picked on a uniform collocation grid Y of size 1000 in \mathcal{Y} . The test data set for filtering the solution was generated similarly but on a finer uniform grid of 5000 observation points. To generate the test datasets for forecasting and extrapolation errors, we used the same numerical solver, but, we introduced three new initial conditions, each satisfying $u(0) = 0$, while the initial time derivative $\partial_t u(0)$ was set to 0.5, 1, and -1 , respectively.

For the kernels, we selected \mathbf{U} as a RQ kernel and \mathbf{P} as RBF, both with $\Sigma = \text{Id}$. We employed a fixed basis with $I = 500$ inducing points for learning the equation (see SI C.1).

For the loss function SI C.1, we used

$$(40) \quad \lambda = 1, \quad \sigma_u^2 = \sqrt{\frac{NM}{\theta_u}}, \quad \text{and} \quad \sigma_P^2 = \sqrt{\frac{MI}{\theta_P}},$$

with $\theta_u = 5e - 8$ and $\theta_P = 1e - 9$, selected manually. The loss history for the optimization of 1-step KEqL can be seen in Figure 5 for learning the Duffing ODE. We see that the algorithm has converged in about 200 iterations.

⁵<https://github.com/TADSGroup/kernelequationlearning>

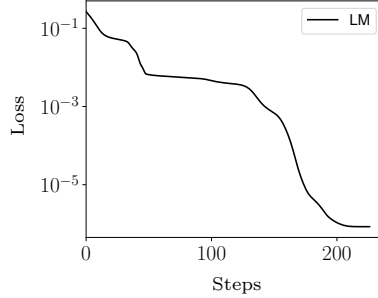


FIGURE 5. Convergence history of LM for 1-step KEqL for the Duffing ODE (18).

D.2. The Burgers' PDE. In this example we compared 1-step KEqL with SINDy and the PINN-SR algorithm. Here we describe the choice of initial conditions, generation of training and test samples, hyperparameters, and optimization details used for this example.

Let us recall our problem setting. We took $\mathcal{Y} = (0, 1] \times (0, 1)$ and considered the Burgers' PDE

$$(41) \quad \begin{cases} \mathcal{P}(u) = \partial_t u + \vartheta u \partial_x u - \nu \partial_{xx} u = 0, & (t, x) \in \mathcal{Y}, \\ u(0, x) = u_0(x), \\ u(t, 0) = u(t, 1) = 0. \end{cases}$$

We remind the reader that whenever we state in any of the subsequent experiments that (19) was solved, we mean that a second-order Strang splitting method with a small step size was used, followed by spline interpolation to obtain a solution that can be evaluated at any point of its domain. Additionally, when using the 1-step KEqL method, we always assumed the use of the standard implementation of the algorithm described in (36).

D.2.1. Experiments with increasing number of observations. Here, we used the PDE (19) with coefficients $\vartheta = 1$ and $\nu = 0.01$ and prescribed initial conditions (IC) u_0 from a Gaussian process with Karhunen–Loève expansion

$$(42) \quad u_0(x) = \sum_{j=1}^{50} \frac{1}{j^2} \sin(j\pi x) Z_j, \quad \text{with } Z_j \sim N(0, 1), \quad x \in [0, 1].$$

The condition used for the fixed IC case is depicted in Figure 6(A) while some samples of ICs are shown in Figure 6(B–D) for the case when ICs vary also in the experiment.

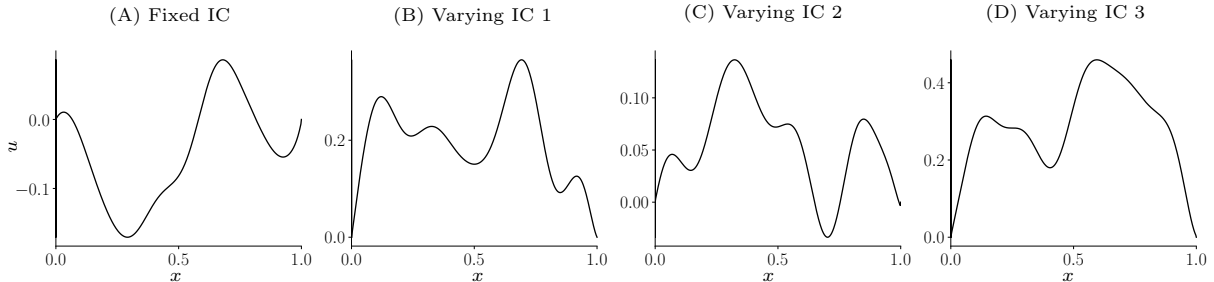


FIGURE 6. Initial conditions sampled from the process (42) for examples of Burgers' PDE (19) increasing number of observations: (A) Condition used in the fixed IC case; (B–D) Sample conditions for the varying IC case.

We then solved each PDE and subsampled the observed data for values $N_y = 10, 30, 50, 100, 200, 300, 400, 500, 600$ in the interior and $N_{\partial\mathcal{Y}} = 131$ at the boundary from a set of 26×31 Chebyshev collocation points in space-time. In Figure 7, we present example training data overlaid on the contour plots of the solutions for the fixed initial condition, as shown in Figure 6(A), while varying the number of observations $N_y = 20, 50, 200$. Additionally, we include instances of the training data for the case where the initial condition varies, corresponding to the ICs introduced earlier in Figure 6(B–D).

We took \mathbf{U} , to be RBF with a diagonal matrix Σ , where its entries were determined using maximum likelihood estimation (MLE) based on the available observation points $u(Y^1)$ for each number of observations case, basically by a first application of the 2-step method. In both cases for this experiment, we chose \mathbf{P} to be a polynomial kernel of degree 2, with the shift parameter set to $c = \text{mean}(S_2)$ and the scaling matrix given by $B = \text{diag}(\text{cov}(S_2))^{-1}$, where $\text{cov}(A)$ represents the sample covariance of A . Specifically,

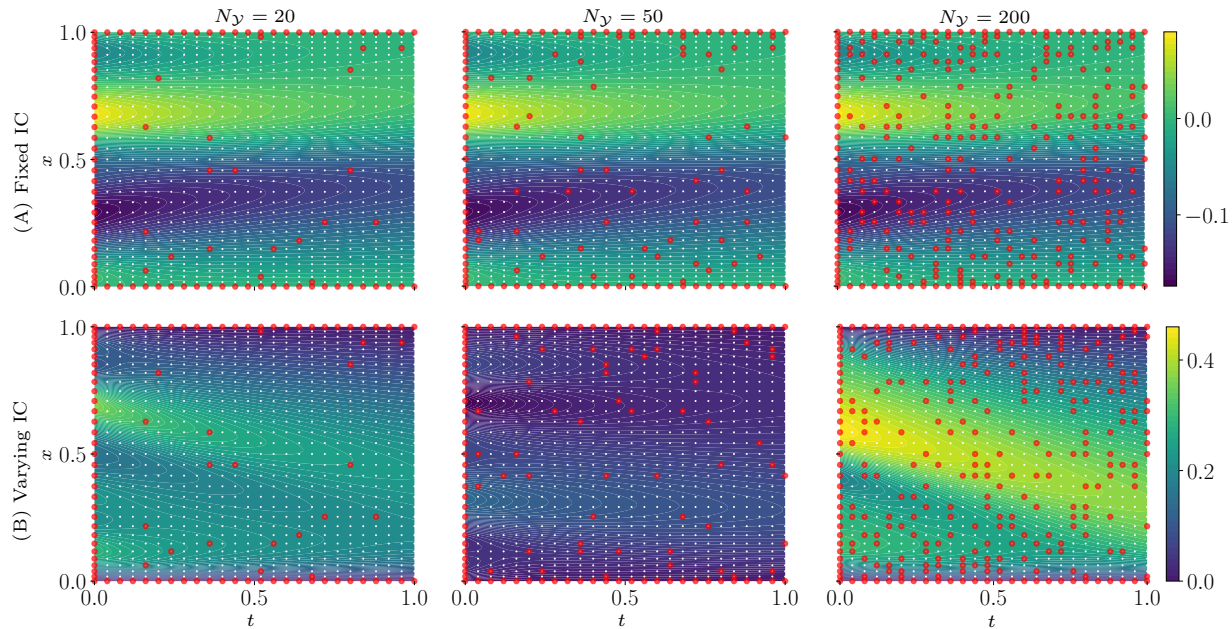


FIGURE 7. Samples of training solutions along with their N observation points (red) and the collocation points (white) for Burgers’ PDE (19) with ICs sampled from the GP (42): (A) Solution obtained using a fixed IC depicted in Figure 6(A); (B) Three solutions obtained from solving the PDE with different ICs depicted in Figure 6(B-D).

$$(43) \quad S = \Phi(\hat{u}_2, Y^1) := \begin{bmatrix} \Phi(\hat{u}_2, y_1) \\ \vdots \\ \Phi(\hat{u}_2, y_N) \end{bmatrix} \in \mathbb{R}^{N \times 5},$$

where \hat{u}_2 is the learned solution obtained from the first step of the 2-step KEqL method, using the MLE-fitted hyperparameters mentioned above.

Recall that for SINDy, we used the same kernel \mathbf{U} for derivative approximation and employed a polynomial library for the dictionary terms, which matched the features of the degree-2 polynomial used in KEqL. These same features were also used by PINN-SR. For PINN-SR, we fixed the hyperparameters across different experiments. For example, in the fixed IC case, where we aim to learn a PDE by varying the number of observation points, we selected a set of hyperparameters—such as network size, loss function weights, and iteration steps—and kept them the same for every experiment with different numbers of observation points. The same approach was applied when varying the initial condition. This strategy is consistent with the kernel method and SINDy, as we also maintained the same hyperparameters across different experiments for those methods.

For the loss function (36), we followed the definitions in (40), with the exception that $I = 26 \times 31$ and we set $\theta_u = 1e - 9$ and $\theta_P = 1e - 11$ as manually chosen hyperparameters.

We analyzed the filtering and equation learning errors for one-shot learning of Burgers’ equation with different numbers of observation points and different ICs. The results are presented in Figure 8, where we report the errors for different smooth initial conditions. Since both the observation points and initial conditions are chosen randomly, we report the average errors along with the best and worst errors across multiple runs. Convergence history of the optimization algorithm for some sample cases of learning the equation is shown in Figure 11(A-B).

A similar conclusion can be drawn here as in Figure 3(A), where the 1-step KEqL method continues to achieve the lowest filtering and equation learning errors, with a larger performance gap when N_Y is small. However, we now observe that the KEqL and SINDy methods exhibit greater robustness across different experiments with varying initial conditions, whereas the performance of the PINN-SR method deteriorates. This decline is reflected in the increased variance in the results, which we attribute to the use of the same model across different experiments. This suggests that PINN-SR may require tuning for each specific set of observations and initial conditions, whereas such tuning was not necessary for the other two methods.

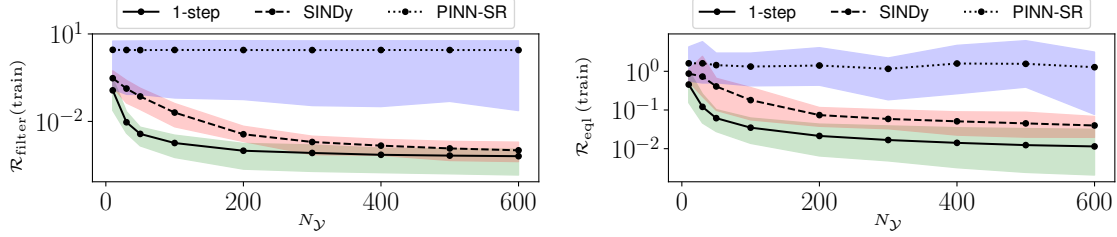


FIGURE 8. The filtering and equation learning errors computed for the training functions for 1-step KEqL, SINDy, and PINN-SR using $M = 1$ training pairs with different number of interior observations N_y for Burgers' PDE (19) with different ICs.

D.2.2. *An experiment with a smoothed shock.* Here, we considered the PDE (19) with coefficients $\vartheta = 5$ and $\nu = 0.001$, using the prescribed IC

$$(44) \quad u_0(x) = \frac{1}{4} (x \sin(\pi x) - \sin(5\pi x) - \sin(3\pi x)).$$

We then solved the PDE, and the solution's behavior at the initial and final times is shown in Figure 9(A). Then we subsampled observation points for $N_y = 60$ in the interior and $N_{\partial y} = 131$ at the boundary from a chosen 26×31 Chebyshev collocation grid in space-time.

We took \mathbf{U} , to be RBF with a diagonal matrix Σ , where its entries were determined using MLE based on the N observation points. We chose \mathbf{P} to be a polynomial kernel of degree 2, with the shift parameter and the scaling matrix constructed using S as in (43). Thus, once again we used the hyperparameter information from the 2-step KEqL methodology to guide the selection of hyperparameters for the 1-step KEqL. For the loss function (15), we followed the definitions in (40), with the exception that $I = 26 \times 31$ and we set $\theta_u = 1e - 9$ and $\theta_P = 1e - 11$ as manually chosen hyperparameters. For SINDy we used the same kernel \mathbf{U} for derivative approximation and employed a polynomial library for the dictionary terms, which matched the features of the degree-2 polynomial used in KEqL. These same features were also used by the PINN-SR method.

We clearly observe that the 1-step KEqL method remains competitive in shock filtering. This is evident from the relative filtering errors presented in Figure 10, where the 1-step KEqL achieves comparable results in shock recovery to those of SINDy and PINN-SR. Convergence history of the optimization algorithm for learning the equation is shown in Figure 11(C).

D.2.3. *A one-shot learning experiment.* Here, we considered the PDE (19) with coefficients $\vartheta = 0.5$ and $\nu = 0.01$, using the prescribed IC given by (44). We then solved the PDE, whose solution behavior at initial and final times are shown in Figure 9(B). Here we subsampled $N = 100$ points placed on the boundary, see first column in Figure 3(A). The placement of the points amounts to observing the initial and end conditions along with the boundary values in the physical domain. To generate data for operator learning, we additionally solved the same PDE with a new initial condition, $u_0(x) = -x \sin(2\pi x)$. The solution behavior at the initial and final times is shown in Figure 9(C).

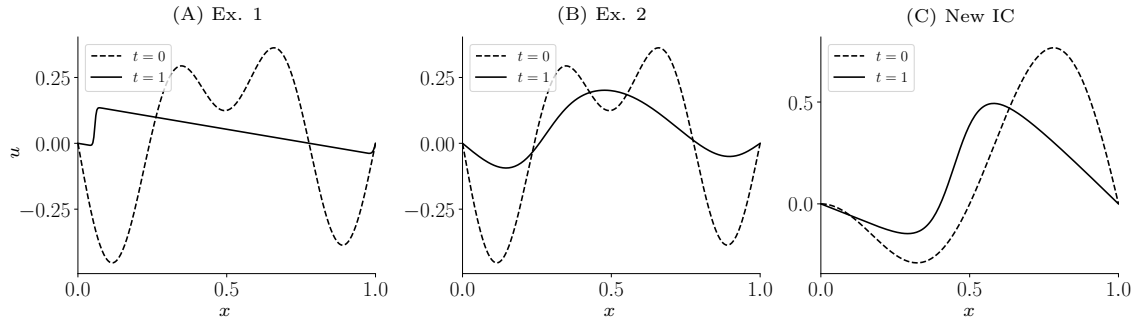


FIGURE 9. Behavior of solutions at initial and final time for one-shot learning examples of Burgers' PDE (19): (A) Shock development (SI D.2.2); (B) Smooth transition (SI D.2.3); (C) Solution behavior to the PDE in (B) for the depicted new initial condition.

In this experiment we took \mathbf{U} to be RBF with the diagonal matrix $\Sigma = 0.0125I$. To learn the equation, we used $\hat{\mathbf{P}}$ as a polynomial kernel of degree 2, where the shift parameter and scaling matrix were constructed using S , as described in (43). Here again, we used the hyperparameter information from the 2-step KEqL methodology to

		Method		
	Ex.	1-step	PINN-SR	SINDy
$\mathcal{R}_{\text{filter}}$	1	$3.9e^{-1}$	$3.4e^{-1}$	$6.2e^{-1}$
	2	$3.5e^{-3}$	$1.5e^{-1}$	$2.9e^{-1}$
\mathcal{R}_{opl}	2	$1.9e^{-2}$	$4.7e^{-1}$	$5.4e^{-1}$

FIGURE 10. Quantitative values of relative filtering and operator learning errors for Burgers’ PDE Equation (19) with different ICs corresponding to the one-shot learning examples Ex. 1 (SI D.2.2) and Ex. 2 (SI D.2.3) in Figure 3(B-D).

guide the selection of hyperparameters for the kernel \mathbf{P} of the 1-step KEqL. Recall that a similar rationale was used for selecting hyperparameters in SINDy and PINN-SR, including the choice of dictionary terms, as in the previous experiment discussed in SI D.2.2. For the loss function (15), we omitted the terms associated with the RKHS norms, divided all the terms by 10 and selected values for σ_u^2 and σ_P^2 as defined in (40). For which we set $I = 26 \times 26$. Additionally, we manually chose $\theta_u = 100$ and $\theta_P = 1$ as hyperparameters.

We clearly observe that the 1-step KEqL method outperforms the other methods in filtering the smooth solution. This is evident from results presented in Figure 10, where the one-step KEqL achieves a two-order-of-magnitude improvement over the other methods in filtering and a one-order-of-magnitude improvement in the operator learning task for the smooth case. The one-shot learning example for the smooth case further confirms that effective filtering is essential for accurately capturing the operator. While PINN-SR and SINDy provided a reasonable reconstruction of the solution, the superior filtering of the 1-step KEqL method resulted in a significantly better operator learning error for a new initial condition. We recall that the variational solution proposed in (11) was used to solve the recovered PDE in each of the methods for this experiment, employing the same kernel \mathbf{U} , to report the operator learning results. Convergence history of the optimization algorithm for learning the equation is shown in Figure 11(D).

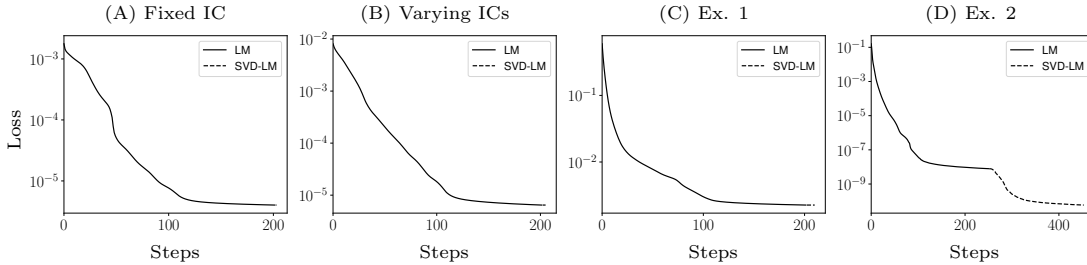


FIGURE 11. Convergence history of the LM algorithm for 1-step KEqL for Burgers’ PDE (19): (A-B) Sample cases using fixed and varying IC, using $M = 1$ training pairs with number of observations $N_{\mathcal{Y}} = 20$ corresponding to the two cases depicted in the first column in Figure 7; (C) Shock development (SI D.2.2); (D) One-shot smooth case where only observed on the boundary (SI D.2.3).

D.3. Darcy’s flow PDE. In this example we performed a systematic study of the performance of 1-step (its reduced version) and 2-step KEqL for learning an elliptic PDE with a variable diffusion coefficient. In particular, we investigate the ID and OOD performance in terms of filtering, equation learning, and operator learning.

Let us recall our problem setting. Here we took $\mathcal{Y} = (0, 1) \times (0, 1)$ and considered the problem

$$(45) \quad \begin{cases} \mathcal{P}(u) = \operatorname{div}(a\nabla u) = f(x), & a(x) = \exp(\sin(\cos(x_1) + \cos(x_2))), & x \in \mathcal{Y}, \\ u = g(x), & & x \in \partial\mathcal{Y}. \end{cases}$$

To generate the training data we drew $M = 2, 4, 8, 16, 32$ functions $u \sim \mathcal{GP}(0, \mathbf{U}_{\text{RBF}})$ with $\Sigma = 0.5^2 I$ and took $f := \mathcal{P}(u)$, also considering the value of u at $\partial\mathcal{Y}$ as the boundary condition. Each u was then subsampled observation points with $N_{\mathcal{Y}} = 2, 4, 8$ in the interior and fixed $N_{\partial\mathcal{Y}} = 56$ at the boundary that were picked randomly from a 15×15 uniform collocation grid where the PDE was enforced. Some training tuples with their observation and collocation points are depicted in Figure 12. We recall that the ID data was drawn from the same distribution that the training data was drawn from. The test data sets were generated similarly, with the OOD data drawn from a less regular GP using an RBF kernel with $\Sigma = 0.4^2 I$. Some ID and OOD samples are shown at Figure 13(A). The fine grid $\mathcal{Y}_{\text{test}}$ where we tested the equation and operator learning error was chosen to be a uniform grid of size 100^2 .

We used $\mathbf{U} = \mathbf{U}_{\text{RBF}}$ with $\Sigma = 0.5^2 I$ for learning u and $\mathbf{P} = \mathbf{P}_{\text{hybrid}}$ where an RBF with $\Sigma = 0.4^2 I$ was used for the spatial variables x_1, x_2 and a polynomial kernel of first degree for the variables $\{L_1 u, \dots, L_6 u\}$ where the shift was

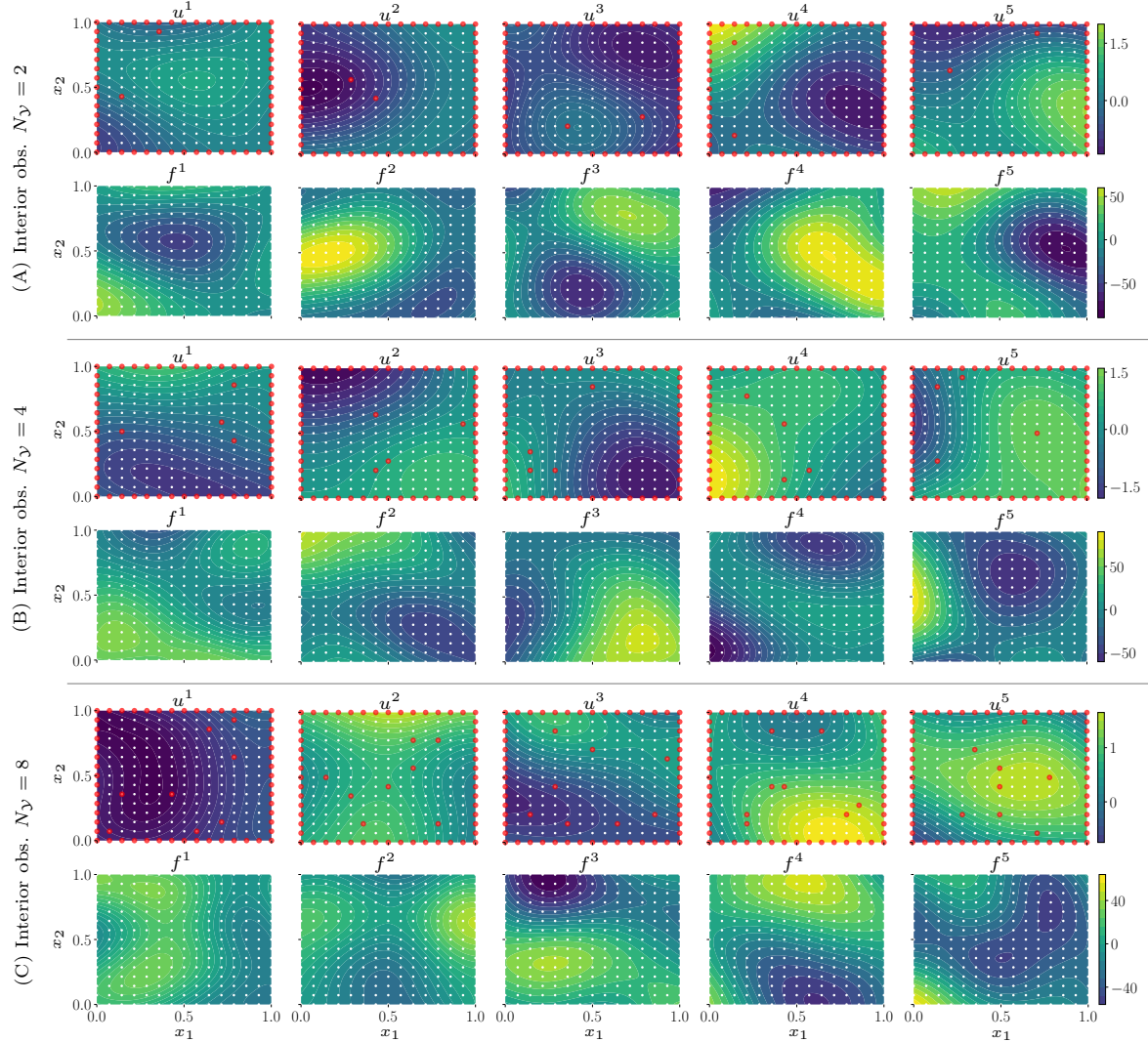


FIGURE 12. Samples of training tuples (u^m, f^m) with different number of observation points for Darcy's flow PDE (20): (A-C) Training tuples observation points (red) and collocation points (white).

chosen to be $c = \text{mean}(S_2)$ and the scaling matrix $B = (\text{diag}(\text{cov}(S_2)))^{-1}$ where

$$S = \begin{bmatrix} \Phi(\hat{u}_2^1, Y^1) \\ \vdots \\ \Phi(\hat{u}_2^M, Y^M) \end{bmatrix} \in \mathbb{R}^{\sum_{m=1}^M |Y^m| \times 8}.$$

where \hat{u}_2^m is the learned solution obtained from the first step of the 2-step KEqL method, using the MLE-fitted hyperparameters mentioned above. In summary, we also used the hyperparameter information from the 2-step KEqL methodology to guide the selection of hyperparameters for the kernels in 1-step KEqL.

To scale up equation learning when using many function tuples, we employed a fixed basis (see SI C.1) with $I = 200$ for learning the equation. Additionally, we leveraged the block arrowhead matrix structure within the optimization algorithm (see SI C.3). For the loss function (36), we followed the definitions in (40) except we took $\sigma_P^2 = \sqrt{I/\theta_P}$ and set $\theta_u = 5e - 12$ and $\theta_P = 1e - 12$ as hyperparameters, selected manually.

To further illustrate the equation and operator learning errors in relation to the error plot in Figure 4, we show samples of the contour error plots in Figure 13 and the convergence history in Figure 14 that uses the block arrowhead matrix structure LM-type algorithm for the case where the equation is learned using $M = 8$ training tuples and $N_y = 8$ observation points of the solution. We recall that the variational solution proposed in (11) was used to solve the

recovered PDE for both the 1-step and 2-step KEqL methods, employing the same kernel \mathbf{U} , to report the operator learning results.

In Figure 13(A), we show some ID and OOD solution samples used to test the learned equation for both the 1-step and 2-step KEqL methods. In Figure 13(B), we present the equation learning errors, where the values typically differ by one order of magnitude between 1-step and 2-step KEqL in favor of the joint methodology, with larger errors appearing near the boundaries. Similarly, in Figure 13(C), we observe that the 1-step method consistently outperforms the 2-step method by an order of magnitude. Notably, for this case the equation learning errors were an order of magnitude smaller than the operator learning errors.

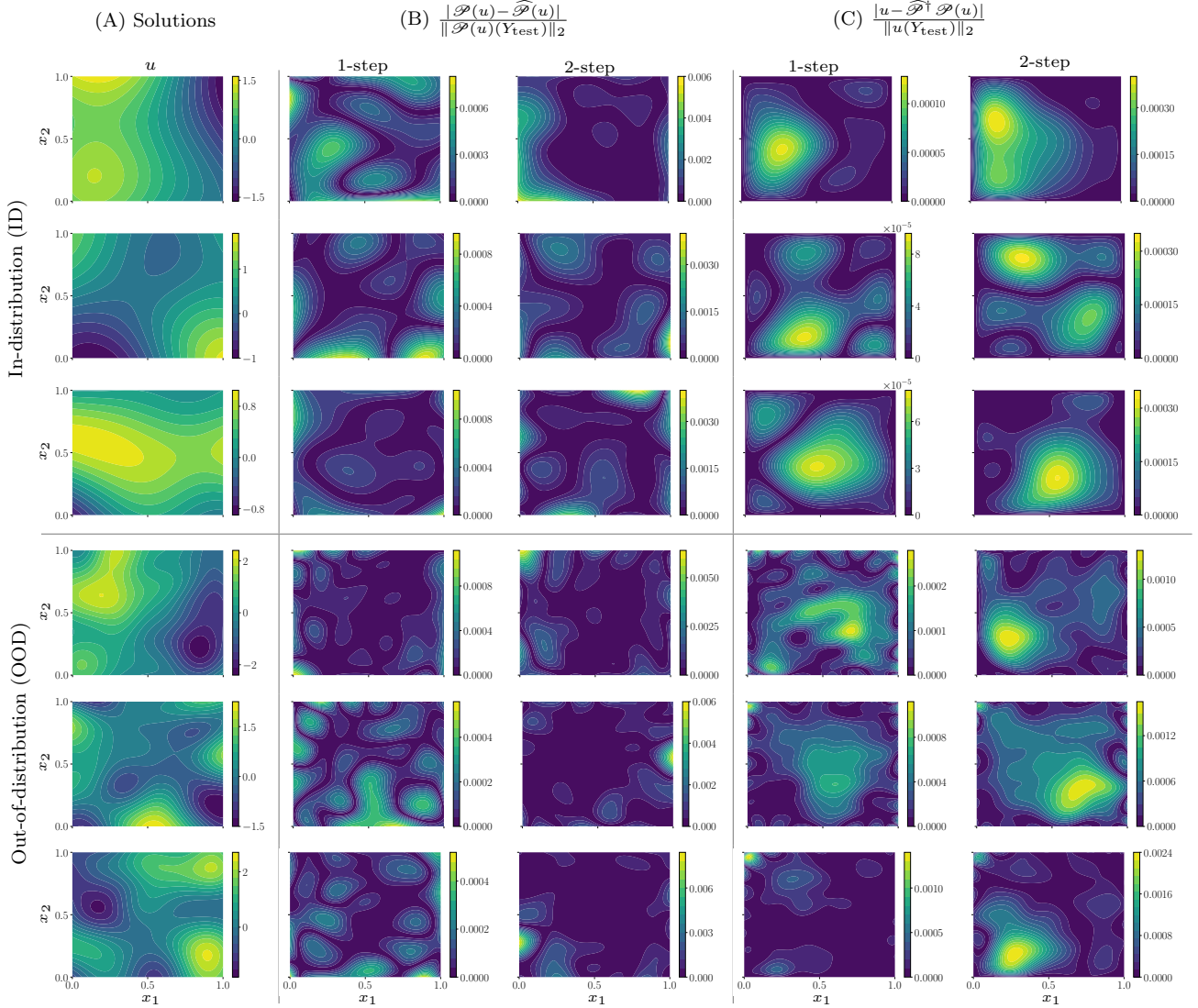


FIGURE 13. Samples of test solutions u (ID and OOD) and their contours of the equation and operator learning errors for 1-step and 2-step KEqL methods for Darcy's flow PDE (20): (A) Sample solutions u ID and OOD for the PDE ;(B) Contour plots for equation learning errors; (C) Contour plots for operator learning errors.

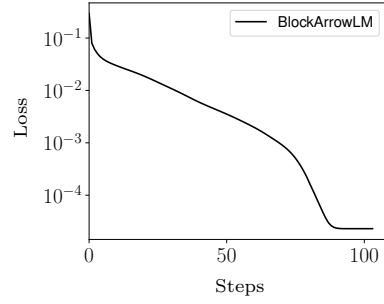


FIGURE 14. Convergence history of the block arrowhead matrix structure LM-type algorithm for the reduced 1-step KEqL when using $M = 8$ solution tuples at $N_y = 8$ observation points in the interior for Darcy's flow PDE (20).